Editor: Gerd Förch

CICD Series Vol.6:
Bogale Gebremariam - Basin Scale Sedimentary and Water Quality Responses to External Forcing in Lake Abaya, Southern Ethiopian Rift Valley, PhD Thesis

May 2007

CICD Series

Editor

Prof. Dr.-Ing. Gerd Förch,
Universität Siegen,
Centre for International Capacity Development,
Paul-Bonatz-Str. 9-11
57076 Siegen

E-Mail: info@cicd.uni-siegen.de

Printing Printing Office, Universität Siegen, Germany

ISSN: 1868-8578

CICD Series Vol.6: Bogale Gebremariam - Basin Scale Sedimentary and Water Quality Responses to External Forcing in Lake Abaya, Southern Ethiopian Rift Valley, PhD Thesis

Abstract

This study has attempted to investigate experimentally the distribution of surficial sediment and variation of water quality parameters under major influences of wind forcing and major rivers inflows in Lake Abaya, the largest Ethiopian Rift Valley Lake. A field study in Lake Abaya was conducted to understand and conceptualize better the lake dynamic process and functioning of main factors. Comprehensive field data consisting of water quality measurements, lake bed sediment grab samples and meteorological observations along the western shoreline have been obtained from Lake Abaya. Spatial and temporal variability of physical parameters are presented and the interrelationships between variables are discussed. Results indicate that the lake basin can be viewed as consisting of two main physiographic units, defined as sub basins, with behaviour defined by their response to external forcing over time.

Distribution pattern of lake bottom sediments bears information about the interaction of physical processes and the resultant motion that controls the transport and distribution of suspended solids. The relationship between sediment texture and bottom topography was discussed. The distribution pattern of sediments was interpreted in the light of the different energy zones and major rivers loading. The spatial distribution diagrams of major minerals found in recent deposits on the lake bottom show that understanding of the sedimentary pattern is of vital importance for proper interpretation of the dynamic process operating on the lake. The downstream tendency of fine sediments suggested the general wind-controlled circulation pattern of the top layer to the north and the return flow in the bottom layer southwards.

As well the inflow current of the tributary rivers as wind driven wave energies have an important influence on the spatial distribution of sediments. Persistent wind energy continuously mixes the lake water vertically and transports sediment in suspension horizontally resulting homogenous water column and extremely high turbidity throughout the whole open water zone. The intense wind mixing together with shallow depth apparently result an essentially homogenous water column.
The observed spatial and temporal variability of physical variables allowed estimating general circulation pattern. The results were discussed in terms of the direction and magnitude of wind forcing, nature of sediment distribution, bathymetry (water depth and bottom slope), and major inflow that determine possible pattern and strength of circulation.

Acknowledgement

The funding for this study by the German Technical Cooperation (GTZ) to Arba Minch University is deeply acknowledged. I would like to express my gratitude to Universität Siegen for providing basic and invaluable supports. Furthermore, I gratefully acknowledge the use of facilities at Freie Universität Berlin and Universität Siegen.
I would like to thank my supervisors Prof. Brigitta Schütt and Prof. Gerd Förch who gave me the inspiration, trust and freedom that paved my way for this study. Their many fruitful suggestions and careful review of the draft have made the production of this thesis possible. It was a great pleasure for me to conduct this thesis under their supervision. I wish to express my sincere thanks to Dr. Stefan Thiemann for the encouragements and many useful contributions both in the field and laboratory works.

I wish to thank the Department of Agriculture (Mirab Abaya Woreda) for proving loan of one of the boats used for the fieldwork, and the Arba Minch University for logistical support during the fieldwork. I acknowledge the Ministry of Water Resources for providing discharge records of the main tributaries of Lake Abaya and rainfall data for stations in the drainage basin of the lake.

I would like to express my thanks to Dr. Ropper for conducting X-ray diffraction test of sediment samples. Useful discussions on lacustrine processes with Ropper were most productive for the progress of this thesis.
A special dept of gratitude is owed to Susan Blumberg for permission to use her X-ray diffraction data for samples taken from the bottleneck connection of the two main basins. My special thanks go to Dr. Phillipp Hoelzmann and Dr. Steffen Möller for many useful comments on an early version of the thesis. Staff and PhD students in the Department of Physical Geography (Free University of Berlin) provided an excellent working environment. Special thanks to Dinh for the great time in our common office.
Thanks are due to Ato Melaku Hailemichael, Wrt. Ayelech Abate Ato Fikre Assefa and Ato Zekarias Gedo for their invaluable assistance in the field and laboratory. I am grateful to all of my university colleagues for their support and encouragement over all these years.

Bogale Gebremariam, May 2007.

Contents

List of Figures

1 Introduction

The ability to determine the responses to changes in external or controlling factors in the form of cause-and-effect relations is the corner stone for management of a natural lake system like Lake Abaya. One of the main aims of this study is to obtain quantifiable parameters which directly or indirectly indicate the variable physical processes in space and time on the lake system. As a baseline study to understand the principles of the lake system, it is the objective of this study to characterize lower and upper bound values of physical variables in the study site. The spatial distribution characteristics of surficial sediments and profiles of water quality parameters are used to characterize the lake response to external forcing. It is well recognized that understanding of the mean circulation of a lake is important for many ecological and management issues because it strongly influences the transport pathways and depositional zones of sediments with variations in composition reflecting changes in inputs from different sources. The understanding of lake sediment process (erosion - transportation - accumulation) is a continuing need in Lake Abaya, as it is the major problem threatening the quality of the water body. Excessive deliveries of solids into the lake by rivers and their transport within the lake by currents and waves have environmental, economic and aesthetic impacts.

The prime objective of this study is to understand the dynamics of sediment transport and lake water circulation in the large and shallow natural Lake Abaya using a combination of field and laboratory techniques. It is based on extensive field work (July 2003 - November 2004) to learn about the system behaviour by observing conditions both internal to the system and forces exerted externally on the system. The field investigation component involved experimental arrangement and accomplishment of focused objective surveys of water quality parameters at regular time intervals from fixed monitoring stations and water depths. Surficial

sediment samples were collected throughout the lake from predefined sampling sites. Methodology for laboratory analyses included identification of mineralogical and chemical compositions of lake floor samples and determination of water quality parameters of lake water samples. Additionally, the effect of the spatial variation of atmospheric forcing and its interaction with lake water circulation and the associated transport process is assessed.

Simplified conceptual model for mean water circulation in Lake Abaya is constructed in order to account for the processes reflected in recently observed field data and past records of hydrometeorological variables as well as for those concepts that are most consistent with the measured data and observations.

2 The Study Site

Lake Abaya is part of the Lake Abaya-Lake Chamo basin (Bekele, 2001), located in the southern sector of Ethiopian Main Rift (WoldeGabriel, 2002). It is the second largest lake in Ethiopia and the largest of eight Ethiopian Rift Valley lakes (Figure 2.1). Lake Abaya is elongated in shape and oriented in a north-east-south-west direction, parallel to the main trend of the Main Ethiopian Rift. Recent bathymetry has been published by Bekele (2001), and the basin parameters are shown in Figure 2.2. Lake Abaya is a quasi-endorheic lake-system fed by rivers originating from adjoining highlands in the west and east escarpments (Figure 2.3). It drains ephemerally to the south into the adjoining Lake Chamo by overflow of the separating, ca. 2 km wide sill during high lake levels. The surface of its open water body (excluding the islands) totals ca. 1070 km^2, with a shoreline length of approximately 1000 km.

From morphological perspective, Lake Abaya drainage basin includes two main provinces-uplands consisting of faulted ridges and dissected piedmonts in the west and east escarpments and lowlands in the rift floor (Makin *et al.*, 1975). Climate, hydrology and geology are distinctly different in these two main physiographic provinces. The land surface of the drainage basin generally slopes gently from the edge of the valley floor toward the Lake Abaya in the valley floor from both the eastern and western sides. The distance between the edge of the valley floor and the shoreline is variable, the maximum in the western and eastern sides being about 7 km and 20 km, respectively. The western slopes of the basin, which cover the major part of the drainage basin, are steeper and more rugged than the eastern slopes. The elevation differences of the tips of the rolling hills at both shoulders also vary considerably, reaching up to 2800 m a.s.l. within horizontal distance of 20 km from the shoreline in the west and, up to 2325 m a.s.l. within 15 km from the eastern shoreline.

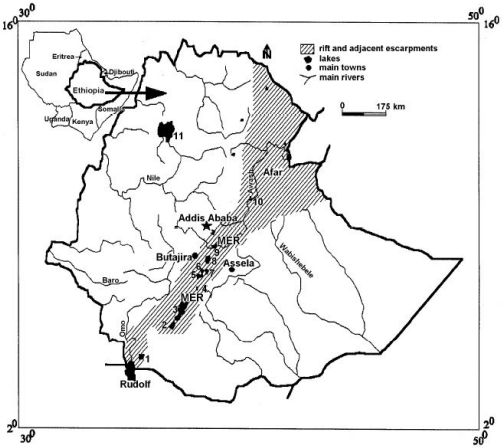

Figure 2.1: Ethiopia and the Ethiopian Rift Valley (hatched signature). In the Main Ethiopian Rift Valley natural lakes are endorheic. Lakes are indicated by numbers: 1:Chew Bahir; 2: Chamo; 3: Abaya; 4: Awassa-Chelelka; 5: Shala; 6: Abiyata; 7: Langano; 8: Ziway; 9: Koka Dam;

Elevation, m	1169
Lake surface area (including islands), km^2	1139.8
Tributary area, km^2	16342.2
Volume, V, km^3	9.82
Mean depth, m	8.6
Maximum depth, m	24.5
Mean width, km	14.1
Maximum width, km	27.1
Shoreline, km	1001*
* Modified from Ethiopian Mapping Agency map of 1979 based on Satellite Image of NASA (2002).	

Figure 2.2: Lake Abaya catchment and basin parameters: Source Bekele (2001)

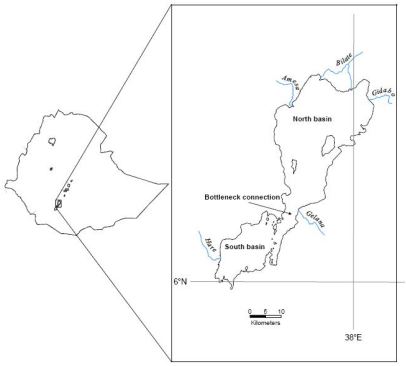

Figure 2.3: Main basins of Lake Abaya and location of main tributaries.

2.1 Climate

The drainage basin of Lake Abaya has a diverse climate, mainly owing to the range in altitude (from 1169 m a.s.l. at lake water surface to 3568 m a.s.l. at Wisha Ridge), and latitude corresponding to the position of the Inter-Tropical Convergence Zone (ITCZ) (Grove *et al.*, 1975; Gemechu, 1977; Bekele, 2001). The broad characteristics of the climate are alternating wet and dry seasons following the annual movement of the ITCZ, which separates the air streams of the northeast and southeast mansoons (Nicholson, 1996; Muchane, 1996). They are determined largely by the convergence of dry north-easterly winds with moist winds of south-easterly or south-westerly origin (Makin *et al.*, 1975; Baxter, 2002). Passage of ITCZ is associated with intensified convective activity within the air column, which usually leads to abundant rainfall (Rozanski *et al.*, 1996). Stations located at the region of maximum southward or northward displacement of ITCZ reveal one rainy period, whereas those stations in the equatorial region experience two rainy periods associated with northward and southward passage of the ITCZ (Rozanski *et al.*, 1996; Muchane 1996). The dry season occurs when the rainfall belts shift south and the area is influenced by dry northeastern trades originating in Arabia and Northeast Africa (Muchane 1996).

The large-scale tropical controls of climate variability in eastern Africa, which include several major convergence zones, are superimposed upon regional factors associated with influences of lakes and topography, resulting in markedly complex climatic patterns that change rapidly over short distances (Nicholson, 1996). As a result, the climatic patterns are markedly complex and change rapidly over quite short distances and altitudes (Grove *et al.*, 1975; Nicholson, 1996).

Rainfall is the most significant climatic factor in tropical Africa, which affects the water resources including replenishing lakes and ground water storages (Balek, 1977). The nature of spatial and temporal variability of precipitation in Lake Abaya drainage basin is examined in detail using the 27 year monthly precipitation database corresponding to 22 stations first described by Bekele (2001). The spatial distribution of the rain gauge stations shown in Figure 2.4 is sparse and heterogeneous. The distance between the rain gauges varies between 11 and 86.4 km, with an average value of 81.5 km. Maximum over all distance between two stations is more than 240 km. The stations are situated in a complex topography with elevations ranging from 1199 to 2840 m *a.s.l.*

Figure 2.4 shows the average annual rainfall measured in the period 1970-1966, according to the data from Bekele (2001). Topographic effects cause substantial variability in mean annual precipitations in the drainage basin. Average annual values for the study period vary from below 800 mm in the vicinity of Lake Abaya to more than 1200 mm along the eastern and western highs, and reach more than 1600 mm along the eastern highs. Mean annual values reveal that precipitation is considerably enhanced by elevation and the rift valley floor posses the lowest annual average precipitation. Highlands flanking the Rift valley intercept most of the monsoonal rainfall in the region, resulting in a strong moisture deficit in the rift valley floor in general and near the lakes in particular (Legesse, *et al.*, 2003; Legesse, *et al.*, 2004).

Recent rainfall variations with elevation in Lake Abaya-Chamo drainage basin have been documented by numerous authors. Relationship of rainfall with altitude is compared using 27 years records 1970-1996 (Bekele, 2001; Theiman and Förch, 2004), and 7 years records 1988-1994 (Krause *et al.*, 2004) at different stations in the drainage basin. Bekele (2001) suggests moderate correlation, whereas Krause *et al.* (2004) provide strong relationship until 2000 m a.s.l. be-

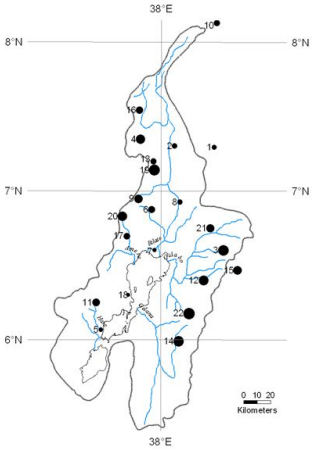

Figure 2.4: Location of Lake Abaya and positions of rain gauge stations: 1, Aje; 2, Alaba Kulito; 3, Aleta Wondo; 4, Angecha; 5, Arba Minch; 6, Bedessa; 7, Bilate Farm; 8, Bilate Tena; 9, Boditi; 10, Butajira; 11, Chencha; 12, Dila; 13, Durame; 14, Fiseha Genet; 15, Hagere Selem; 16, Hosaina; 17, Humbo Tebela; 18, Mirab Abaya; 19, Shone; 20, Sodo; 21, Yirga Alem; 22, Yirga Chefe. Circles correspond to the mean annual precipitation.

tween elevation and rainfall. On the other hand, Theiman and Förch (2004) found that precipitation patterns during the dry seasons of the wet years do not seem to be dependent on altitude at all. Thiemann (2006) found that the average monthly precipitation totals for a period 1970-1996 can be described by an exponential equation for 9 months; for January the equation is linear, while no correlation between elevation and altitude could be detected for October and November.

The pattern of increasing rainfall associated with increasing altitude is modified in the high altitude area by the influence of the high mountains which may cause either rain shadows or areas of heavy orographic rainfall (Makin *et al.*, 1975). In the tropics rainfall variation with elevation is influenced by factors such as water vapour available for condensation and rate of ascent of air (Nieuwolt, 1977; Jackson, 1977; Linacre and Geerts, 1997; Barry and Chorley, 2003). While an

increase in rainfall with height is commonly experienced this does not necessarily continue to the summit of the highlands (Jackson, 1977). Rainfall tends to decrease at places above a kilometre or two up a mountain, after the air has lost water lower down and temperatures of the ascending air have fallen to the extent that little water can be hold as vapour (Linacre and Geerts, 1997). The presence of trade-wind inversion may limit ascent above a certain altitude with resultant decrease in rainfall above it (Nieuwolt, 1977; Jackson, 1977; Barry and Chorley, 2003). A further explanation for the occurrence of maximum precipitation below the extensive highlands in the tropics, where horizontal advection of moisture is often limited, is based on the high instability of many tropical air masses (Nieuwolt, 1977; Barry and Chorley, 2003). Where mountains obstruct the flow of moist tropical air masses, the upwind turbulence may be sufficient to trigger convection, producing a rainfall maximum at low elevations (Barry and Chorley, 2003).

All rain gauge stations considered in the drainage basin show considerable degrees of precipitation seasonality. Traditionally, four seasons are considered in regions where distribution is bimodal: dry period from December-to-February (known as *Bega*), small rain season from March-to-May (known as *Belg*), main rain season from June-to-August (known as *Kiremt*) and transitional period from September-to-November (known as *Tsedey*). The general trend in seasonal precipitation across the drainage basin is shown in Figure 2.5 using arithmetic average monthly rainfall for the nine constituent stations with three stations from each of eastern and western highs and rift valley floor. The means of four seasons for selected stations is also shown in Figure 2.5. Both monthly and seasonal averages variability of the graphs for constituent stations in Figure 2.5 reveals noticeable areal homogeneity.

A bimodal seasonal distribution of rainfall occurs throughout the stations considered, with peaks usually in April-May and July-September. Months of primary peak in the western upland and secondary peak in the valley floor appear to be variable. The annual cycle of rainfall depicted in Figure 2.5 reveals that precipitation is more seasonal in the eastern highlands, with months of maximum main and secondary rains at all stations consistently being in May and October, respectively. The rift valley floor has, on the average, the main rain in *Belg* cen-

tring in May or in *Kiremt* centring in July. In the western highs there is higher monthly average rainfall in the rainy *kiremt* season from June to August, whereas the eastern highs have higher monthly averages during *Belg* season.

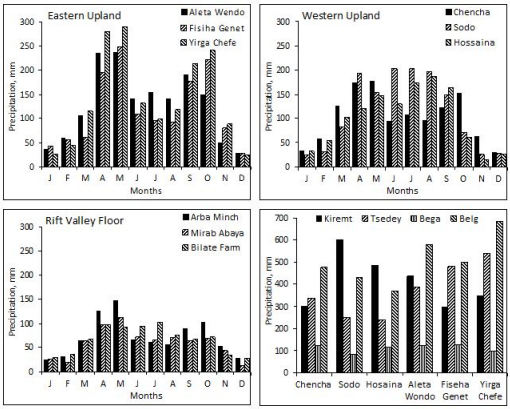

Figure 2.5: Mean precipitation by station location. Right bottom, Seasonal mean precipitation in the western and eastern uplands.

Seasonality of precipitation is further analysed quanititatively using Seasonality Index, SI, which provides a measure of the spread of the monthly rainfall with-respect to an idealy uniform monthly distribution in all 12 months (Celleri *et al.* 2007; Sumner *et al.* 2001). The SI derived by Walsh and Lawler (1980) is given by:

$$\mathrm{SI}_i = \frac{1}{R_i} \sum_{j=1}^{j=12} \left| \mathrm{M}_{ij} - \frac{R_i}{12} \right|$$

Where R_i is the total annual precipitation for the year i under study and M_{ij} is the monthly precipitation for month j. The above expression indicates that *SI* would be zero if the annual rainfall is distributed equally over all 12 months. Near zero values indicate that there is little or no seasonal variation of precipitation, with higher *SI* values representing a greater departure from uniform distribu-

tion through the year (see Figure 2.6). However, Sumner *et al.* (2001) suggest that since such single figure corresponding to each station under investigation does not by itself provide a month-to-month detailed look at seasonal variation, it should be complemented by a detailed analysis of monthly precipitation across an area.

SI	Precipitation regime
<0.19	Precipitation spread throughout the year
0.20–0.39	Precipitation spread throughout the year, but with a definite wet season
0.40–0.59	Rather seasonal with a short dry season
0.60–0.79	Seasonal
0.80–0.99	Markedly seasonal with a long dry season
1.00–1.19	Most precipitation in less that 3 months
>1.20	Extreme seasonality, with almost all precipitation in 1 to 2 months

Figure 2.6: Seasonal precipitation regimes as classified by Seasonality Index (after Walsh and Lawler, 1981)

The long-term mean index for each station can be calculated in two ways (Sumner *et al.*, 2001; Celleri *et al.*, 2007). First, SI_i was computed for all 22 rain gauge sites within Lake Abaya drainage basin for each of 27 years of the data base. The long-term mean, SI_{mean}, for each site was derived by averaging the SI_i values computed for each year of the record over the study period, 27 years in the current study:

$$\mathrm{SI}_{mean} = \frac{1}{27} \sum_{i=1}^{i=27} \mathrm{SI}_i$$

The second alternative index, denoted by SI_a, was computed for each station using mean monthly and annual rainfall data in Equation (1) directly, but the resulting index will possess a lower magniture as a result of smothening by averaging the noise in the year to year distribution of monthly precipitation values (Sumner *et al.*, 2001).

The distribution of wetter periods throughout the year are indicated using the Replicability Index, *RI*, defined by Walsh and Lawler (1981) as:

$$RI = \frac{SI_a}{SI_{mean}}$$

Higher values of Replicability Index indicate that the wettest month of the year generally occurs in only the same few months, resulting a stable long-term intra-annual rainfall distribution. Conversely, a highly variable timing of wet and dry seasons will result in a smaller *RI* index.

The values of SI_{mean} for the period 1970-1996 at rain gauge stations in Lake Abaya drainage basin (Figure 2.7) revealed reduced seasonality of eastern uplands, with higher values in the range 0.52-0.67, when compared to the the rift valley floor and western highs, where indices varying between 0.58 and 0.73. In the rift valley floor, value of SI_{mean} fall below 0.6 only at Bilate Farm, with the precipitation seasonality being reduced in the central areas. Higher values in the western margines of the rift valley floor attributed to the fact that the precipitation is relatively concentrated in two periods separated with marked dry season.

As Sumner *et al.* (2001) pointed out, mean values may mask considerable annual variability in the SI_i. Indices exceeded once or twice 1.0 in individual years within the study period, and have occurred along the western part of the rift valley floor and sholder. In the eastern uplands, the lowest SI_i values recorded for individual years are generally around 0.3 or 0.4, while the highest values exceeded rarely 0.8 only at Yirga Chefe. This indicates that most of the eastern uplands do not experience a marked seasonality even in extreme years, suggesting eastern part of the drainage basin is more reliable year-round water provider. The highest value obtained for individual years is 1.07 (Sodo and Butajira stations) and the lowest is 0.29 in the western upland towards far south (Chencha Station) and around the central area (Bedessa and Boditi stations).

The occurrence of the minimum and maximum values of the indices in Figure 2.7 simultaneously at nearby stations indicates the existance of rainfall subregions. The lowest indices occurred over many parts of the western and eastern uplands during 1989, when they experienced wet year with only one or two dry months (<50 mm monthly rainfall) and little marked variation in precipitation in remaining months. Increased seasonality occurred in some areas in the western uplands during 1973, when >50% of the annual precipitation occurred within 2 or 3 months with 2 or 3 conseccutive months having <50 mm monthly rainfall

Location	Station	SI_a	SI_{mean}	$SI_{minimum}$	Year	$SI_{maximum}$	Year	*RI*
Western Highland	Angacha	0.46	0.61	0.38	1992	0.85	1973	0.76
	Bedessa	0.45	0.60	0.29	1992	0.92	1988	0.76
	Boditi	0.48	0.58	0.29	1989	0.83	1984	0.83
	Chencha	0.39	0.60	0.29	1989	0.80	1970	0.65
	Durame	0.44	0.62	0.41	1976	0.90	1973	0.71
	Hossaina	0.52	0.65	0.41	1989	0.87	1973	0.80
	Humbo Tebela	0.51	0.64	0.45	1989	0.83	1981	0.80
	Shone	0.41	0.58	0.30	1977	0.86	1974	0.70
	Sodo	0.61	0.69	0.32	1989	1.07	1973	0.88
Rift valley floor	Aje	0.51	0.70	0.39	1992	1.04	1984	0.73
	Alaba Kulito	0.42	0.61	0.32	1977	0.89	1981	0.69
	Arba Minch	0.43	0.64	0.34	1978	0.86	1985	0.66
	Bilate Farm	0.35	0.59	0.31	1982	0.85	1981	0.59
	Bilate Tena	0.41	0.60	0.30	1982	0.84	1974	0.69
	Butajira	0.53	0.73	0.49	1977	1.07	1984	0.72
	Mirab Abaya	0.38	0.69	0.45	1980	1.02	1981	0.54
Eastern highland	Aleta Wendo	0.47	0.57	0.39	1989	0.71	1983	0.81
	Dila	0.41	0.55	0.31	1978	0.72	1979	0.74
	Fisiha Genet	0.53	0.62	0.43	1989	0.75	1982	0.85
	Hagere Selam	0.40	0.52	0.35	1972	0.71	1975	0.76
	Yirga Alem	0.44	0.58	0.31	1982	0.77	1989	0.76
	Yirga Chefe	0.56	0.67	0.44	1989	0.90	1980	0.84

Figure 2.7: SI_i mean values and years with extreme SI_i for each rain gauge station.

amount. Overall, the importance of local orography over the large-scale anomalies is implied by the fact that minimum and maximum values of the indices do not occur simultaneously all over the drainage basin as shown in Figure 2.7.

Replicability Index (*RI*) values varied between 0.54 and 0.88, with overall higher values found in the western and eastern uplands and the lower values in the rift valley floor. The smallest value corresponding to the station at Mirab Abaya reflected that every month (with the except of January and February) has been at least once the wettest month of the year. Therefore relatively smaller *RI* values in the rift valley floor represents the characteristics of having a higher flactuation of the timing of the wettest period of the year compared to the surrounding highlands. The highest value corresponding to Sodo station indicates that months with the highest rainfall in individual years are more restiricted consistently to

a few months (between June and August in 18 out of 27 years), resulting fairly stable annual precipitation pattern.

Overall, the above results of seasonality analysis demontrated the complexity of rainfall pattern in the drainage basin. The occurrence of different rainfall patterns over relatively small distances and altitudes in the drainage basin implies that the climate is controlled to a large extent by the regional factors (Nicholson, 1996). As noted by Nieuwolt (1977) for east Africa climate variability, Lake Abaya and Chamo in the valley floor produce huge amounts of water vapour and also create local disturbances conducive to rainfall. Other local factors leading to complex pattern of rainfall include numerous highlands and differences in exposures.

The dry season usually extends between November and February when ITCZ is in the south of Ethiopia, and the northeasterly trade winds traversing Arabia dominate the region (Muchane, 1996; Vallet-Coulomb et al., 2001; Legesse, et al., 2004). Two rainy periods (known as *belg* and *kiremt* rains) are associated with northward and southward passage of the ITCZ, respectively (Rozanski *et al.*, 1996; Muchane, 1996). In general, the main rains in most of the drainage area occur during the period July to October when the ITCZ lies around the north of the country so that the resulting convergence of the wet monsoonal current from the Indian and Atlantic Oceans brings much rain to the region (Malkin, 1975; Vallet-Coulomb *et al.*, 2001; Legesse, *et al.*, 2004). At the same time, low pressure over India and the Arabian Sea dominates airflow and generates strong, persistent southwesterlies to the southern part of Ethiopia. Convective instability, due to the intense heating of the high plateau land, is also a cause of a high percentage of the rainfall (Legesse, *et al.*, 2004). Incursions of the humid, unstable westerly Congo air stream during this time (Niuvoult, 1971, Nicholson, 1996) bring high rainfall over the western part of the drainage basin. Lesser rainfall in the western highlands and main rainfall in the eastern highlands in the *belg* season coincide with a decrease of the Arabian high as it moves towards the Indian Ocean causing warm, moist air with a southerly component to flow over the southeastern half of the country (Vallet-Coulomb *et al.*, 2001; Legesse, *et al.*, 2004).

Rainfall intensity is the most important parameter for the investigation and prediction of flood generation and soil erosion (Merz *et al.*, 2006). However, rain-

fall intensity information at high temporal resolution is scarce in Lake Abaya drainage basin due to absence of recording rain gauges. The high-resolution (0.1 mm/impulse) recording rain gauge at Wajifo Weather Station established for this study measured maximum 1 minute rainfall amount of 9.3 mm (equivalent to 588 mm hr^{-1}) on 3 September 2004. The maximum 5 and 10 minutes intensities observed at this station were 176.4 and 94.2 mm hr^{-1}, respectively, during the period March 2004 - February 2005. The highest 1 hr measurement observed at this station was 23.7 mm 0n 7 April 2004.

Annual rainfall recorded at Wajifo Weather Station during March 2004-February 2005 was about 815 mm (Figure 2.8). One main rainy month (April with >200 mm) enclosed by pronounced dry months (March and May each with <25 mm). June to October and November to December were fairly rainy months, each with >55 mm. Close examination of continuous records reveals that the most intense 3 hour storm with a total of 60 mm form 30% of the monthly total precipitation in April 2004. About 40% of the annual rainfall emerged from June through September. These evidences illustrate that in the tropics a high proportion of annual rainfall is concentrated into a relatively small number of days (Makin *et al.*, 1975; Balek, 1977).

Examination of rainfall events on a daily base further shows that 83 rainy days (i.e. days with rainfall amount of 1mm or more) measured annually (from March 2004 - February 2005). These rainy days mostly measured between 1 and 10 mm (about 65 percent of all the rainy days). In terms or rainfall amounts, these days contribute about 23 percent of the total annual rainfall. The frequency distribution of daily rainfall is highly skewed to the left showing that low-magnitude rainfall is much more frequent that high-magnitude rainfall. Days of more than 25 mm account for only 6 percent of the rainy days with a maximum of 66.2 mm measured on 13 April 2004.

Diurnal variation of rainfall indicates that most of the rainfall occurs from 1800 to 0600 hr local standard time (LST). About 72 percent of the annual rainfall from March 2003 to February 2004 occurred during the night, in particular early in the morning between midnight and 0600 LST. This suggests that the nocturnal-early morning rain type did appear to predominate, which confirms the costal type diurnal rainfall regime in the tropics (Nieuwolt, 1977; Reihl, 1979).

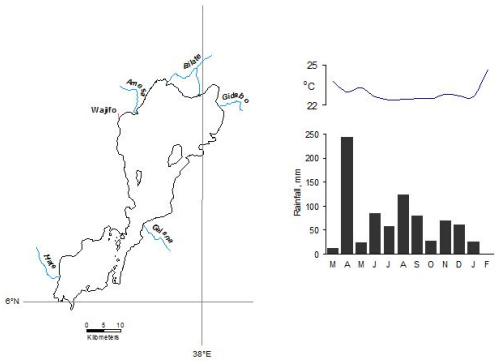

Figure 2.8: Left: Location map; Right: monthly rainfall and average air temperature at Wajifo.

In the tropics, the character of rainfall in a particular month (e.g. intensity, duration, frequency) and the elements of atmosphere-soil-plant system determining the effectiveness of the rainfall in relation to evaporative demand make it impossible to strictly define a 'wet' month (Jackson, 1977). Next to rainfall, evaporation and evapotransportation, both under the influence of sunshine, are the most significant phenomena in the hydrological cycle (Balek, 1977; Jackson, 1977). In the lowlands of the Lake Abaya drainage basin temperature and water losses are high and rainfall amounts are low (Gemechu, 1977). Because evapotranspiration exceeds the rainfall in the Ethiopian Rift Valley area, the closed drainage basins may suffer seasonal or annual water deficits (Todorancea and Taylor, 2002). The humid and rugged conditions in the highlands, from which the streams flow, encourage rapid runoff, low retention in soil layers and soil erosion (Gemechu, 1977).

2.2 Hydrology

Lake Abaya receives water from precipitation on the lake as well as tributaries around it. The arrangement of rift segments affects the location, pattern and flow

direction of major drainage system (Wescott, *et al.*, 1996). The major rivers rise from the plateau on either side of the rift and follow in a radial manner into the lake. The north basin has four main inflows, which have their sources in the Ethiopian highlands. The south basin has only the Hare River as larger inflow, with its headwater area in the Western Ethiopian Highlands. All rivers are perennial in their upper reaches, and have the character of allochtonous rivers at the graben floor. Yet most of the runoff is captured during dry season for irrigation in the lowland areas around the lake (Bekele, 2001; WoldeGabriel, 2002). Lake Abaya lacks a direct surface outlet and drains down to Lake Chamo by overflowing the sill in its south end (Schütt *et al.*, 2005).

The catchment area of the gauged main tributaries varies between 199 and 5224 km^2 (Schütt *et al.*, 2005; Bekele, 2001). Bilate River, which has the largest catchment area among the main rivers, rises 100 km south of Addis Ababa and flows south between the headwaters of the Omo River to the west and the central Main Ethiopian Rift lakes to the east (Grove, 1975; Bekele, 2001; Schütt *et al.*, 2005). Runoff of the major rivers is unregulated. They receive water from several tributaries on their way to Lake Abaya. Next to these major tributaries numerous first and second order streams, mainly torrential, enter into the lake. Most of these river courses can be characterized upstream as straight and with high velocity-steep gradient runs, and downstream as flood plains with braided systems. The bulk of the infill material accumulated in large fans at the rift floor is of high pore volume and, thus, serves as an important near-surface groundwater storage (Makin *et al.*, 1975; Grove, 1986).

Freshwater discharge into the south basin contributes only small amount compared to the total input in the north basin. Volumetric records at gauged main tributaries (1970-2003) show that Bilate River, mouthing in the north end of the lake basin, provided the largest (38%) of the mean annual total inflow, while the Hare River, the largest tributary of the south basin, provided only 9% of the mean annual total inflow (Figure 2.9b). An overwhelming majority of its mean annual water supply is provided by surface runoff from the major tributaries Amesa, Bilate, Gidabo, and Gelana in the north basin (Figure 2.9a). Moreover, except during flooding Hare River flow is basically intercepted for irrigation and inflow to the lake is virtually zero. In general, it is assumed that there is flow from the north basin to the south basin through the bottle neck, regulated and triggered by

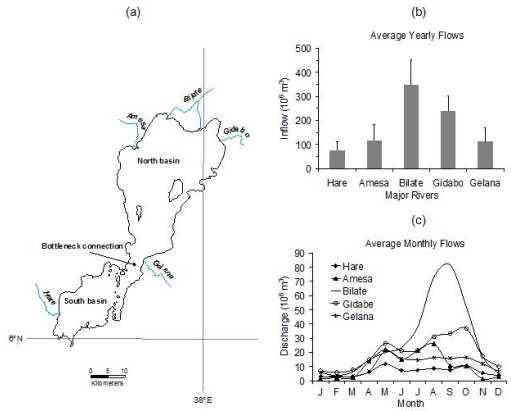

Figure 2.9: Location map of major tributaries around Lake Abaya (a), and their yearly average (+s.d.) (b) and monthly average (c) inflows. Data Source: Ministry of Water Resources.

the inflow of the northern basin tributaries to satisfy continuity requirement.

Averages of monthly stream flow volumes of 34 year records are generally highest in the rainy months and decline during months with small or little rainfall in the drainage basin (compare with Figure 2.5). There is a clear variation in the seasonality of major rivers flow, which is demonstrated in Figure 2.9(c) using mean monthly flows for the period 1970-2003. While Figure 2.9(c) highlights months which have experienced large events, it should be remembered that the periods of record from the main rivers do not strictly overlap. Minimum stream flows occur from January to March, and begin increasing slowly in March in response to first rainy season (*belg*), with minor peak in May and annual peak between August and October resulting from direct runoff during the main rainy season for rivers draining from the north. On the contrary, rivers draining from southern drainage basin have main pick in May due to the greater intensity of the *belg* rain season and secondary peak in October as a result of general lack of or small rain between June and August. Discharge in the south is relatively stable

from June to October, and overall declines quickly from October onwards.

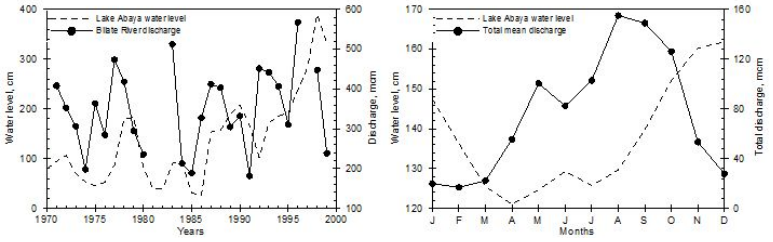

Figure 2.10: Interannual evolution and monthly distribution of lake water level at Arba Minch Station and discharge of Bilate River at Alaba Kuluto Station. Mean monthly distribution of discharge correspond to the sum of major tributaries.

The lake levels over time (1970-1999) are shown in Figure 2.10 and can be compared with the largest tributary Bilate River flow recorded at Alaba Kulito gauge station. However, according to Schuett and Thiemann (2004), who studied modern water level and sediment accumulation changes of Lake Abaya, a direct interrelation between inflow from tributaries and lake-level changes can not be stated mainly due to interception of flow downstream for increased irrigation demand and other purposes over recent years. Schuett and Thiemann (2004) further suggest that continuous increase of lake-level in the recent past could be attributed to increased sediment input due to land use changes and neo-tectonism due to location of the lake in the most active tectonic zone. Some changes in lake levels in the Ethiopian rift are possibly due to the formation and/or reactivation of rift faults (Yalew, 2004).

During 30 years period (1970-1999), the available data show that the lake have undergone water level variations of more than 4 m in amplitude. The large proportion of rainfall and evaporation in the balances of the African lakes makes their levels particularly sensitive to climate change (Spigel and Coulter, 1996). Plots of mean monthly lake level records near Arba Minch and total inflow of major tributaries (Figure 2.10) demonstrated their seasonality. The sum of mean monthly inflow of major tributaries showed seasonal input with annual maximum in August and secondary peak in May, whereas the monthly distribution of mean

lake level is found to have its respective maxima in December and June. Seasonal influences on the East African lakes are dominated by the annual cycle of monsoon winds and the accompanying changes in air temperature and humidity (Spigel and Coulter, 1996).

The beginnings of increase in lake level at Arba Minch station situated near the south end of the lake during primary and secondary rainy seasons lag by one and two months, respectively, the start of total inflow to rise. This onset of lake water lever rise at the south end earlier after beginning of increase in total mean inflow suggests that stronger lake water circulation prevailing during main rainy season distributes faster the freshwater and sediment input by major tributaries principally from the north basin. Put another way, the average strength of circulation during the main rainy season (*kiremt*) is about twice the average speed of lake water currents prevailing in the *belg* season.

2.3 Lake Water Quality

The water of Lake Abaya is characterized as alkaline - saline with dominant ions of sodium, bicarbonate and chloride, and smaller concentrations of potassium, calcium and magnesium among cations and suphate and fluoride among anions (Kebede *et al.*, 1994; Baxter, 2002; Teklemariam, 2005). It is found to be the most concentrated water of the lakes in the country having outlets, perhaps because its discharge into Lake Chamo is only intermittent (Baxter, 2002). Concentration of fluoride is high enough to induce fluorosis with mottling of the teeth in the inhabitants in Gidicho Island in the northern basin and around the lake.

The transparency of the lake water is very low as the Secchi disc readings show (Kebede *et al.*, 1994). Light attenuation in these lakes appears to be mostly due to suspended inorganic material (Baxter, 2002). The lake water is of a reddish colour due to very stable suspension of colloidal ferric oxide particles in the water column, which are introduced by most of the tributaries and distributed all over the whole water body (Schröder, 1984). This is documented by the fact that the concentration of Iron is found to be quite high (10 mg/l) (Baxter, 2002). The electrolyte concentration of the water seems to be critical in maintaining the stability of this suspension (Wood *et al.*, 1978).

Comparison of data on salinity of Lake Abaya over years showed marked increases between the 1930s and the early 1960s (Wood and Talling, 1988; Baxter, 2002), and it falls until 1980, after which there is a rapid increase in salinity and later evening out to a gradual increase.(Teklemariam, 2005). The former trend may suggest that the lake received saline flows and lies in an area of intense heat and consequently a high rate of evaporation. For example, Bilate River receives saline springs in its lower reaches and this contributes to the salinity of Lake Abaya (Makin *et al.*, 1975). Evaporation, which is considered as a major component of tropical African lakes water balance, played an important role in giving the unique hydrogeochemical signature of most of the lakes (Vallet-Coulomb *et al.*, 2001; Alemayehu *et al.*, 2006).The later phenomenon may be correlated with the decrease in water level of Lake Abaya in the period 1980 - 1989 mainly caused by a meteorological drought phase leading to reduced peaks and volumes in precipitation (Teklemariam, 2005). Generally, water input-output relationships are the dominant feature of the status of the salinity series of the rift lakes (Wood and Talling, 1988). If accompanied by a maintained lake level or volume and negligible seepage-out, evaporation loss can balance inflow plus direct rainfall; thus, with time, the lake becomes more saline (Alemayehu *et al.*, 2006).

Overall, the present day hydrochemistry of the rift lakes is the result of long-term hydrogeochemical evolution of the lacustrine system and the flux of coming and going out of the lakes through the Quartnary sediments (Teklemariam, 2005; Alemayehu *et al.*, 2006). These lakes accumulated solutes from inflowing rivers, rainfall and groundwater sources. Subsequent evaporative concentration (especially in closed terminal lakes) has led to the precipitation of certain minerals and concentration of others. This profoundly affected the composition of the remaining water (Alemayehu *et al.*, 2006). The source of the present day composition of the terminal lake waters is, therefore, particularity difficult to interpret on the basis of present day inflow and outflow conditions alone (Alemayehu *et al.*, 2006).

2.4 Geology

Lake Abaya lies in the main graben of the Ethiopian Rift System, which consists of three major rift zones with distinct volcanic and tectonic characteristics

that are at different stages of rifting: the broadly rifted zone of south western Ethiopia, the Main Ethiopian Rift (MER) of central Ethiopia, and the Afar Rift System (WoldeGabriel, 2002). Lake Abaya, which is situated in the southern segment of the Main Ethiopian Rift, is one of the numerous fresh and saline lakes in the central sector of the Ethiopian rift that form hydrogeologically a unique system within the rift due to the underground interconnection by NE-SW aligned regional faults (Alemayehu *et al.*, 2006).

Volcanism and tectonism have been major controls on the development of lakes and drainage pattern in the East African Rift System (Wescott *et al.*, 1996). Volcanism started in the southern and central sectors of the MER as early as in Eocene time with important basaltic eruptions, associated with an early stage of rifting characterized by uplift and faulting (WoldeGabriel, 1990; Ebinger *et al.*, 1993). From Late Oligocene to Early Miocene times, the first major phases of rifting within the MER resulted in a series of asymmetric half-grabens with alternating polarity (Le Turdu *et al.*, 1999). The volcanic products in many places were fissural basaltic lava flows, stacked one over the other, alternating with volcano-clastic deposites derived from tuff, ignimbrite, and volcanic ash (Alemayehu *et al.*, 2006).

Volcanic and tectonic activities that were responsible for the formation of volcanic plateau, uplift, eastern and western faulted margins of the MER, and development of rift basins began in the middle to late Miocene (Grove, 1986; WoldeGabriel *et al.*, 2000). Then, evolution from alternating half-grabens to full symmetrical graben occurred, and low angle volcanic piles were built up both at the margins of the rift floor and within it in the late Miocene and Pliocene (Grove, 1986; Le Turdu *et al.*, 1999). Smaller volcanoes within the rift, active until a few centuries ago, are now dormant or emit only steam (Grove *et al.*, 1975; Ayalew, 2004). A widespread thermal activity mainly characterized by hot sprints, fumaroles and altered grounds exists on the northwest shore of Lake Abaya (Grove *et al.*, 1975; Teklemariam and Beyene, 2005).

The opposing stepped fault zones forming the margins of the rift and spaced not more than 32 km apart (Jackson, 1971) cut across plateau lavas, tuffs, and ignimbrites of Tertiary age (Grove *et al.*, 1975). Both escarpments expose crystalline basement, sandstone of unknown age, and thick sections of Eocene to late

Miocene mafic and silicic lavas and tephra (Ebinger *et al.*, 1993). Northwards along the rift floor and east of Sodo, the Bilate River and its tributaries expose Pleistocene fluvial and lacustrine sediments interbedded with basaltic lavas and ash flows and fallout (Wolde, Gabriel *et al.*, 2000). Sediments and tephra mostly cover the rift floor east of the Bilate River (Wolde, Gabriel, 2002). The Abaya (Ganjuli) basin is separated from the Chamo basin to the south by Tosa Shucha (Bridge of God), which is a chain of eruptive volcanic centres that crosses the rift valley (Ebinger *et al.*, 1993). The simplified geological map of the southern sector of Ethiopian Rift System that includes the main drainage basin of Lake Abaya is shown in Figure 2.11.

While the primary control on the origin of the lake is the faulting due to rift formation, difference in the length and offset of the normal faults will determine the original morphology of the troughs (Yuretich, 1982). On the rift floor, topographic barriers created by lava flows, uplift, and faulting created basins and lakes that act as a sediment trap (Grove, 1986; WoldeGabriel *et al.*, 2000). The bulk of the infill consists of material of volcanic origin, much of it airfall pumice and ash derived directly from eruptions, the rest transported by rivers (Grove, 1986). The most recent deposits around the lake and along the river valleys are alluvial fans and landslides (Makin *et al.*, 1975; Halcrew and Patrners, 1992).

2.5 Present Day Morphodynamics

Rivers draining through steep and severely gullied volcanic slopes to the rift floor bringing in heavy loads of fine detritus into the lake as it can be seen from the reddish-brown colour of the lake water (Grove *et al.*, 1975; Schröder, 1984; Schütt *et al.*, 2005). The abundance of easily-weathered volcanic material forming structurally weak topsoil that is highly prone to erosion contributes to the high rate of suspension load of the tributaries and sedimentation in the lake basin (Yuretich, 1982; Halcrow and Partners, 1992). Furthermore, dramatic population growth since the 1970s and clearing of forests and bush lands as a consequence, changes in land ownership and cultivation manners have induced increasing soil erosion processes, even aggravating erosion processes (Grove *et al.*, 1975; Schütt and Thiemann, 2004; Schütt *et al.*, 2005; Hurni *et al.*, 2005). Soils are potentially most erodible during rainy seasons before significant crop cover exists. Major

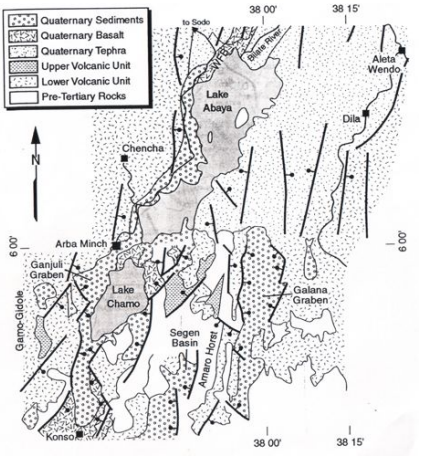

Figure 2.11: Geological map of southern sector of Ethiopian Rift Valley and adjacent plateau (WoldeGabriel, 2002).

part of rainfalls occur usually prior to significant crop cover - any leaf growth that has started was insufficient to shelter soils from raindrop impacts - thus, soils are highly susceptible to erosion. The scale of erosion is devastating in Bilate basin, north of Hasaina, north of Lake Abaya and between Dilla and Lake Abaya, with large expanses of land being lost each year (Halcrow and Partners, 1992). As a result, soil erosion and sediment loading to streams are concerns in Lake Abaya drainage basin.

Soil types in the drainage basin are closely related to parent material and degree of weathering; weathering has generally predominated over leaching and the presence of distinct layers within the soil profile is rare (Makin *et al.*, 1975; King and Birchall, 1975). The main parent materials are basalt, ignimbrite, lava, gneiss, volcanic ash and pumice, and riverine and lacustrine alluvium (Makin *et al.*, 1975). Much of the highland area frigging the Southern Rift Valley is characterized by deep reddish clay loams or clays developed from weathered basalt, where as the lowlands, including fans, deltas and floodplains around Lake

Abaya, are characterized by soils formed on materials recently deposited by rivers (Makin *et al.*, 1975). Lacustrine deposits include bedded pumice, siltstone, sandstone and tuff (King and Birchall, 1975). On the plateau, above 2000 m, the basalt, tuff and ignimbrite with additional volcanic ash give rise to soils with high silt and clay contents (Makin, *et al.*, 1975).

Short sediment cores taken from the deltas of Bilate and Gidabo rivers in the north basin posses mainly soft and poorly consolidated clay size fraction deposits of 30-70 cm depth overlaid highly compacted sandy deposits (Schütt and Thiemann, 2004; Schütt *et al.*, 2005). Very fine laminations are typical for most samples collected from both deltas. This suggests that the sediments of Lake Abaya are laminated despite the fact that the shallow depth is subject to continuous wind-driven wave action. In other words, laminations are preserved because sedimentation rate is too fast to allow complete reworking by wind-driven wave action.

Quartz is the dominant mineral in the Bilate delta, but its concentration varies between minor to major at Gidabo delta. Organic carbon concentration is generally very low. Its distribution at Bilate delta shows uneven oscillation with depth yet generally decreases within 10 cm from the top. Samples from Gidabo delta have higher concentration of organic carbon, and showed similar variations with depth and sampling locations (i.e., at the centre and near margin of the delta). High concentration of clay minerals in the most recent delta deposits of the major rivers point out soil erosion process due to human impact in the drainage basins (Schütt *et al.*, 2005).

The paucity of organic carbon is a reflection of both the high rate of detrital sedimentation and the well mixed oxidizing environment of the overlying water mass (Yiretich, 1979). Since organic matter in natural waters in present in different forms, in suspended living and organic detritus, in true solution, and in colloidal solutions, variations in organic carbon content with depth is attributed to the efficiency of decomposition in relation to supply from different forms (Schütt *et al.*, 2005; Bordovskiy, 1965a, 1965b). Calcites, which are the only carbonate found in the lacustrine sediments from Lake Abaya, originated from organisms or evaporation respectively as the occurrence of limestone in the drainage basin is unknown (Schütt *et al.*, 2005).

2.6 Land Use and Land Cover

Agriculture is the predominant land use throughout Lake Abaya drainage basin. High percentage of land is devoted to farming except steep rocky hillsides, where the preserved natural vegetation cover has been suffering from clearance by cutting and burning (Makin *et al.*, 1975; Grove, *et al.*, 1975). The strong altitudinal gradient is reflected a rapid ecological change from *qolla* growing below 1500 m a.s.l., through *woina dega* growing between 1500-2500 m a.s.l to *dega* growing above 2500 m a.s.l. This strong altitudinal dependency of plant growth ensures that plant growth conditions are extremely varied within a small area (Jackson, 1971). The land use system in the highlands is dominated by small-scale subsistence agriculture that integrates livestock, mainly small stock (Thiemann, 2006). South of Hosaina to Sodo, west of Bilate River, and in the Gamo Highlands, the plateau of rolling hills and isolated green valleys is charaterized by groves of *enset edulis* clustered around each compound (Jackson, 1971; Halcrow and Partners, 1992). East of the Bilate River, intensive maize production grades into open grassland, shrubland and woodland (Halcrow and Partners, 1992).

The lowlands, receiving less than 500 mm of annual rainfall, are thinly populated and devoted to cattle-rearing except where highland rivers debouch on the plains surrounding Lake Abaya (Jackson, 1971). Here open and dense bushland occurs mixed with banana, sweet potatoes, maize, dryland cotton and sorghum, grown on fan deposits and often irrigated applying simple techniques (Jackson, 1971; Halcrow and Partners, 1992; Assefa, 2001). Use of tributary rivers for Irrigation has been fairly practiced for private and state owned farms in the lowland around the lake (Bekele, 2001). The valley floor north of Lake Abaya is characterized by open and dense bushland (Jackson, 1971; Halcrow and Partners, 1992). Towards the eastern divide as the land rises, intensively cultivated arable farm land occurs, with coffee, fruits and enset been cultivated merges with disturbed upland forest.

The vegetation varies from open Acacia woodland in the neighbourhood of the lakes, now extensively overgrazed, with tall forest trees on the shoulders of the rift, to large areas of grassland on the plateaus between 2000 and 2500 m, and heaths, tussock grass and tropical alpine vegetation on the high mountains (Grove, *et al.*, 1975; Woldu and Tadesse, 1990; Valett-Coulomb *et al.*, 2001). Lake shores partly carry a dense vegetation of the shrubs (*Aeschynomene elaphraxy-*

lon), a light wood of which floats and used to make transport boats (locally known as "hogolo") (Schröder, 1984). In the flooded zones spreads a more or less broad reed belt of *Typha*, *Phragnites*, *Juncus* and *Scirpus*, which merges into the community of submerged vegetation of *Potamogeton pectinatus*, *P.nodosus* and *Ceratophyllum* (Schröder, 1984). Overall, forest represents a rather insignificant and declining proportion of the drainage area (Makin *et al.*, 1975).

3 Water circulation and sediment dynamics of large shallow lakes

Investigations to understand dynamics of lakes are all about seeking answers to basic questions such as (Bennett, 1974):

(i) What are the general patterns of large scale currents under different types of wind forcing?

(ii) What is the relative importance of physical factors such as geometry, friction, and waves in determining the current patterns?

Over more than a century attempts have been made to answer these and related questions by using both current measurements and theoretical analysis to explain observations. Theoretical studies (e.g. Rao, 1967; Csanady 1997; Koçyiğit and Koçyiğit, 2004) applying various simplifications have been supported with observations to reveal fundamental physics and significance of different factors. Water current measurements to derive resulting circulation patterns have been split in two distinct groups of either the drift bottle, drift card, or other type of surface water drift measurement, or measurement with fixed current meter on the other hand (Beletsky *et al.*, 1999). The former method, where the trajectories of moving tracer objects are used, is known as Lagrangian approach, while the later method, where time series of observations at fixed points are considered, is known as Eulerian approach.

Theoretical investigations to explain quantitatively the observational evidences employ assumptions either to simplify mathematical formulation or to isolate only a few of the physical factors and processes to identify their significance. Since the basic physics applies equally well to inland water bodies as well as to the continental shelf regions of the oceans, revision of theoretical studies and

experimental results from different types will allow to draw some general conclusions about lake circulation patterns with varying environmental settings. It is therefore natural to begin with revising developed theories.

Much of the review materials in this chapter refer to numerous theoretical models and extensive works about circulation and mixing that have been published on the physical limnology of the North American Great Lakes. Spegel and Coulter (1996) note that significance differences in climate, latitude and basin shape make the direct application of some of the results to the East African Lakes questionable. For example, although the strength of density stratification in both tropical and temperate lakes is sufficient enough to influence water movements, the annual cycles of temperature stratification and prevailing wind over the tropical lakes follow important differences from temperate lakes. Nevertheless, the basic physics applies equally well to different types of lakes as well as to the coastal shelf regions of the oceans (e.g. Bennett, 1974). It is therefore felt that comparisons of developed models and observation results for lake basins with identical physical setup do provide both a framework for explanation of observations in the current study and develop working hypotheses to help organize further investigations.

3.1 Dynamics of Winds in the Coastal Regions

The relative importance of the various relevant physical factors in determining the character of each type of wind classified according to dynamical principles is discussed by Jefferys (1922). He noted that not all of the forces due to the rotation of the Earth, friction and gravity are equally important under all circumstances. The large-scale upper layer air motion, corresponding to the geostrophic wind, is generated mainly by the balance between pressure gradient and Coriolis forces due to earth's rotation and flows nearly parallel to the isobars with velocities proportional to the pressure gradient force. The effect of friction, which is always opposite to the direction of the air motion and therefore tends to decrease the wind speed, cannot be neglected near the surface of the earth.

When the pressure difference between places at the same level is mainly occupied in overcoming friction, the resulting wind is called antitriptic wind. The

Eulerian winds are characterized by accelerated motion of each particle of air due to the horizontal pressure gradient. The small-scale phenomena, which include all atmospheric disturbances whose horizontal dimensions in at least one direction are of the order of kilometres or tens of kilometres, embrace tropical cyclones, tornados, land and sea breezes and mountain and valley winds (Fleagle, 1950; Gleeson, 1953). Jefferys' analysis shows that tropical cyclones and tornados are Eulerian winds, whereas mountain and valley winds and sea and land breeze winds are mainly antitriptic.

The land and sea breeze circulation is one of the interesting mesoscale atmospheric phenomena occurring in coastal regions during periods of clear weather. A great deal of very detailed information from theoretical investigations and studies of observational evidences has come to light on land and sea breeze since the late 1940's (e.g., Haurwitz, 1947; Schmidt, 1947; Johnson and O'Brien, 1973; Arritt, 1993; Laird and Kristovich, 2001). In general, the occurrence of the land and sea breezes is due to the temperature difference between the air over land and that over water in the course of the day. This means that the phenomenon can be observed in its purest form when there is no general pressure gradient causing an offshore or an onshore wind, for in this case all air motions perpendicular to the coastline are due to the unequal heating mentioned above (Schmidt, 1947). On the other hand, if the winds connected to the large scale weather situation are strongly developed, their influence may overshadow that of the temperature difference (Haurwitz, 1947; Leopold, 1949; Estoque, 1962; Frizzola and Fisher, 1963; Johnson and O'Brien, 1973).

Diurnal variation of onshore wind in a costal area depends on the distance from the shoreline (Yu and Wagner, 1970; Crawford and Hudson, 1973; Johonson and O'Brien, 1973). A distinct wind maximum near shore follows the sea breeze front inland. The sea breeze can be classified as a gravity current (or density current) whose formation often intensifies during the early afternoon when the density difference between the land and sea air becomes large (Buckley and Kurzeja, 1997). The maximum sea breeze intensity occurs before the temperature difference between the air over land and over water has decreased to zero because of the effect of friction (Haurwitz, 1947; Weber 1979). Positive temperature difference is required to overcome the frictional force. As soon as the temperature

difference has fallen below this critical value, the sea breeze starts to slow down. The stronger the friction, the larger is the critical value of the temperature difference necessary to maintain a sea breeze and, consequently, the shorter is the time between the maximum temperature difference and the maximum speed of the sea-breeze circulation. Stagnation point represents equilibrium due to balance between heating of the air column from below and advection of cold air from over the water (Staley, 1957). Another factor of possible significance for stagnation was the inertial oscillation associated with abrupt change at sunrise or sunset of the frictional force to a new relatively constant value.

The veering of the land and sea breeze in extratropical latitudes is due to the deflecting force of the earth's rotation (Schmidt, 1947; Haurwitz, 1947). In tropics, the sea and land breezes change direction when the general wind meets at an angle (Garbel, 1947). The resultant wind gradually changes direction during the day as the sea breeze component varies. Topographical constraints, such as irregular shoreline and the presence of mountains, result in non-uniform rate of turning of the direction of the sea and land breezes over the diurnal cycle (Frenzel, 1962; Alpert *et al.*, 1984; Kusuda and Alpert, 1983; Balling and Sutherland, 1988; Simpson, 1996).

Leopold (1949) described the interaction of trade wind and the sea breeze in Hawaii and the flow of air over the mountain masses of various shapes and sizes. He suggested that the interactions depend primarily on three factors:

1. the breadth of the area on which the heating and cooling will occur to cause the land and sea breeze, and which presumably governs the strength of the breezes so developed;

2. the height and shape of the mountain range which, in relation to the subsidence temperature inversion, will determine whether the trade wind will rise over the top or tend to split into two currents, passing one on either side; and

3. the aspect of the area on which the sea-land wind regime develops (exposure windward or leeward with respect to the trade wind).

With respect to the sea breeze over an area with irregular topography, its circulation is closely related in both theory and observation to other local winds resulting

from differential heating, since the same forces are of importance (Fleagle, 1950; Gleeson, 1953; Stalely, 1957). The local topography is most important to air flow at individual locations. The land may contain valley or slope upward from the sea, causing the sea breeze to combine with other local winds such as air drainage and valley winds (Staley, 1957; Frenzel, 1962; Balling, 1988). Narrow valleys cause funnelling and greater variation in direction observed where the valley is relatively wide (Frenzel, 1962; Lemmin and Adamo, 1996).

The effects of various types of prevailing large-scale winds and thermal stratification on the development of the sea breeze circulation in straight costal regions are such that offshore prevailing geostrophic winds developed stronger sea breeze than onshore geostrophic winds (Estoque, 1962). Onshore large-scale flow produces weaker sea-breeze perturbations compared to those generated by an offshore flow (Zhong and Takle, 1992). This difference is due to development of strong pressure gradient as a result of the strong temperature gradient produced by advection of warm air over land towards the sea by offshore large-scale wind. On the other hand, the advection of cold air over sea towards over land inhibits the rise in temperature of the atmosphere over land. Consequently, the horizontal pressure gradient is weaker and a weaker circulation is developed.

A further effect of large-scale background winds on the characteristic of the sea-breeze circulations is that an onshore synoptic wind causes an earlier onset of the sea breeze, but delays the onset of land breeze, and a strong onshore flow of more than 5ms-1 does not allow the land breeze to develop at all (Zhong and Takle, 1993). The maximum offshore wind speed and vertical motion at night are less sensitive to the magnitude of surface cooling than to the large-scale flow and daytime surface heating, which together determine the initial flow at the beginning of the land-breeze phase. In addition, the magnitude, the sense of rotation, and the diurnal variation of the dominant forces governing the wind-vector rotation change as the orientation of the synoptic wind direction changes (Fisher, 1960; Neumann, 1977). The rate of rotation in the sea-breeze phase is dominated mainly by the balance between the mesoscale pressure gradient and friction; at night, the Coriolis effect also contributes significantly to the balance of forces in the land-breeze phase further away from tropics.

Examination of the characteristic features of sea breeze encompassing a broad

range of onshore and offshore synoptic winds revealed that onshore synoptic flow of only a few meters per second was sufficient to suppress the thermally induced circulation, whereas for offshore synoptic flow as strong as 11 ms^{-1}, the circulation was still apparent (Arritt, 1993). Thus, a sea breeze circulation can exist entirely offshore, if the opposing flow is strong. The gradient wind is such that any land-breeze effect is only to reduce the night-time velocity but not to reverse the direction (Frenzel, 1962) Alongshore large-scale wind with low pressure over the sea produces the seaward frictional inflow in the lowest layers strengthens the horizontal pressure gradient in the same way as that produced by an offshore prevailing geostrophic wind (Estoque, 1962).

The most prominent feature of the general circulation occupying the lower levels in a vast area around the equator, broadly between 30°S and 30°N, is the trade winds that converge into the doldrums while being deflected westward (Petterssen, 1969; Nieuwolt, 1977; Riehl, 1979; Barry and Chorley, 2003). Trade winds, which originate at low latitudes on the margins of the subtropical high pressure cells, are strong and fairly steady (Petterssen, 1969; Riehl, 1979). Thus, the two general wind systems prevailing in the East Africa are the Northeast and Southeast Trade Winds (Bugenyi and Magumba, 1996; Barry and Chorley, 2003). The southeast and northeast trade winds prevail during the high and low sun seasons, respectively, and the associated oscillation of Inter Tropical Convergence Zone (ITCZ) north and south in an annual cycle (Nicholson, 1996; Barry and Chorley, 2003). For example, ITCZ is situated in January at about 15°S and most of the East Africa is under the influence of northeasterly winds, whereas in July the ITCZ is about 15°N and over East Africa southeasterly winds prevail (Nieuwolt, 1977).

Although the land and lake breeze regimes with a clear diurnal cycle in the tropics takes a course similar to that of higher latitude in summer, they generally show their most regular occurrence and strongest development in the tropics - as the heating of the tropical air over land can be up to five times that over adjacent water surfaces (Nieuwolt, 1977; Rierl, 1979; Nicholson, 1996; Barry and Chorley, 2003).

By way of summary, the dynamics of winds at coastal regions is a combined result of the passage of large scale pressure cells and small scale local winds.

The land-sea breeze, the generation of motion by differential heating in coastal regions, is one of the most fundamental atmospheric processes. Interactions with other local wind systems and large-scale synoptic flow as well as physiographic characteristics may cause it to differ considerably from place to place. Thus, since the sea breeze is strongly affected by terrain, coast line shape, sea surface temperature, land temperature, and many other factors associated with the particular locale where the observations are made, it is felt that an many series of observations should be attempted at different locations in order to determine more accurately how much variation one might expect in the characteristics of the sea breeze from region to region.

3.2 Response of Lakes to Wind Stress Forcing

Work done by wind stress on a water surface generates turbulence that causes mixing in the surface layer, and horizontal currents and long waves that distort the thermocline, tilting it downward and bringing warmer surface water toward the leeward end of the lake (Spigel and Coulter, 1996). In a homogeneous lake with moderately strong, steady winds, steady currents are established whose directions are largely controlled by the wind direction and the presence of the shoreline (Murthy, 1971). However, steady and uniform winds rarely persist for more than a few hours, and in the normal course of events the winds often change slowly or vigorously or may be even cease entirely for sometime. Since the hydraulic circulation (from inflow-outflow) is always small and thermally driven flow in nearly isothermal water must be small, lake currents should be wind driven (Pickett, 1977). Wind stress must play a key role in governing the transport and fate of riverine inputs (Balnton and Atkinson, 1983).

In general, the response of a lake to wind stress forcing depends both on the strength and the scale of the atmospheric disturbance (e.g. Spigel and Coulter, 1996). Since the stress of the wind over water is known to be a quadratic function (Charnock, 1955), the major prime movers of currents are short bursts of strong winds (Csanady, 1973). Strong winds usually have uniform spatial structure (Estoque, 1962). Because strong wind stress impulses are exerted on the water at random times, and because the strength and direction of these impulses vary in a random manner, water movements produced by them are always essentially in a

transient state, there being never enough time to obtain any sort of a steady-state flow patter. It is quite possible that some residual, long-term average circulation still exists, but the intensity of this is certain to be much less than that of the transient patterns (Csanady, 1973). This suggests that both the time history of the wind and the instantaneous value are important to understand wind-driven lake circulations.

Wind stress, which is caused by moving atmospheric disturbance, is known to have a major influence in lake water circulation and associated material transport. In the discussion of the dynamic response to a moving atmospheric disturbance, the scale of external disturbance is important (Rao, 1963). Because the scale of most natural lake bodies is small in comparison with the scale of cyclonic disturbances, the geostropic wind is usually uniform over one lake (Rao, 1967, and Csadady, 1968). Theoretical studies considered such cases as uniform wind. In addition, the rotary characteristics of the applied wind stress may be very important (Saylor and Miller, 1987).

Contrary to the uniform stress case which could be considered for very short duration, the spatial and temporal structure of the wind-stress field is variable. The manner in which the circulation in the lake adjusts depends, in addition to other lake's physical parameters, on the spatial and temporal structure of the wind field (Mohammed-Zaki, 1980). The rate at which energy is supplied by a time-dependent wind stress to the lake depends on the extent of the resonant coupling, which arises when the propagation speed of the atmosphere is nearly equal to that of free waves on the lake (Rao, 1967). Resonance, which corresponds to the maximum setup, is obtained when the speed of propagation of the stress band is the same as the free gravity wave for bandwidths less than the length of the lake. For bandwidths greater than the length of the lake, resonance is obtained for a speed of propagation of the stress band, for which the time taken by the band to cross a fixed point in the lake is the same as the time taken by the free gravity wave to cross the lake.

A good deal of discussion on forced motions of the model Great Lakes under three simplified wind systems: steady and uniform wind, uniform but periodic wind, and uniform potential vorticity built up by the curl of the wind stress over the past period presented by Csanady (1968). The steady and uniform wind cor-

responds to the geostropic wind, which is often uniform over one lake and of longer lifetime, whereas periodic wind is a relaxation of the steady and uniform wind to allow changes with the typical period of weather cycles. The horizontal stress variations to build the uniform potential vorticity may be caused by either the horizontal wind shear present in cyclonic disturbances or the relationship of the geostrophic wind to wind stress on the surface of the lake or both.

Csanady reported that the developed flow pattern, under no lateral and bottom friction assumption, when a uniform wind starts to blow over a circular lake at rest consists of two gyres, the maximum elevation (and velocities) occurring at the downwind end. When acted upon by periodic and uniform winds, the setup varies from maximum 90° to the right of the wind at higher frequency to a maximum downwind, as in the steady uniform case, at very low frequencies. On the other hand, although wind stress of constant curl, applied to the lake surface for a certain period, setup a close circulation pattern of an amplitude proportional to the wind stress, Round-the-basin coastal jets setup by the wind stress curl are not likely to contribute significantly to current patterns observed (Rao, 1967).

In summary, the particular response of a lake depends on the characteristics of the forcing wind event. Wind energy is a most important physical, year-round control on circulation of tropical lakes in East Africa, where daily cycles in wind strength is one of the probable mechanisms to promote mixing of water column (Olago and Odada, 1996; Spigel and Coulter, 1996; Halfman, 1996). The annual wind cycle over the tropical lakes, with stronger southerly winds blowing along the axes of the lakes and persisting from May or June through August or September, results seasonal pattern of strong circulation and most mixing taking place during this period (Eccles, 1974; Coulter, 1968; Spigel and Coulter, 1996; Ochumba, 1996).

3.3 Large Scale Motion in Lakes

The study of large scale motions in closed basins has received considerable attention over several decades. Bottom currents of a few centimetres per second on average may appear to be rather small, but steady flow of a 2 $cm \cdot s^{-1}$ equals about 50 $km \cdot month^{-1}$ (Saylor and Miller, 1987). Observations (e.g. Pickett,

1977) indicate that currents speed up, slow down, and change direction at different locations and depths. Even so, Pickett confirmed from inspection of the original data that most of the time, especially when speeds are high, the meters conform to the monthly mean pattern. Hence, one should be able to consider this mean pattern as the steady background flow driven by the monthly mean wind, but disturbed by wind variations.

The general circulation patterns identified from both numerical calculations (e.g. Gedney and Lick, 1972; Csanady, 1973; Bennett, 1974) and current meter records (e.g. Pickett, 1977; Saylor and Miller, 1987; Beletesky *et al.*, 1999) show that a top surface mass flux is being transported in the direction of the prevailing wind. A subsurface current driven by the surface gradients returns the surface mass flux in the opposite direction to conserve the volume of the lake water. The surface currents computed to 0.4 meters from the surface in the deepest and central basins are, in general, found to be smaller than near the shore for an actual shallow lake, Lake Erie (Gedney and Lick, 1972). It is noted that this effect is essentially due to the relatively large subsurface return current down the centre of the lake, which is opposite in direction to the surface current and subtracts from it. Furthermore, it was reported that the flow at all levels at many locations is essentially parallel to the shore.

The vertically integrated flow follows the same pattern; the water in the shallow region is accelerated in the direction of the longshore component of the wind and the flow is return in the deeper central region of the lake (Bennett, 1974). The transport distribution identified by Csanady (1973) in a long lake directly forced by suddenly imposed wind stress, for example, is such that the wind stress and pressure gradient are in balance at the average depth of a section and the computed transport is, hence, zero. Where the depth is less than the average depth of the section, wind stress overwhelms the pressure gradient and accelerates the water. Where the water is deeper, the reverse happens and the return flow develops.

The vector resultant currents computed on a monthly basis from current meter records yield a complicated set of charts on which concise and strong flow patterns did not persist for lengthy intervals of time stretching into many months, but they did sort into several frequently observed modes (Saylor and Miller, 1987). It

is noted that the monthly or longer period averaged currents were composites of numerous wind-driven episodes as evidenced from the spectra of the wind stress which showed energy accumulations that represent some average values for the major weather system passages. A whole basin mixing episode of strong wind event that modifies the monthly averages plays a big part in determining the distribution of monthly resultant currents (Pickett, 1977; Saylor and Miller, 1987).

The overall circulation pattern could be either cyclonic (unticlockwise) or anticyclonic (clockwise) or consist of both gyres depending on the size of the lake: cyclonic pattern for large lakes and two gyre circulation pattern for small lakes (Beletesky *et al.*, 1999). The possible explanations suggested for such circulation patterns are that the meso-scale vorticity in the wind field due to large surface area and atmospheric temperature gradient would be the reason for cyclonic pattern in large lakes, and more uniform wind fields over small lakes to create two gyres pattern that resembles theories developed for circulation patterns under uniform wind. Csanady (1975) and Spigel and Coulter (1996) argue that a cyclonic circulation is required to achieve geostropic equilibrium, the balance between pressure gradient due to greater mixing and heating in the coastal regions than in pelagic regions and Cariolis forces that one would expect to hold in the long-term. Studies on tropical lakes (e.g. Eccles, 1974; Yuretich, 1979; Olago and Odada, 1996) show that wind-driven circulation, which appears to dominate any residual or long-term circulations, causes a closed-gyre circulation, with circulation centred on the main axis of the lake basins.

In summary fundamental principle of wind-driven flows in closed or partially closed basins states that in the shallow water, the dominant force balance is between surface wind stress and bottom friction, yielding a current in the direction of the wind. In the deeper water, the dominant force balance is between the horizontal pressure gradient (induced by surface slope) and bottom friction, yielding a current flowing in opposite to the wind (Hunter and Hearn, 1987). Major physical factors such as bottom friction, topography and presence of waves play interrelated roles that determine the hydrodynamics and associated transport process.

3.3.1 Effect of Friction

The effect of bottom friction is to produce resistance opposing wind stress. Increasing effective bottom friction therefore reduces the strength of circulation. The controlling effect of the bottom friction to transport caused by wind stress depends on the depth distribution of the basin and the time scale of the wind stress forcing. In an initial period of depth-integrated transport directly forced by suddenly imposed wind stress is found to increase linearly in time; later, friction slows down this increase (Csanady, 1973). Thus, if the wind blew with constant force a very long time, the linear increase in transport would certainly be reduced by bottom friction. If the wind blew with constant force for a very long time, the linear increase in transport would certainly be reduced by bottom friction. Furthermore, frictional effects are strong very close to the shores (within 7-9 km), but do not modify qualitatively the flow pattern which may be simply calculated from the frictionless, linearised equations (Csanady, 1973).

The straightforward damping effect of friction was revealed by the results of two models, where the one included friction and the other did not (Bennett, 1974). On the other hand, the relative importance of the lateral (depth-integrated) and overturning (vertically varying) circulations is dependent on the bottom roughness (Hunter and Hean, 1987). Increase in bottom roughness decreases lateral transport and hence flushing efficiency of the existing wind stress.

3.3.2 Effect of Water Depth

A uniform wind stress applied at the surface of a basin of variable depth sets up a circulation pattern characterized by relatively strong barotropic coastal currents in the direction of the wind, with return flow occurring over the deeper regions (Csanady, 1973; Bennett, 1974). Under quite general conditions the baroclinic response is confined in a narrow coastal region while the response in the main part of the basin is essentially barotropic. The barortopic large-scale low frequency motion follows contours of constant depth (Walin, 1972). The velocity distribution to suddenly applied wind stress shows the development of strong barotropic coastal currents (Csanady, 1973). The intense baroclinic motion in the coastal region will undoubtedly be a very important energy source for vertical mixing (Walin, 1972). For example water from deeper layers occasionally brought up to

the surface will be more or less diluted with surface water before fining its way back to an equilibrium position in the deep layers.

The response of hydrographic systems to time dependent forcing caused by synoptic meteorological disturbances is such that unless the slope of the bottom is much smaller than the mean slope, the motion will be along the counters of constant depth (Walin, 1972). The time dependent response may be divided into two parts with distinctly different properties (Walin, 1972): (1) a barotropic part non zero in the whole basin, (ii) a baroclinic part non zero only in a relatively narrow coastal region. The width of the coastal region in which baroclinicity is a dominating feature is found to be of the order of 10 km. A constant slope bottom causes a single gyre that intensifies the flow at portions of the boundary (Gedney and Lick, 1972). The variable slope effects of bottom topography cause the two gyre configuration, the asymmetries in the gyres being a direct result of the asymmetries in the bottom topography. Presence of narrow underwater ridges causes gyre and prevents subsurface return flow exchange (Saylor and Miller, 1987). The circulation pattern is complicated further by islands that limit basin interactions through the restricted passages.

Hunter and Hearn (1987) investigated the influence of basin bathymetry and bottom friction in determining the relative importance of depth-integrated transport at right angles to the motion vector (lateral) and vertically varying (overturning) circulations. They noted that these two elements of the total circulation can act to flush the natural system. However, under conditions of uniform wind stress and a flat-bottom basin the circulation consists only a vertical variation in the current (overturning). The interaction of variable topography leads to the development of lateral circulation in the basin. Their analysis showed that the ratio of the lateral to total circulation decreases with increasing bottom roughness or a flatter topography, due to reduction in lateral circulation. The ratio approaches a maximum value of unity for low bottom roughness (or small drag coefficient) and a broad distribution of depths.

There is a large difference in flushing rate (or exchange transport) between flat bottom and sloping bottom case (Singell *et al.*, 1990). In the flat bottom case, continuity requires the depth-averaged flow to vanish; thus the exchange transport limited by the amount of vertical shear that can develop. The bottom stress

is small because the bottom velocity is small, and the primary balance is between wind stress and depth integrated pressure gradient. In the sloping bottom case, the depth averaged flow at any particular depth value need not vanish to satisfy continuity, and strong horizontal structure develops with downwind transport in the shallows and upwind transport at depth. In shallow water, the primary stress balance is between wind stress and bottom stress, while in deep water, wind stress balances the integrated pressure gradient. As a result there is a downwind transport driven by the wind stress, and upwind transport in the deep water by the pressure gradient. Departure of the depth from the mean, therefore, increases the efficiency of the wind-driven flushing. For homogeneous flow in realistic basins, most of the exchange transport occurs in the horizontal (Hunter and Hearn, 1987; Singell *et al.*, 1990).

3.3.3 Effect of Surface Waves

When waves and currents exist jointly in a coastal region, the shear stress identified with the wave and current are altered because of the nature of the turbulence generated by wave-current interaction at the bed and are different from the stresses expected in the case of pure waves or currents. The turbulent momentum transfer from the near-bottom mean flow to the bottom is increased by the additional turbulence generated at the bottom in the thin wave boundary by the oscillatory wave velocities (Signell *et al.*, 1990). The resultant is that the current in the region above the wave boundary layer feels a greater resistance that associated with the physical bottom roughness.

Analytical theory presented by Grant and Madson (1979) described the significance of waves in modifying the flow in the vicinity of the bed. They noted that waves are capable of entraining significant amount of sediment from the seabed when current of comparable magnitude may be too weak even to initiate sediment motion. On the other hand, waves are an inefficient transporting mechanism, and to the first order, no net transport is associated with the wave motion over a wave period. However, the simultaneous presence of even a weak current will cause a net transport. Their theory shows that when waves and currents exist jointly in a region, the shear stresses identified with wave and current are altered because of the nature of the turbulence generated by the wave-current interaction at the bed

and are different from the stresses expected in the case of pure waves or currents. The net result is that the region above the wave boundary layer feels a greater resistance than that associated with the physical bottom roughness.

The magnitude of wind-driven currents in shallow bodies of water may be significantly influenced by wave-current interaction (Signell *et al.*, (1990). Surface wave in shallow water can increase the resistance felt by the bottom currents by an order of magnitude over the case of a current flowing over a rough bottom without waves present. Signell *et al.* (1990) compare results obtained using flat and sloping bathymetry cases. The results show that reduction of the exchange transport is larger for the sloping bathymetry case, whereas the reverse is found to be true for the increase of setup due to the presence of waves. If the wind stress is of sufficient strength and duration to generate surface waves which feel the bottom in at least the shallower part of the bay, the near-bottom current feels an enhanced drag which yields diminished velocities in the shallow water and reduces the overall exchange transport. If wave response varies with wind direction, then an oscillatory wind with a quasi-steady current response could generate a vertically uniform horizontal circulation that could increase the flushing. Overall, the magnitude of wind-driven currents in shallow bodies of water is significantly influenced by wave-current interaction.

3.4 Sediment Dynamics

It is widely accepted that the major sources of sediments are inflow from rivers, shoreline erosion, dead organic material and dumping of dredged materials (e.g. Madsen *et al.*, 2001; Brigham *et al.*, 2001). The rate of infilling by sediment depends on the sediment supply from the catchments and aquatic sources, and the original volume of the lake basin (Ryan *et al.*, 2003). A thorough understanding of the process of sediment-water interactions and the dispersion of sediments in a lake will have significant implications for many important problems (Sheng and Lick, 1979). The way in which sediments accumulate in a lake is important because sediments provide a record of past events in the lakes and in their watersheds (Davis and Ford, 1982; Blais and Kalff, 1995). Lake deposits reflect environmental conditions within the whole drainage basin - climate, hydrology, sediment production, land use, water pollution, etc (Sundborg, 1992). Large

amounts of contaminants such as nutrients and pesticides are transported into large lakes while being absorbed onto or associated with fine-grained sediment particles.

River mouth morphologies and depositional patterns comprise a broad spectrum of types (Wright, 1977). Wright (1977) discusses that when the wave power of the receiving lake basin is negligible or small relative to the strength of river outflow, effluent behaviour and consequent depositional patterns depend on the relative importance of three primary forces: (1) inertia and associated turbulent diffusion; (2) turbulent bed friction; or buoyancy. The role played by each force depends on factors such as the discharge rate and outflow velocity of the stream, water depths in and lake-ward of the river mouths, the amount and grain size of the sediment load, and the sharpness of density contrasts between the river and basin waters. High outflow velocities, small density contrasts, and deep water immediately lake-ward of the mouth permit inertial forces to dominate, causing the effluent to behave as a fully turbulent jet. When bed-load transport is large and water depths lake-ward of the mouth are shallow, turbulent diffusion becomes restricted to horizontal while bottom friction increases deceleration and expansion rates. Where the river mouth is deep relative to the riverine discharge, lake water enters the mouth as a salt wedge, and the buoyancy of the lighter river water becomes dominant; the effluent then spreads and thins as a relatively discrete layer.

River mouths located in relatively protected environments of fronted by flat offshore slopes may experience minimal wave effects. In a surface-trapped river plume, an external forcing (e.g. wind or ambient current) is required in order for entire fresh water volume discharged by a river to be transported downstream (Fong and Geyer, 2002; Fong and Stacey 2003; Warrick *et al.*, 2004; Piñones *et al.*, 2005). On the other hand, river mouths fronted by steep nearshore slopes in high wave-energy environments are profoundly influenced by waves. Outflow from river mouths reflects and steepens incident waves in such a way as to concentrate power on the effluent and to cause breaking in water depths greater than the normally breaking depth. The resultant wave-induced setup opposes the outflow, while wave-breaking enhances the mixing and momentum exchange between the effluent and ambient lake water. The effect is to cause very rapid deceleration and loss of sediment transporting ability within short distances from

the outlet.

The initial direction of sediment transport at river mouth is determined by outflow pattern, but the subsequent dispersal of sediment is regulated by the mixing rates of the buoyant plume with ambient water (Van Maren and Hoekstra, 2005). Dynamically, advection is likely to dominate the transport in the primary flow direction, while the lateral and vertical structure and the temporal variability of the plume is determined by environmental dispersion (Fong and Stacey, 2003). Frequently, well-mixed conditions can be reached quickly in the vertical direction and the dispersion of sediment will occur primarily in the lateral horizontal direction, orthogonal to the dominant advective direction. When the mixing rate of surface waters with underlying water is low, then the removal rate of sediment from the plume is dominated by sediment settling velocities; otherwise mixing processes contribute to sediment removal and further downstream transport as well. River discharges into saltwater bodies also have been found to form sharp frontal boundaries, across which density changes abruptly, at times of high discharge (Garvine and Monk, 1974).

The resuspension and deposition of fine-grained cohesive sediments in lakes are dependent upon the shear stress applied at the sediment-water interface, on the bulk sediment water content, on the mineral and size composition of the sediment and the absence or presence and amount of benthic infauna and bacteria (Sheng and Lick, 1979; Fukuda and Lick, 1980). Waves breaking on the shore of a lake will create turbulence and resuspend material in the shore zone that will then be redeposited in deeper waters (Håkanson, 1977). In general, increase in water content, bottom shear stress, or clay content of the sediment results increase in resuspension rate. The energy parameter with the most direct impact on the bottom dynamic situation is the wave length, which in turn depends upon the effective fetch, the wind velocity and wind duration (Håkanson, 1977; Sheng and Lick, 1979; Douglas and Rippey, 2000). Johnson (1996) suggests, based on review of the evidence for various sedimentary processes that have been inferred from seismic reflection and side scan sonar profiles from the east African lakes, that sedimentation pattern in the large lakes of the East African Rift Valley that surface waves generated by strong winds can sort and redistribute sediments in water depths as great as 100m. The strong prevailing winds blowing over the rift

valley lakes set up longshore currents in the nearshore zones that can generate significant lateral transport of sediment (Yuretich, 1979; Johnson, 1996).

Among 10 mechanisms identified to control distribution of sediments in lakes (Hilton *et al.*, 1986), the redistribution of settled material or occurrence of sediment focusing, resuspension of sediment in the shallower zones by waves and water currents with subsequent transport to and settling in the deeper zones of lakes, can be rationalized in terms of the dominance of four processes: peripheral wave attack, sliding/slumping on the slopes, intermittent complete mixing, and random redistribution (Hilton, 1985). These mechanisms, except random distribution, may cause sediment focusing (Hilton et al, 1986).

Based on their potential for resuspension, lake bottoms can be divided into erosion zone, transportation zone, and accumulation zone (Hakannson, 1977; Blais and Kalff, 1985). Erosion zone is marked by course-grained, non cohesive sediments and is found in areas of high water turbulence. Areas of sediment accumulation are characterized by soft deposits of fine material with relatively high water content, whereas areas of bottom transport may be characterized by discontinuous deposition of fine materials (Håkanson, 1985).

Overall, the basic textural trends and compositional variations of sediment distribution in lakes is known to conform to an inshore-to-offshore prograding associated with declining energy as water depth increases (e.g. Holmes, 1968; Thomas and Kemp, 1972). The rapid energy decrease at stream mouths appears to allow deposition of much of the sand and silt (Holmes, 1968). Transport dynamics of fine-grained sediments are functions of the energy imparted to the immediate surroundings (Petticrew and Kalff, 1991). Due to their small fall velocities, fine grained particles (i.e. those in the silt and clay size range) are transported easily by flow (Luettich *et al.*, 1990). The fine material is not deposited in high energy environment, e.g. in the beach zone, at lower water depths relative to large fetch, or when the water velocity for different reasons is high (e.g. in connection with topographical bottle-necks) (Håkanson, 1977). As the energy level further decreases out into the lake clay particles begin to flocculate and the floccules are deposited (Holmes, 1968).

Further, the mineralogical composition of modern lake sediments is intertwined

with geological, climatic, biological, chemical and physical processes within the basin (Thomas, 1968; Yurtich, 1979; Hilton and Gibbs, 1984; Johnson, 1996; Halfman, 1996). For lakes in the East African Rift System, the timing and style of tectonic movements has influenced drainage pattern development, hydrological budget, and the amount and type of sediment supplied to the rift (Wescott *et al.*, 1996). The length of the rift segment has a significant impact on how effective the axial drainage is in affecting sediment distribution and sedimentation rates within a segment (Wescott, *et al.*, 1996). The great length means that the effect of axial drainage in limited to the north most part of the rift segment, whereas the shorter lake segment in contrast is greatly affected by axial drainage in either direction. Localized compositional character of sediments in the vicinity of river deltas and near-shore localities is closely controlled by the detrial load and local source areas (Horowitz, 1974; Yuretich, 1979). Variations in distributional patterns of lake sediments offshore define specific sedimentological provinces (Yurtich, 1979; Hilton and Gibbs, 1984). Differences in mineral densities may also reflect mineralogical trend in lake sediments (Kennedy and Smith, 1977).

3.5 Study Objectives

In view of its large horizontal extent (more than 80 km), topography of surrounding land and existence of blocking islands distributed in the lake (about 2.5% of the lake area), the hydrometeorological condition of Lake Abaya may vary from place to place. This in turn could give rise to different zones characterized by spatiotemporal patterns of lake water circulation and associated transport processes. Consequently, the characterization of the spatial and temporal variability of physical parameters and sediment distribution is the main subject of this research. More specifically, this study addresses the following distinct, but related issues:

- Study the importance of meteorological forcing on lake water circulation, which influences many processes, including sediment transport and mixing for water quality considerations;

- Determine the depositional zones for sediment transported within the lake;

- Define the lake basin-scale magnitude and variability of fundamental water quality parameters; and
- Characterize the mean lake water circulation in terms of sediment distribution and lake geometry (local bathymetry, shape and islands) and their interactions with top-level forcing of the lake.

4 Methods

4.1 Meteorology

Two automatic meteorological stations were established at the western shoreline of Lake Abaya. Fura Station is located at 37.67° Easting, 6.16° Northing in 100 m distance to the shoreline, and Wajifo Station is located at 37.28° Easting, 6.5° Northing in 30 m distance to the shoreline.

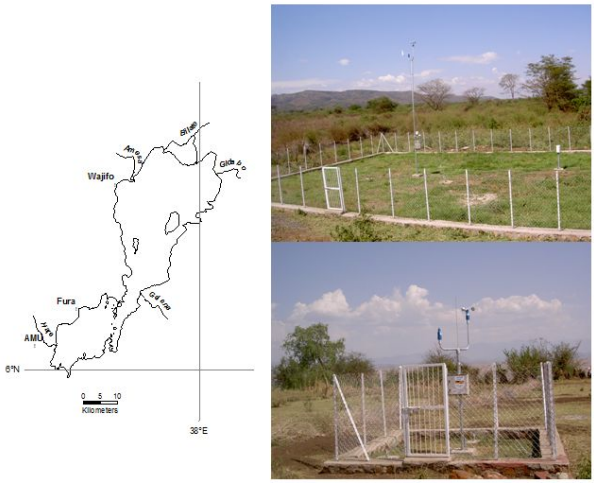

Figure 4.1: Left: Location map of meteorological stations and base site (AMU); Right: Wajifo (top) and Fura (bottom) stations.

The selection of the localities for the establishment of observational stations involved various meteorological and logistical problems. For instance, in order to simplify the meteorological complications, a straight coastline in a region of flat terrain is desirable (Fisher, 1960). Although the two selected sites do not fully satisfy these requirements, they offer some advantages that led to their selection. Only the western shoreline of Lake Abaya can be accessed for routine operation of the instruments. Relief at the stations is fairly flat enough to capture winds from all directions. In addition, locations are as close as possible to the shoreline, to the west of the longest transverse lengths and around the middle of the main basins in the south and north (Figure 4.1).

For the two sits selected for the meteorological stations there are some disadvantages which should be mentioned. The pronounced bend at Fura and indentation to the north of Wajifo in the coastline, and the presence of valley floor edges within few kilometres to the west of the stations certainly have some effect on the main features of the wind field resulting from differential heating at a lake shore.

The Fura station is located in the south basin, and records wind speed (measuring range: 0.5 - 35 m/s) and direction (angle of rotation: 0 359°) at 2 m elevation from the ground surface using SEBA HYDROMETRIE sensors. Wajifo station is located in the north basin; it records wind data at 6 m elevation along with air temperature (resolution: 0.1°C, accuracy: $\pm$0.3°C), atmospheric pressure (accuracy: 1% relative error), global radiation (spectral range: 0.3 - 3μm, temperature dependence: <0.15%/°C), and rainfall using rain gauge with impulse output (resolution: 1 pulse = 0.1 mm precipitation, pick-up for data logger system and ball-beared tipping bucket). Both stations are equipped with data logger and the data were recorded as either two or five minute averages since 7th of February, 2004. In the present study data from 1 March 2004 through 28 February 2005 are used. Although the available data set is not sufficient for formal statistical analysis to investigate the general structure of the meteorological elements around the lake, it provides important information to capture local phenomena observed during the study period.

Various analyses were performed in order to understand the variation of wind field at different time scales along the western shoreline of Lake Abaya. The

resultant values of the wind records were computed by adding and averaging the west and south components of the two or five minute interval wind observed at a given time. Diurnal variation of the wind is analyzed using half-hourly averages of 2 minute interval records of wind speed and direction. Frequency histogram was plotted to compare onset of lake-breeze at two stations. Hourly wind roses were obtained from the mean wind vector for each observation time at the stations to study the average variation of wind speed and direction over each hour of a day. The monthly wind statistics is presented using the monthly wind roses and speed class histograms. Periodicity analyses were performed to identify the most oscillatory components using the monthly spectra estimates from hourly average speed along dominant directions. The dominant directions were explored using wind direction histograms.

The tipping bucket data were converted to series of daily and monthly total and 1 minute, 5 minute, 10 minute and 1 hour rainfall intensities. Temperature variation at Wajifo Station is analyzed using hourly averages. The descriptive statistics together with frequency distribution histograms and plots of monthly averages over individual hours during the study period are used to observe closely diurnal and monthly variability of temperature. Interdiurnal variability was computed as the difference between either the daily mean or a fixed hour of a day and that of the next day to identify the variability of warming and cooling in each month during the study period. The monthly atmospheric pressure oscillations about the monthly means were plotted to illustrate the diurnal cycle of pressure changes as well as some atmospheric dynamics causes for extreme events.

4.2 Sedimentology

948 surficial sediments were collected from the Lake Abaya lake floor (Figure 4.2) using a Van Veen grab sampler type during the 2003-2004 field years from both south and north basins (Figure 4.3). Additional 238 samples were collected by Blumberg and Schütt (2006) in 2002 from the area around the Lake Abaya bottleneck connecting two basins. Sampling stations were geo-positioned using the topographical maps (scale 1:50,000) and Garmin III GPS. The water depth was recorded at each sampling locality using the markings on sampler line. For the fresh samples colour, grain size composition and odour were recorded.

In the Hydraulics and Water Quality laboratories of Arba Minch University the sediment samples were dried at 60°C, disaggregated and stored. For further analysis samples were homogenized using an agata ball mill at Siegen University and at Freie University of Berlin. The geochemical and mineralogical analyses were carried out in the Geographic laboratories of Freie University of Berlin.

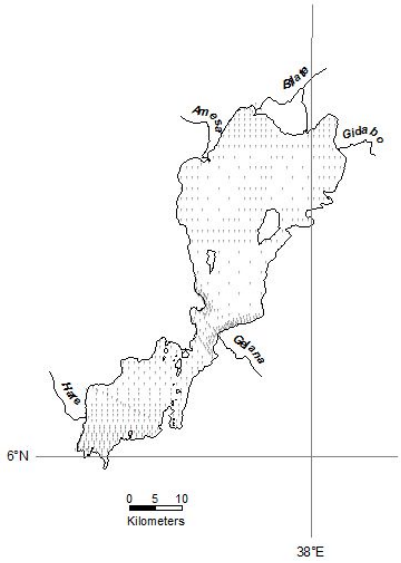

Figure 4.2: Location of sampling sites of Lake Abaya lake floor sediments.

The total carbon content (TC) was determined by burning 100 mg of grounded sample material in an oven under oxygen atmosphere at a temperature of 1000°C. The released CO_2 changed the electrical conductivity of NaOH-solution in a special measuring cell (WÖSTHOFF, CARMOGRAPH 6). For total inorganic carbon (TIC), 100 mg of sediment material was treated with 42.5% phosphoric acid at a temperature of 80°C, and the released CO_2 was detected in the same manner (see above). The difference between TC and TIC represents the organic carbon

content. The detection limit for all carbon measurements is 0.02 mass %.

X-ray diffraction analysis of 706 powder samples was undertaken to determine the mineral composition of the lake floor sediments from Lake Abaya using a Philips PW 1710 diffractometer connected with PC-APD (version 3.6g) with Ni - filtered copper Kα radiation. To produce reliable diffractogram each sample was tested for preparation error.

The determination and a semi-quantitative analysis of mineral composition of the lake floor sediments were carried out using Philips X'Pert HighScore analysis software. The position change of the major peaks of X-ray diffraction data, which may be inherent mainly due to sample preparation, affects the computed amount of mineral composition. The software feature to correct this computational error produces usually different results when 'allowing pattern shift' is turned on and off. To overcome this effect, the computed results of the percentage composition of identified minerals were compared with the major peak intensities of quartz, feldspar and calcite minerals.

Determination of clay minerals is not possible using X-ray powder analysis. Correspondingly, first the amount of the different minerals without clay minerals was calculated. Since X-ray diffraction failed to reveal the occurrence of other carbonates than calcite in the lake sediments, the inorganic carbon content (TIC) was used to calculate the calcite content (mass %). In comparison with the calcite content obtained by semi-quantitative analysis of X-ray diffraction data, a reducing factor is calculated. After using this factor to reduce the semi-quantitative values of the identified minerals, the difference between 100% and the sum of calculated minerals is taken as the amount of the clay minerals including also allophanes and organic matter.

In general, the diffraction patterns of samples from the central parts of Lake Abaya are extremely similar. This fact was also used to prove the correctness of the calculations.

All basic statistics on the percentage composition of minerals were carried out using SPSS. Kriging interpolation method in ARC GIS environment was used to estimate spatial distribution of water depth and percentage composition of minerals. This method is chosen because it represents better two ends in the spectrum

Figure 4.3: Grab sampling of lake bed sediment from predefined sampling site.

of interpolation method. Plots of frequency distribution of percentage composition for main basins included to display relative distribution structure. Correlation analyses were used to investigate the influence of water depth on the spatial distribution of sediment texture and mineralogical composition. Average mineralogical compositions at deltas of major rivers were compared to identify the influence of drainage basins. The Ward method of cluster analysis with percent mineralogical compositions was used to group different lake sediment samples. The data are reported as mean percent of the sediment samples included in a cluster.

4.3 Water Quality

The water quality data are categorized into two sets of parameters: (1) in situ parameters, measured with multiparameter sonde and Secchi disk, and (2) laboratory parameters. Parameters measured on site using portable multiparameter water quality measuring equipment of SEBA HYDROMETRIE include: pH (accuracy: $\pm$0.1pH, resolution: 0.01pH); water temperature (accuracy: $\pm$0.1°C, resolution: 0.01°C); conductivity (accuracy: $\pm 1 \mu$S (0 - 200 μS), $\pm 0.5 \mu$S (> 200 μS), resolution: 0.001 μS); dissolved oxygen (accuracy: $\pm$0.5 vol. of measured range, resolution: 0.01mg/l); and redox (accuracy: $\pm$10mV, resolution: 0.1mV). Laboratory parameters include concentrations of Total Suspended Solids (TSS)

and Total Dissolved Solids (TDS).

Crosschecks between upcast/downcast near surface quality data of duplicate measurements were used to confirm accuracies suggested by the manufacturer as well as the sensors are operating properly. The quality sensors were calibrated frequently in the Water Quality Laboratory of Arba Minch University before going out in the field (SEBA HYDROMETRIE, 2004b) against company made fresh standards. The calibration process is supported by the calibration software SEBAConfig and infra-red (IrDA-Standard) interface to make wireless connection to a PC.

The primary criterion for the selection of sampling locations was an adequate spatial coverage to determine the effects of different parameters on water quality. Nine fixed monitoring stations were established where three types of sampling stations were defined (Figure 4.4): (1) in the sphere of influence to the major tributary rivers mouths (S2, S3, S7, S8, and S9), where freshwater and transported materials are delivered in large amount; (2) in the central part of the lake (S4 and S6), which are remote from transported materials delivery points to the lake; and (3) in the southern margin of the two sub-basins (S1 and S5) to identify any trend in water quality parameters along the longitudinal axis.

The research vessel was anchored at each fixed station and parameters were measured and water samples were obtained from predefined sampling depths. All lake water samples were extracted using SEBA HYDROMETRIE grab sampler (Figure 4.4). Number of water quality measurements depended on the lake depth at the respective station. For shallow stations (depth $\leq$ 3m), parameters were measured at the surface (0.1m) and at 0.5m intervals working down to the bottom (0.5m, 1m, 1.5m, etc). For stations deeper than 3m, parameters were measured at the surface (0.1m), at 0.5 m, and 1.0 m, and at every meter thereafter until reaching 0.5m above the bottom. The measurements were recorded after the sonde readings were stabilized.

The Secchi disk transparency was obtained with a 20 cm metallic Secchi disk. The disk was lowered into the water over the shaded side of the boat to reduce problems of glare until it just disappeared from view and the depth was recorded. Then the disk was slowly retrieved to the point where it reappeared and the depth was recorded again. The mean of these two measurements was taken as the Sec-

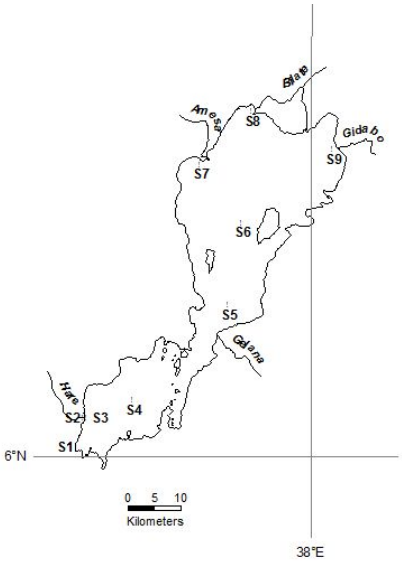

Figure 4.4: Location map of fixed monitoring stations.

chi disk transparency.

The physical analyses conducted in the water quality laboratory of the Arba Minch University included determination of Total Suspended Solid (TSS) and Total Dissolved (TDS) concentrations. TSS concentration was determined gravimetrically by filtering a known volume of a well-mixed water sample and by differential weighing of the dried filters. 250 to 1000 ml were filtered through 55 mm diameter and ashless S & S Filter Paper. After filtration was complete, the filters were washed with 20ml distilled water and then dried for 12 hrs at 105°C. The residue was weighed in an analytical balance (precision = $\pm$0.1 mg) to calculate the total concentration of suspended solids. The mass of total dissolved constituents in water (TDS) was determined by evaporating the filtrate at 180°C and weighing the residue.

Stratification patterns in Lake Abaya were shown by the contour plots of water

Figure 4.5: Water sampling from fixed monitoring station.

Bimonthly monitoring in the south basin								
Station ID	**Mar**	**Apr**	**May**	**Jun**	**Jul**	**Aug**	**Sep**	**Oct**
South basin								
S1	11, 26	14	11, 26	14, 26	12, 28	12, 27	25	12, 27
S2	11, 26	14		26	12, 28	12	25	12, 27
S3	11, 26	14	11, 26	14, 26	12, 28	12, 27	25	12, 27
S4	11, 26	14	11, 26	14, 26	12, 28	12, 27	25	12, 27
North Basin								
S5	20	19	19	21	19	20	21	21
S6	19	19	19	21	19	20	22	21
S7	20	19	19	21	20	20	22	22
S8	19	20	20		20			22
S9					20			22

Figure 4.6: Regular field monitoring sessions for water sampling from fixed sampling station in Lake Abaya (March-October 2004). Figures indicated dates of the month when field samplings were conducted.

quality profiles at fixed monitoring stations. The monthly and bi-monthly values of variables for all the fixed stations were described in terms of the mean val-

ues of depth profiles. The general spatial variation of water quality parameters for fixed stations was depicted based upon the overall average values for each fixed station. Seasonality of quality parameters variations were assessed by plots of mean values during the study period. The relationship between weather and water temperature was examined using plots of average values of 1 hour air temperature and top layer water temperature at the nearby fixed stations. The spatial distribution of water transparency was estimated by the mean Secchi values at fixed monitoring sites combined with single measurements taken from some sediment sampling locations.

Statistical results to quantify the associations and differences between water quality parameters were evaluated with a two-tailed t-test, one-way ANOVA, Tukey's Multiple Comparison and correlations coefficients. Stations which have been monitored more frequently and profile measurements taken at more than one depth are included for analysis. The individual parameters were tested between fixed stations and data set. Statistics were computed in SPSS ® v14.0.

5 Results

5.1 Meteorology

5.1.1 The Wind Field

The primary data for this study include the continuous records of two or five minute averages at two stations established for this study. The first step in the analysis consisted of obtaining the resultant values of the wind records. That is, the records of wind speed and directions were used to obtain the corresponding vector $\mathbf{V} = u\mathbf{i} + v\mathbf{j}$, where u and v are, respectively, from west and south components of the two or five minute interval wind observed at a given time and $\mathbf{i}$ and $\mathbf{j}$ are the unit vectors. The resultant component in a particular direction is equal to the arithmetic sum of respective components divided by the number of readings. Finally, the resultant, or vector mean, is obtained by reconverting resultant components into a single vector. The use of mean vectors for each half an hour or hour of a day reduces perturbations due to changes of the large scale winds or random disturbances to a level that is acceptable for the envisaged variations.
Resultant wind has a value different from zero when there is either a preference for a given direction during the averaging time or there is a tendency for higher speeds for a certain direction. As an example of good representation of the hourly resultants, wind roses for variable light winds observed on 27 March 2004 were compared at Fura (Figure 5.1). The wind from three quadrants persisted nearly equally on the average. The hourly mean winds for 20 hours of the day have separate bins, with two bins in the NE representing more persisting winds during the recorded hours. More detailed examination of the wind roses revealed that the rare wind from SE quadrant is easily identified in both representations of the wind field.

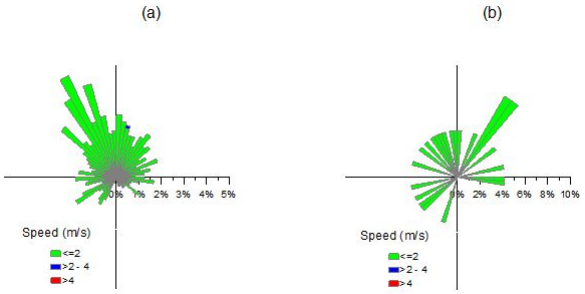

Figure 5.1: Wind roses for 27 March 2004 at Fura station obtained from: (a) 2 min interval records; and (b) derived hourly resultant winds.

Diurnal Variation of the Wind

In order to obtain a more detailed understanding of the general nature of the diurnal wind pattern along the western shoreline, half-hourly averages of 53 individual days (between 7 February and 30 March, 2004) were computed from 2 minute interval records of wind speed and direction. Resultant winds at half an hour intervals are considered to capture the observed short period oscillations. The half-hourly averaging period is centred at the beginning of each hour; for example, 0800 to 0828 for the 0800 value and 0830 to 0858 for the 0830 value. The orientation of the shoreline is such that fully developed lake-breeze comes from SE quadrant at both stations. A descriptive analysis of the diurnal changes in wind structure during this period is presented in the following paragraphs.

A detailed examination of observational data for the 53 days provided that the lake-breeze was observed daily at both stations. Figure 5.2 presents the relative frequency of the time when the lake-breeze started at Fura and Wajifo during the 53 days observations. At Wajifo, the lake-breeze started between 0730 and 0930 Local Standard Time (LST), predominantly around 0800 LST (about 60% of the time). The persistence of the lake-breeze is at least for 8 hours except for two days when the duration was only for 2.5 and 4 hours. Lake-breeze developed with NNE sector dominating during onset, and rotated clockwise to the SE quad-

rant within the next hour. The onshore wind speed increases rapidly before noon, mid-afternoon speeds falling close together. The most important feature of the resultant wind vector is that on individual days there is a strong tendency to turn counterclockwise during the onset of lake-breeze in the morning. Wind vectors turned in a clockwise direction in the remaining hours of individual days. The lake-breeze is followed by the variable wind, and before midnight a weak land breeze begins. The wind continues from the NW quadrant at less than 3 ms^{-1} through the early morning hours; but during the hour immediately preceding the lake-breeze, the wind is again variable. The lake-breeze caries average speed of 0.22-1.48 ms^{-1} in the first half an hour, increasing to 0.84-4.97 ms^{-1} in the next 2.5 to 9 hours.

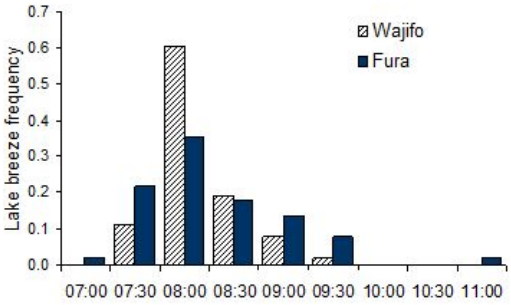

Figure 5.2: Observed lake-breeze starting time and frequencies at Wajifo and Fura stations from 07 February through 30 March 2004.

A more detailed investigation of the diurnal wind variations for individual days revealed that erratic day-to-day changes of the half-hourly mean wind speeds at both stations. At Wajifo, winds fall of in strength during the night, reaching a maximum at various hours between 1000 and 1800 (all times in Local Standard Time) predominantly (for about 75% of the time). Maximum easterly winds occurred on 28 days between 0930 and 1330, on 13 days between 1430 and 1800, on 11 days between 1900 and 0030, and one day at 0830. Maximum westerly component occurred on 32 days between 1830 and 2330, on 16 days between 0030 and 0530, and on one day at 0730, 1330, 1430, 1630, and 1730. Maximum

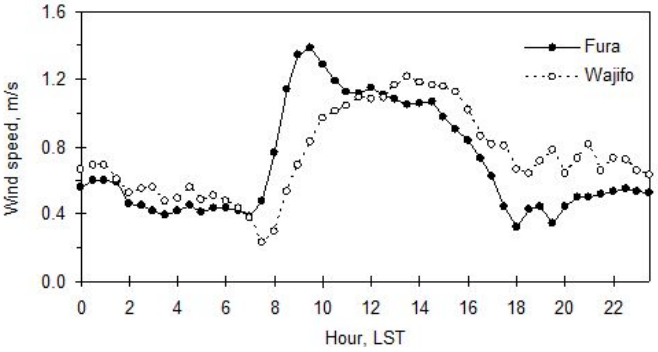

Figure 5.3: Average diurnal variation of wind speed at Fura and Wajifo stations for 53 days (from 07 February through 30 March, 2004).

northerly winds occur on 22 days between 2200 and 0130, on 17 days between 1930 and 2100, on 8 days between 0230 and 0700, on 2 days at 0800, and one day at 1330, 1430, 1730 and 1830. Maximum southerly winds occur on 43 days between 1000 and 1800, on 7 days between 2100 and 0100, and one day at 0400, 1900 and 1930. Maximum winds from the south are much stronger than in the opposite direction from the north. Similarly, the easterly maximum wind components are stronger than westerly components. A definite stagnation occurs during the early morning and late afternoon hours before the lake-breeze begins and shifts to land breeze. The outstanding features of the diurnal wind on individual days at Wajifo are the high resultant speeds persisting on SE quadrant with little variation in direction after the lake-breeze developed around midmorning.

At Fura in the south, the first lake-breeze observed between 0700 and 1100 (Figure 5.2), predominantly being between 0730 and 0830 (about 75% of the time). The persisting large scale wind in the direction of the lake-breeze overlapped on two days and obscured the identification of the first observations. The persistence of the onshore wind is between 6.5 and 11.5 hours. Wind occurred on the SW quadrant on 29 days, on SE quadrant on 10 days, and 14 days on NE quadrant during onset. Variable wind during onset rotated clockwise direction on 15 days,

turned in a counterclockwise direction on 38 days. The resultant wind carries an average speed in the range of 0.05 and 2.76 ms^{-1} in the next half an hour, which increases to 1.28 or 3.25 ms^{-1} between the next 1.5 and 6.5 hour. At the late hours when the onshore wind wanes, winds rotated in clockwise direction on 46 days and showed tendency to turn counterclockwise on 7 days. Nighttime wind speeds are weak and close together.

The diurnal variation of arithmetic mean wind speed at Fura and Wajifo stations is shown in Figure 5.3. It is shown that daytime portion of both curves is different from the nighttime portion. Furthermore, the average wind speeds rise rapidly between 0700 and 1000, relatively steady between 1200 and 1600, and fluctuate more between 1800 and 2100 LST.

The frequency of occurrence of maximum half-hourly average wind components on individual days is found to be more erratic at Fura. Maximum easterly winds occurred on 27 days between 0800 and 1000, on 12 days between 1030 and 1400, and on 10 days between 2030 and 0130. Maximum westerly component occurred on 21 days between 1900 and 2230, on 13 days between 0030 and 0300, on 9 days between 0430 and 0830, and on 7 days between 1630 and 1830. Maximum northerly winds occurred on 22 days between 0800 and 1000, on 14 days between 2200 and 0030, on 9 days between 0100 and 0600, and on 6 days between 1830 and 2100. Maximum southerly winds occurred on 39 days between 1230 and 1430, on 7 days between 1500 and 1700, and on 5 days between 1900 and 0030. Maximum winds from the south are much stronger than from the north, like in Wajifo. Similarly, the easterly maximum wind components are much stronger than westerly components in the opposite direction.

Figures 5.4 and 5.5 contain hourly wind roses for Wajifo and Fura for the resultant winds of 53 days. The two minute interval records were averaged over the 53 days of March and April 2004 to obtain the mean wind vector for each observation time at the stations. At Wajifo, the resultant winds are predominantly from the west and southeast with a rather distinct diurnal variation in speed. Winds are lighter during the night and the onshore wind increases rapidly until mid-morning, reaches a maximum early afternoon, and then returns to a lower value around 1800 LST. Generally lower resultant velocities occur in the early morning hours and between hours of 1800 and 2000. Wind speeds between noon and mid afternoon, and between 0300 and 0600 LST tend to fall close together.

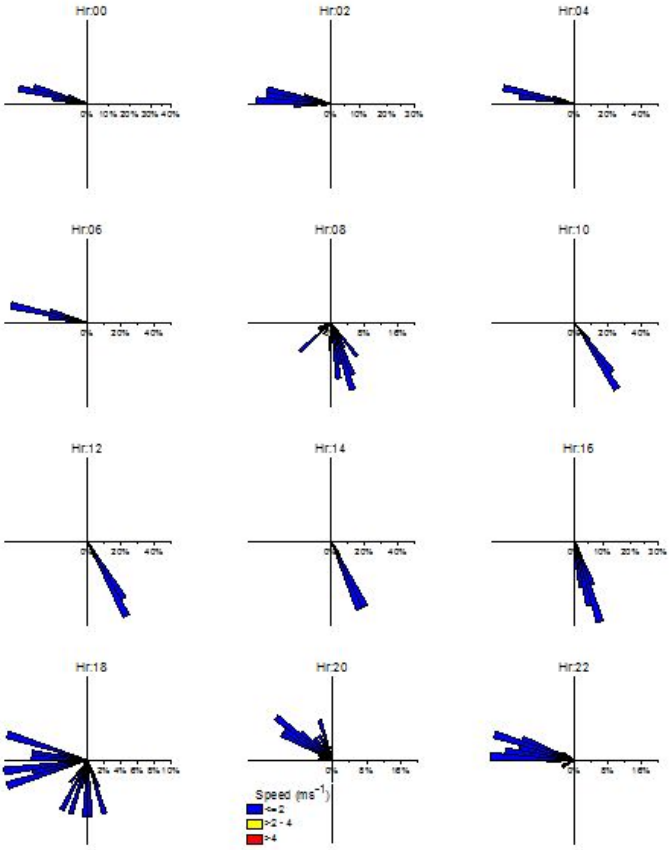

Figure 5.4: Wind roses at Wajifo station, 07 February-30 March 2004.

The fluctuation of wind speed and direction at 0800 and 1800 LST clearly marks the onset of lake-breeze and land breeze, respectively. The outstanding features of the wind roses for Wajifo are the counterclockwise rotation of the wind vectors during onset of lake-breeze and little variation in direction after midmorning.

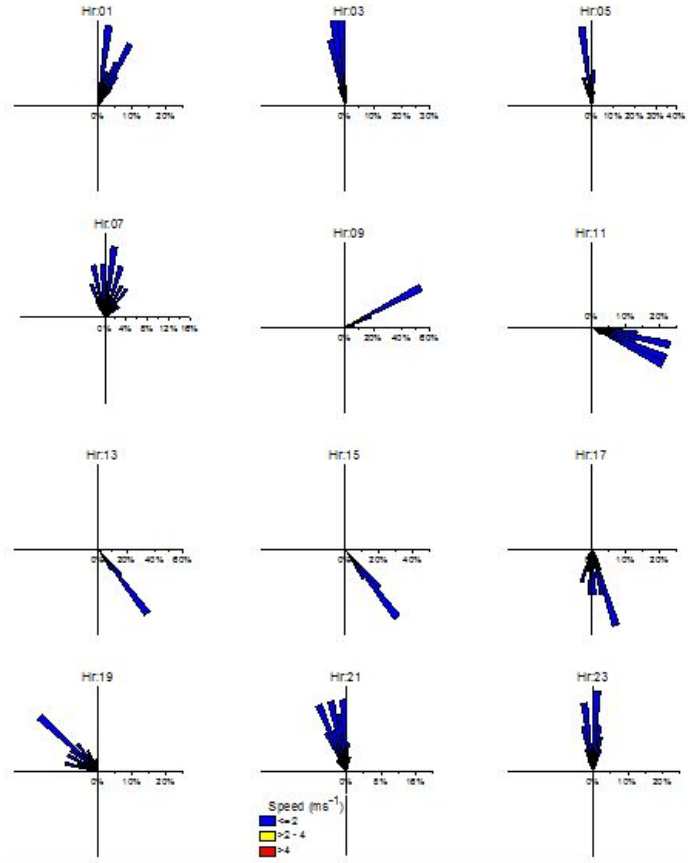

Figure 5.5: Wind roses at Fura Station, 07 February-30 March 2004.

Rotation of the resultant winds is clockwise during daytime and onset of land breeze. There is a great tendency to veer and back alternatively before midnight. The resultant directional change between 0700 and 0800 LST and between 1800

and 2300 LST (limits included) are greater than the remaining hours of the 24-hr period.

The resultant winds at Fura (Figure 5.4) show clockwise rotation before midnight and the tendency to veer and back after midnight. The onset of lake-breeze and land breeze were marked by increased oscillation of the wind vector at 0700 and between 1700 and 1800 LST. The wind field persisted in the ENE sector mostly between 0800 and 1000 LST, completely shifted to ESE sector at 1100 LST. There was a great tendency of the actual wind rotating clockwise throughout the 24-LST period at Fura. The average daytime wind speed increased steadily to the maximum at the midmorning, fluctuated between midmorning and early afternoon, and finally deteriorated to minimum at 1800 LST. There is a tendency, as at Wajifo, for nighttime wind speeds to fall close together. More diurnal directional changes observed at Fura than at Wajifo.

By way of summary, the diurnal winds for February and March 2004 indicate the following characteristics. During the 53 days observations, the lake-breeze was in general able to dominate at both stations the over-riding and ever-changing large-scale flow. Along the western shoreline of Lake Abaya, lake-breeze develops by one hour earlier in the southern basin than in the north. Wind roses for both stations show clockwise rotation, but Wajifo show definite counterclockwise rotation during onset of lake-breeze. The westerly winds rotate to northward when they exit Fura in the south during nighttime. At Wajifo, winds are generally westerly during nighttime and the north components are very light. Resultant winds are in the NE quadrant during some period of the day at Fura and become nearly parallel to winds at Wajifo later in the afternoon in the SE quadrant. It is noted that the rate of turning of the direction of the lake-breeze and land breeze is not uniform over a 24 hour period.

Afternoon winds are found to rotate slightly in clockwise direction at both stations. The directional changes to the reverse directions during the onset of lake-breeze at Wajifo and land breeze at Fura are abrupt. Time of maximum resultant wind is in the midmorning at Fura, but tends to be four hours later at Wajifo station. The light lake-breeze in the morning at Fura is partially distorted by changing large-scale flow pattern.

Monthly Variability of Wind Field

Figures 5.6 and 5.7 present the statistics of monthly winds of 2 or 5 minutes records observed for one year from March 2004 to February 2005 at two stations situated at the west boundary of Lake Abaya. The observed wind speeds, u, are classified in three ranges ($u \leq 2\text{ms}^{-1}$, $2\text{ms}^{-1} < u \leq 4\text{ms}^{-1}$, $u > 4\text{ms}^{-1}$). The considerable difference between graphs of two stations corresponding to the same month obviously indicates the importance of the winds of local origin at a given site around the lake. On the other hand, remarkable similarities and differences between monthly wind roses at a station mark the presence of characteristic seasonal pattern.

The outstanding feature of the monthly wind roses at Wajifo (Figure 5.6) is that winds showed strong directional preference. A persistent southeast wind occurred throughout the year (23-47% of the monthly period), but is most prominent during the period approximately from May through July 2004 (36-47% of the monthly period). Little directional change noted in the SSE sector from May through June and October through December 2004, when winds were stronger for significant portions of these months. Westerly winds observed continuously, being nearly at right angle to the SE winds. From March through April 2004, westerly winds occurred predominantly. Southeasterly and westerly winds were nearly equally important from September through October 2004 and from January through February 2005. Generally, southeasterly winds are stronger than westerly winds, and winds from NE quadrant are rare.

Fura station experienced winds from different quadrants over a significant portion of the time (Figure 5.7). The northeasterly winds occurred only between 3-7% of the monthly periods from May through August 2004, during which southwesterly winds from opposite direction occurred predominantly. Northeasterly winds observed to be predominant over southwesterly counterparts in the reverse direction during the remaining months of the year considered in this study. Northwesterly winds occurred predominantly over southeasterly winds all the time, except February 2005 when winds in both direction were nearly equally important.

Next Figure 5.8 gives the speed class histograms for monthly winds in the ranges 0-2 ms^{-1}, 2-4 ms^{-1}, and exceeding 4 ms^{-1} for the months of calmest and high-

est wind speeds and the average of 12-month period at Wajifo and Fura stations. During the study period considered in this study the observed wind speeds were predominantly < 2 ms^{-1} (between 92 and 98% of the monthly periods at Fura, and between 62 and 95% at Wajifo). At Wajifo in the north, the moderate and strong winds occurred more frequently in June, but at Fura in the south December winds were in general stronger than any other month of the year considered. The maximum wind records in different months at Wajifo and Fura, respectively, were about 5.2-8.9 ms^{-1} and 3.9-6.5 ms^{-1}. The maximum recorded wind speed occurred on May 05, 2004 at 1810 LST at Wajifo and later at 2035 LST at Fura. Since the collected wind data were 2 or 5 minute interval records, the actual maximum wind speed that occurred during the year may not have been captured although it would not be expected to differ greatly from the measurements. The calmest month was August at Fura and January at Wajifo (Figure 5.8) which had peak frequencies of occurrence in the 0-2 ms^{-1} bin.

Periodicity Analysis

This section is concerned with periodic components that may contribute to measured wind. Spectra presenting the distribution of kinetic energy as a function of frequency are useful in picking out some of the more energetic oscillatory components (Saylor and Miller, 1987) in the wind speed records. To this end, the monthly spectra were estimated from hourly average speed along dominant directions for both stations in units of wind speed squared per cycle per hour. The dominant directions were identified for each month from wind roses (Figures 5.6 and 5.7) and wind direction histograms, but not reported here. Observed spectra have very similar shapes, and typical spectral plots of for two months are shown in Figure 5.9.

All spectra indicate pronounced peak at about 0.0417 cycle per hour (cph) frequency, which corresponds to a period of 1 day (the diurnal frequency). The magnitude of this peak is higher at Fura across-shore in all months, except July and August 2004. At Wajifo, the magnitude of the spectra peak at diurnal frequency appeared higher for across-shore wind component than along-shore component of the wind in all months, except in March, April and August 2004. Another remarkable feature from monthly spectral estimates is that the energy distribution is in general broader across-shore component at Wajifo and along-shore component

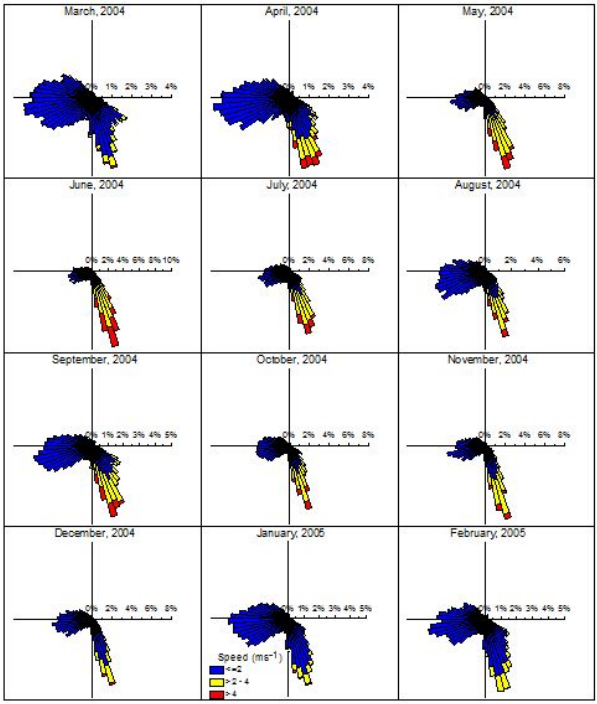

Figure 5.6: Monthly wind roses at Wajifo Station.

at Fura. Thus the estimated power spectra of wind speed in the frequency range between 0 and 0.5 cph fall into two more or less distinct groups depending upon the broadness of the energy distribution as shown in Figure 5.9. It should be noted that the only significant periodicity contained in the spectra, in the frequency interval between 0 and 0.5 cph, is that associated with the diurnal oscillations, as evidenced by the sharpness of the peak and its harmonics. Furthermore, most of the spectral energy at both stations is concentrated in the across shore direction, as suggested by the wind roses.

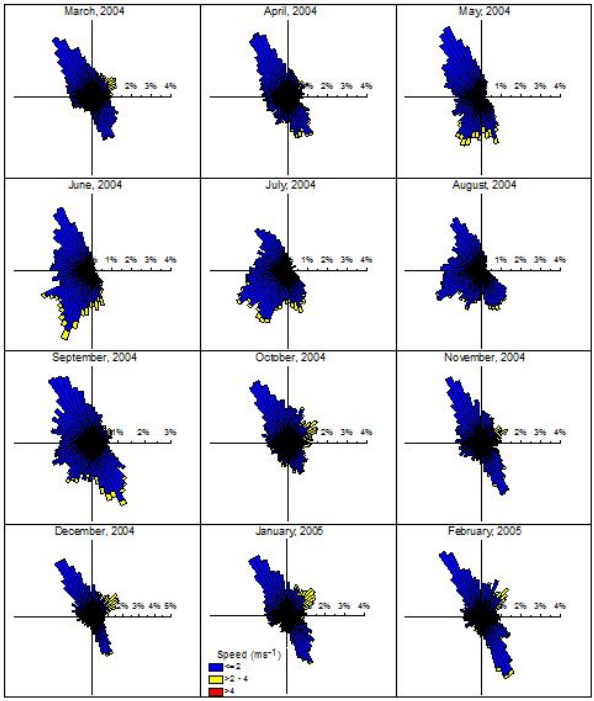

Figure 5.7: Monthly wind roses at Fura Station.

5.1.2 Temperature

Frequency distributions of hourly temperatures at Wajifo station (Figure 5.10) from March 2004 through February 2005 have been analysed in order to obtain detailed information as to what actual temperatures encountered during the months. Five minute interval records are the bases of all temperature data: the hourly mean is defined as the average of 12 values. Averaging by individual hours enables us to establish the average daily march of the temperature. Similarly, the daily means are computed as arithmetic means of 24 hourly means derived from

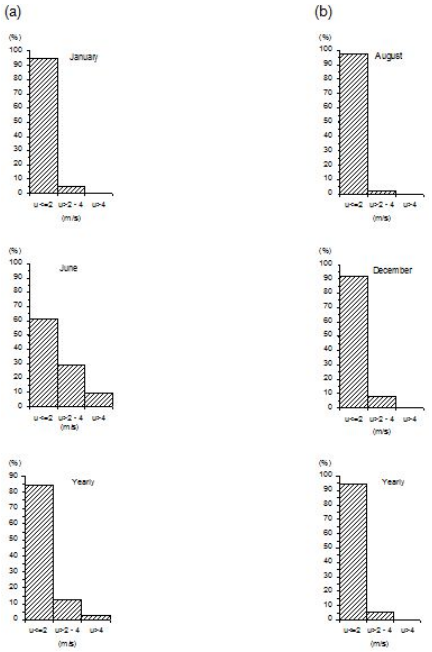

Figure 5.8: Speed class histograms at Wajifo (a), and Fura (b) stations during calmest (top), strongest (middle) and yearly average (bottom).

5 minutes interval records mentioned above.

Figure 5.10 presents the frequency distribution histograms of hourly temperatures using totals for each month. Here the problem to be investigated concerned the distribution of hourly temperature, regardless of the time of occurrence. Six temperature ranges distinguished ($\leq$ 10°C, >10-15°C, >15-20°C, >20-25°C, >25-30°C, > 30°C). Plots for each month are easily compared by observing the relative frequency of temperature ranges. These show considerable month-to-month variability in the temperature regime at Wajifo. The hourly temperatures were predominantly >20°C, (about 70-80% of the monthly hours).

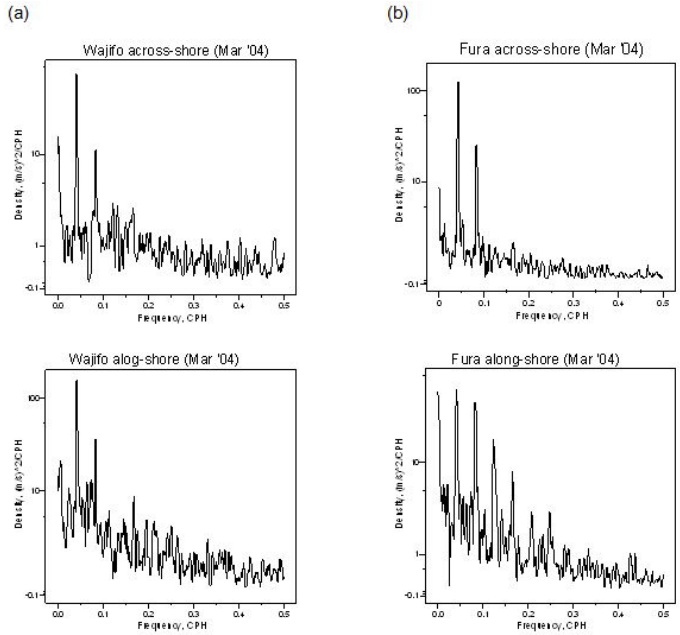

Figure 5.9: Typical monthly spectra of the two components of the wind vector at two stations.

Another marked feature in the temperature class histograms is the larger variability in March 2004 and from January through February 2005, and the smaller in July through September 2004. A third remarkable feature occurred in January and February 2005, respectively, where the coldest month (the hourly average temperature was < 15°C, for about 6% of the time) was fallowed by warmest month (the hourly temperatures were >30% for about 15% of monthly hours). The hourly average temperature gradient reached its maximum in August 2004.

It is of interest to investigate the descriptive statistics were computed for monthly totals (Figure 5.11) to obtain further information on the hourly temperatures variations during the year considered in this study. The annual mean temperature at

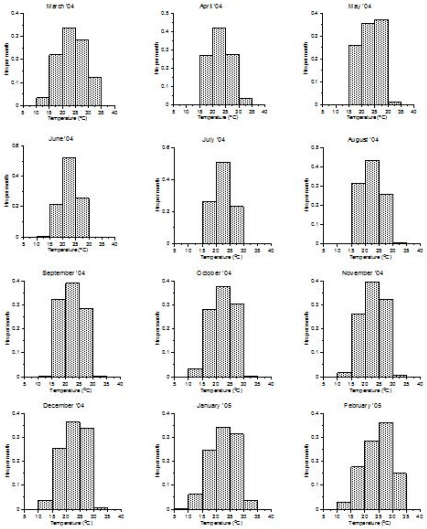

Figure 5.10: Monthly hourly average temperature frequencies at Wajifo Station.

Wajifo station was 22.9°C. Monthly variations in standard deviations found to be in good agreement with corresponding variations in the customary index of temperature, the mean daily range. The greatest average daily range of the year occurred in the warmest month of the year January 2005, while the least daily range averaged to 3°C in July 2004. A second general feature is that skewness of the monthly totals tended to be equally positive and negative during the year considered, but the differences from the normal are minor in general. The largest positive skewness and largest monthly minimum noted in April 2004, whereas a large negative skewness and a small monthly mean observed in January 005.

Month	n	Range	Minimum	Maximum	Mean	St. Dev	Skewness
Mar '04	744	14.3	12.2	35.3	23.8	4.937	0.004
Apr '04	720	10.5	17.1	31.5	23.0	3.647	0.423
May '04	744	10.2	16.8	31.4	23.3	3.598	0.060
Jun '04	720	8.6	14.7	28.8	22.6	2.896	-0.159
Jul '04	744	9.3	15.3	29.3	22.4	3.074	0.149
Aug '04	744	9.6	16.4	29.8	22.4	3.360	0.391
Sep '04	720	10.6	15.1	30.4	22.5	3.560	0.247
Oct '04	744	12.1	12	29.9	22.5	4.089	-0.124
Nov '04	720	11.6	12.2	30.5	22.8	3.835	-0.160
Dec '04	744	12.7	10.9	31.7	22.7	4.256	-0.207
Jan '05	744	13.4	10	31.4	22.7	4.746	-0.288
Feb '05	672	14.8	12.7	35.1	24.5	4.797	-0.280

Figure 5.11: Descriptive statistics of hourly average temperature in different months from March 2004 to February 2005 at Wajifo.

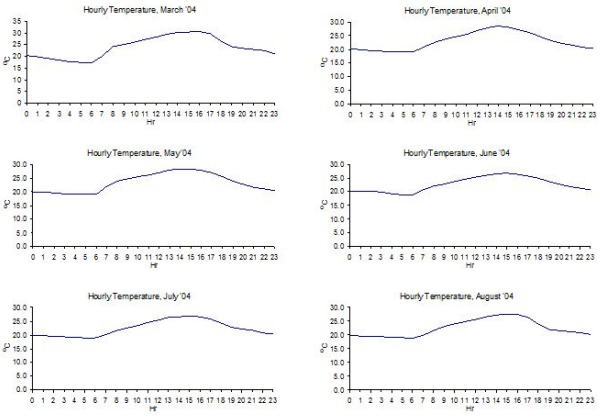

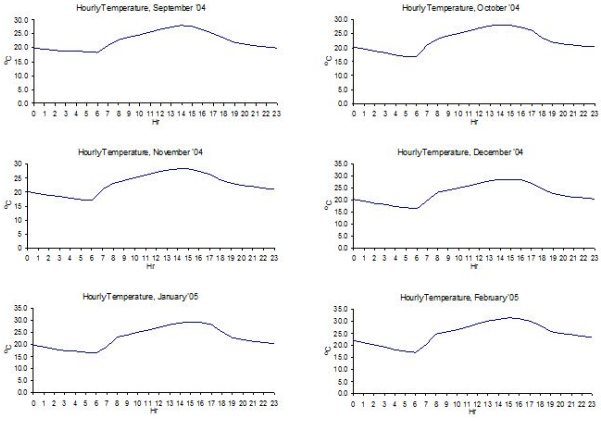

Figure 5.12: Diurnal variability of temperature at Wajifo Station.

Diurnal Variability of Temperature

As an indicator of human comfort, and also for purpose of applied climatology, it is important to know what percentage of the time various temperature are exceeded (at the earth's surface) during particular months at a given location (Spreen, 1956). Next in Figure 5.12 are shown the average values of air temperature, by hour of the day, for each month separately. The average 24 hourly values of a month are obtained as simple arithmetic means of the particular hours of an entire month. The resulting monthly averages over individual hours appear to be much more smoothened than would be expected from the hourly averages of daily observation considered alone. Nonetheless, close inspection of individual graphs shows systematic changes of the hourly variation of mean temperature. From 0600 to 0800 LST, rapid rise on the average appeared in all months, except from June through August 2004. Notice that maximum rise from 0600 to 0800 LST by 7.6°C noted for February 2005, minimum rise by 2.6°C for July 2004. The average traces show the temperature maximum oscillating during the period from 1400 to 1600 LST. In general, regular increase in temperature observed from 0800 LST to the period of maximum temperature, followed by a

mean temperature drop of less than 1°C on the next hour.

Interdiurnal Variability of Temperature

The discussions in the previous section about the range of variability of temperature considered the variations to which the average values are subjected. The task of this section is to investigate the variations from day to day. These are called interdiurnal variability (or IDV), and computed as the difference between either the daily mean or a fixed hour of a day and that of the next day (Conrad, 1947). Increasing temperature from one day to the next is called "warming", decreasing "cooling" (Conrad, 1942). Using these definitions the interdiurnal variability is computed for a daily averages and extremes for a time which lies close to the daily minimum on the one hand and to the daily maximum on the other hand.

Figures 5.13 and 5.14 show the interdiurnal variability of daily average temperature at Wajifo station. The primary modes of the frequency distributions of interdiurnal variability of warming tend to persist in the 0-1°C class interval throughout the year. On the other hand, two noticeable exceptions observed for the persistence of the primary modes in the 0-1°C class interval of interdiurnal variability of cooling frequency distribution during April and October 2004. Another remarkable fact to be noted is that the variability of cooling is found to exceed warming, except for May and November 2004 where they were nearly equally variable.

IDV	Mar	Apr	May	Jun	Jul	Aug	Sep	Oct	Nov	Dec	Jan '05	Feb
0 – 1	72.2	66.7	100.0	76.9	62.5	66.7	94.4	76.2	88.9	71.4	76.5	75.0
1 – 2	27.8	33.3	00.0	15.4	37.5	26.7	05.6	19.0	11.1	28.6	17.6	25.0
2 – 3	00.0	00.0		07.7	00.0	06.6	00.0	04.8	00.0	00.0	05.9	00.0
3 – 4				00.0		00.0		00.0			00.0	

Figure 5.13: Percentage frequency of the various values of daily mean IDV of warming (oC) at Wajifo

IDV	Mar	Apr	May	Jun	Jul	Aug	Sep	Oct	Nov	Dec	Jan '05	Feb
0 – 1	61.5	33.4	100.0	82.4	73.3	68.8	75.0	40.0	91.7	82.4	78.6	75.0
1 – 2	15.4	50.0	00.0	11.8	20.0	12.5	16.7	50.0	08.3	17.6	14.3	16.7
2 – 3	07.7	08.3		05.8	06.7	18.8	08.3	10.0	00.0	00.0	00.0	08.3
3 – 4	15.4	08.3		00.0	00.0	00.0	00.0	00.0			07.1	00.0
4 – 5	00.0	00.0									00.0	

Figure 5.14: Percentage frequency of the various values of daily mean IDV of cooling (oC) at Wajifo

Next Figures 5.15 through 5.18 present frequencies of differences from day to day close to hours of extremes. The primary modes of frequency distributions of warming in the 0-1°C and 1-2°C class intervals are nearly equally important at 0600 LST, 0-1°C being dominant at 1500 LST except for June and February when 1-2°C class interval was more significant. The dominant mode for cooling throughout the year is in the 0-1°C class interval, except in April and August 2004, when 1-2°C class interval was more important. The interdiurnal variability of warming and cooling are nearly the same at 0600 LST. At 1500 hrs day to day difference of warming and cooling found to be higher from March through April 2004, July through September 2004 and February 2005. The greatest interdiurnal variability of daily average warming was 2.3°C, while cooling was 3.5°C; at 0600 LST the corresponding values for cooling and warming, respectively, were 4.7°C and 6.1°C, and at 1500 LST greatest warming 7.8°C and cooling was 6.6°C. Thus the observed ranges of interdiurnal variability are smaller for cooling than warming.

The annual marches of the average and extreme values for daily average, 0600 and 1500 LST are to be seen separately for warming and cooling in Figure 5.19. Within one year period, the greatest warming was 7.8°C and the greatest cooling was 6.6°C. Overall, the variability was somewhat higher at 1500 LST than in the early morning. There seems slightly marked annual march of the interdiurnal variability at 1500 LST, with a high maximum in July through September and a deep minimum in November through January. Lack of marked annual march of

IDV	Mar	Apr	May	Jun	Jul	Aug	Sep	Oct	Nov	Dec	Jan '05	Feb
0 – 1	60.0	37.5	35.7	20.0	43.8	46.2	46.6	53.8	50.0	25.0	41.2	33.3
1 – 2	13.3	37.5	57.1	33.3	31.2	38.5	26.7	15.4	06.2	33.3	23.5	33.3
2 – 3	00.0	18.8	07.2	20.0	25.0	00.0	26.7	23.1	31.3	16.7	23.5	33.3
3 – 4	13.3	06.2	00.0	20.0	00.0	15.3	00.0	07.7	12.5	16.7	00.0	00.0
4 – 5	00.0	00.0		00.0		00.0		00.0	00.0	08.3	05.9	
5 – 6	06.7			06.7						00.0	05.9	
6 - 7	06.7			00.0							00.0	
7 – 8	00.0											

Figure 5.15: Percentage frequency of the various values of 0600 LST IDV of warming (oC) at Wajifo

IDV	Mar	Apr	May	Jun	Jul	Aug	Sep	Oct	Nov	Dec	Jan '05	Feb
0 – 1	62.5	57.1	64.7	20.0	40.0	66.6	40.0	44.4	50.0	36.8	50.0	53.8
1 – 2	12.5	21.3	23.5	33.3	33.3	16.7	33.3	44.4	07.2	31.6	14.3	38.5
2 – 3	06.2	07.2	05.9	33.3	06.7	16.7	26.7	05.6	35.6	26.3	07.2	00.0
3 – 4	18.8	07.2	00.0	13.4	20.0	00.0	00.0	05.6	07.2	05.3	21.3	07.7
4 – 5	00.0	07.2	05.9	00.0	00.0			00.0	00.0	00.0	07.2	00.0
5 – 6		00.0	00.0								00.0	

Figure 5.16: Percentage frequency of the various values of 0600 LST IDV of cooling (oC) at Wajifo

the interdiurnal variability at 0500 LST and for daily averages is explained by the shortness of the period of only one year. It is remarkable to note that warmings are slightly greater than coolings from day to day at 0600 LST, while this relation is the reverse at 1500 LST and for daily averages.

IDV	Mar	Apr	May	Jun	Jul	Aug	Sep	Oct	Nov	Dec	Jan '05	Feb
0 – 1	40.0	31.3	76.5	35.7	40.0	55.5	50.0	56.3	53.8	60.0	76.4	36.4
1 – 2	40.0	25.0	05.9	50.0	40.0	22.1	31.3	25.0	23.1	26.7	11.8	45.4
2 – 3	00.0	25.0	17.6	00.0	00.0	05.6	00.0	06.2	23.1	13.3	11.8	09.1
3 – 4	13.3	12.5	00.0	14.3	13.3	05.6	06.2	12.5	00.0	00.0	00.0	00.0
4 – 5	06.7	06.2		00.0	00.0	00.0	00.0	00.0				09.1
5 – 6	00.0	00.0			00.0	05.6	12.5					00.0
6 - 7					00.0	05.6	00.0					
7 – 8					06.7	00.0						
8 – 9					00.0							

Figure 5.17: Percentage frequency of the various values of 1500 LST IDV of warming (oC) at Wajifo

IDV	Mar	Apr	May	Jun	Jul	Aug	Sep	Oct	Nov	Dec	Jan '05	Feb
0 – 1	56.3	21.4	71.4	43.8	43.8	30.8	35.7	66.7	47.1	75.0	71.4	47.1
1 – 2	18.8	35.7	07.2	31.2	25.0	46.1	28.6	13.2	41.2	06.2	21.4	41.1
2 – 3	06.2	14.3	14.2	18.8	18.8	00.0	07.2	06.7	11.7	18.8	07.2	00.0
3 – 4	06.2	21.4	07.2	06.2	06.2	07.7	21.3	06.7	00.0	00.0	00.0	05.9
4 – 5	00.0	07.2	00.0	00.0	06.2	07.7	00.0	06.7				00.0
5 – 6	00.0	00.0			00.0	00.0	00.0	00.0				05.9
6 - 7	12.5					07.7	07.2					00.0
7 – 8	00.0					00.0	00.0					

Figure 5.18: Percentage frequency of the various values of 1500 LST IDV of cooling (oC) at Wajifo

Month	Warmings						Coolings					
	Average values			Maxima			Average values			Maxima		
	Daily	0600 hr	1500 hr	Daily	0600 hr	1500 hr	Daily	0600 hr	1500 hr	Daily	0600 hr	1500 hr
Mar	0.8	1.6	1.5	1.7	6.1	4.7	1.1	1.3	1.7	3.4	3.7	6.4
Apr	0.8	1.3	1.8	1.8	3.2	4.0	1.3	1.4	2.1	3.5	4.5	4.9
May	0.4	1.1	0.9	0.9	2.4	2.2	0.5	1.0	1.0	1.0	4.6	3.3
Jun	0.8	2.2	1.3	2.2	5.1	3.5	0.6	1.9	1.4	2.2	3.9	3.5
Jul	0.7	1.3	1.7	1.6	2.9	7.8	0.8	1.6	1.4	2.2	3.5	4.7
Aug	1.0	1.3	1.5	2.0	3.1	6.1	0.9	1.0	2.0	2.7	2.9	6.5
Sep	0.6	1.3	1.6	1.1	2.9	5.4	0.9	1.3	2.0	2.4	2.4	6.6
Oct	0.6	1.4	1.2	2.1	3.7	3.8	1.2	1.1	1.1	2.1	3.2	4.5
Nov	0.4	1.4	1.2	1.7	3.8	2.8	0.7	1.6	1.0	1.9	3.3	2.6
Dec	0.7	2.0	1.0	1.9	4.6	3.3	0.7	1.5	1.0	1.9	3.6	3.0
Jan	0.6	1.7	0.8	2.3	5.6	2.1	0.6	1.8	0.8	3.4	4.7	2.9
Feb	0.7	1.5	1.6	1.8	2.9	4.8	0.8	1.2	1.3	2.0	3.2	5.3
Yearly	0.7	1.5	1.3	1.8	3.9	4.2	0.8	1.4	1.4	2.4	3.6	4.5

Figure 5.19: Interdiurnal variability of temperature, oC, at Wajifo

5.1.3 Atmospheric Pressure Oscillation

The atmospheric pressure at any place is found to exhibit certain periodicities if averages are taken over a sufficiently long period of time. The best known of these periods are the diurnal, the semi-diurnal and the annual (Spar, 1950). In this section we shall consider one year records of surface observations of atmospheric pressure taken at 5-minute intervals at Wajifo station. Thus the basic data analysed here can hardly be regarded as adequate to represent the general atmospheric pressure oscillation.

In Figure 5.20 are shown monthly atmospheric pressure variations from which the mean has been eliminated. It is seen that the oscillations about the mean are stationary and the amplitude of the diurnal oscillation of the atmospheric pressure varies between 3.5 and 20.2 mb. It appears obvious at first sight that the fluctuations are mainly diurnal and semidiurnal, and larger amplitudes do not seem to occur more than a few days in the year considered in this study. The maximum hourly average atmospheric pressure value of about 891 mb was observed in September 2004, and the minimum value of about 873 mb was occurred in April 2004 and January 2005. The least and most extremes, respectively, were observed in the consecutive months May and June 2004. The lowest pressure was occurred in August, and the highest was observed in June. The total pressure range observed during each month was found to be nearly the same for most portion of the year. The observed large pressure changes occurred over different time intervals. For, example, pressure change of 22 mb in November 2004 occurred after only 2 days. On the other hand in May, the minimum monthly change occurred after 9 and 15 days. On 1 January 2005, the maximum pressure was 988 mb, the highest over 1-year period, 13 days later the pressure had fallen by 118 mb to 871mb.

Daily Variation of Mean Atmospheric Pressure

Figure 5.21 shows month-to-month changes of the daily variation of mean pressure. The data were organized in the form of 1-hr mean pressures for each individual month of the study period. Hourly means are centred at the start of the hour. To obtain a grand mean for a particular hour and particular month, say 0000 LST local time for March, each of the particular hourly means of the days was added together and divided by the total number of days in the month.

The times of maxima and minima wander, in apparently nearly systematic fashion, from hour to hour during the course of the year. A detailed examination of the data shows that double structure appeared in all months, February 2005 showing larger departure from the mean monthly pressures. The morning primary maxima appeared between 0600 and 0900 LST: at 0600 LST in two months, at 0700 LST in seven months, at 0800 LST in two months and only in one month at 0900 LST. Afternoon primary minima found at 1500 LST in three months and at

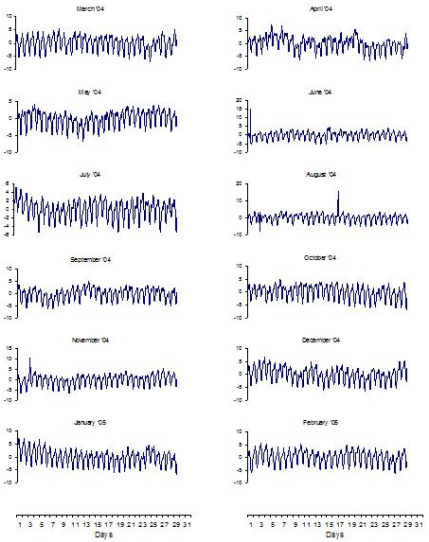

Figure 5.20: Atmospheric pressure oscillations from monthly mean at Wajifo Station.

1600 LST during the rest 9 months. Secondary maxima in the evening occurred at 2300 LST in nine months, at 0000 LST during the remaining three months. All months, except December, displayed the secondary minima at 0200 LST.

5.2 Sedimentology

5.2.1 Sediment Distribution

Four major units of surficial sediment deposits of Lake Abaya were recognized: (1) silty-sand; (2) clayey-sandy-silt; (3) sandy-silty-clay; and (4) silty-clay. These divisions are based on in situ visual inspection of the fresh samples and are used in this study. Most of the sediments of Lake Abaya consist of silty clay; pure sand rarely lies at the mouth of main rivers near shore; yet most sand also contains silt and clay in significant amount. A comprehensive map of sediment distribution

Time	Mar'04	Apr	May	Jun	Jul	Aug	Sep	Oct	Nov	Dec	Jan'05	Feb
00	1.30	1.20	1.24	0.90	0.82*	0.85	0.95	1.21	1.29	1.04	1.16*	0.92
01	1.03	0.78	0.88	0.63	0.65	0.58	0.78	0.98	1.10	0.91**	1.07	0.85
02	0.93**	0.53**	0.60**	0.46**	0.55**	0.48**	0.67**	0.98**	1.03**	0.92	1.00**	0.78**
03	1.12	0.57	0.70	0.52	0.66	0.52	0.83	1.19	1.16	1.03	1.15	1.03
04	1.60	0.91	1.03	0.84	0.99	0.88	1.21	1.58	1.54	1.48	1.65	1.58
05	2.18	1.39	1.57	1.42	1.51	1.38	1.66	2.17	2.15	2.16	2.31	2.33
06	2.84	1.90	2.13	2.04	2.02	1.83	2.27	2.89*	2.82*	2.91	3.00	3.13
07	3.19*	2.33	2.28*	2.33*	2.41	2.26	2.46*	2.71	2.67	3.06*	3.41*	3.52*
08	2.56	2.37*	2.03	2.28	2.43*	2.37	2.25	2.14	2.35	2.34	2.64	2.55
09	2.25	2.09	1.85	2.19	2.27	2.80*	2.05	1.89	1.87	1.92	2.21	2.35
10	1.70	1.64	1.34	1.78	1.89	1.96	1.56	1.25	1.26	1.28	1.65	1.87
11	0.87	0.79	0.64	1.03	1.07	1.24	0.66	0.20	0.24	0.27	0.64	0.92
12	-0.56	-0.46	-0.39	0.04	0.14	0.23	-0.58	-1.08	-1.10	-0.95	-0.64	-0.37
13	-1.85	-1.89	-1.63	-0.78	-0.98	-0.98	-2.04	-2.38	-2.42	-2.19	-1.99	-1.77
14	-3.09	-3.16	-2.80	-1.55	-2.04	-2.19	-3.26	-3.47	-3.54	-3.36	-3.28	-3.06
15	-3.99	-3.89**	-3.69	-3.17	-3.03	-3.25	-3.80**	-4.17**	-4.22	-4.13	-4.17	-4.08
16	-4.42**	-3.86	-3.91**	-3.64**	-3.59**	-3.83**	-3.74	-4.15	-4.27**	-4.28**	-4.48**	-4.47**
17	-4.23	-3.27	-3.32	-3.41	-3.40	-3.65	-3.12	-3.55	-3.58	-3.71	-4.17	-4.24
18	-3.24	-2.30	-2.41	-2.73	-2.66	-2.80	-2.22	-2.34	-2.41	-2.56	-3.06	-3.31
19	-1.81	-1.16	-1.28	-1.80	-1.80	-1.66	-1.11	-1.12	-1.04	-1.18	-1.71	-1.92
20	-0.66	-0.17	-0.23	-0.88	-0.96	-0.82	-0.18	-0.10	0.02	0.00	-0.57	-0.69
21	0.25	0.78	0.69	0.00	-0.17	0.10	0.58	0.71	0.74	0.78	0.40	0.27
22	0.91	1.39	1.21	0.58	0.45	0.76	1.05	1.15	1.09	1.10	0.83	0.86
23	1.32*	1.46*	1.46*	0.93*	0.79	0.94*	1.07*	1.31*	1.27*	1.16*	0.93	0.97*
Mean monthly pressure	873.31	873.69	874.09	876.32	874.76	875.15	873.99	874.25	873.58	873.18	873.58	872.33

Figure 5.21: Mean monthly pressure (mb) and departures from the mean monthly pressures. * denotes maxima of Diurnal Variation of Mean Pressure (DVMP), ** denotes minima of DVMP. Time is in Local Standard Time (LST)

constructed based on visual description of sediment samples is shown in Figure 5.23. The distribution pattern is basically simple with a natural sorting of sediment units reflecting the different energy-regimes of the lake. Figure 5.23 demonstrates the courser nature of sediments near the mouth of the major rivers as well as exposed shallow regions parallel to the shorelines. The nearshore sediments are characterized by the high sand contents.

The general bathymetry of the lake is shown in Figure 5.22. The main basins are generally slop gently or flat bottomed and the shore areas usually have steep slope. The north basin is relatively more flat-bottomed and shallower with maximum observed depth of about 14 m, whereas the maximum water depth measured in the south basin is about 20 m, decreasing towards the east.

In shallow areas, particularly in the northernmost of the lake at Bilate River delta, the sand silt deposit extended southward. Marked Increase in the sand population of samples taken near the mouth of major tributaries and the narrow passage between Gidicho Island and east shoreline in the north basin suggests a possible higher energy environment. This shows that the regions displaying the best-sorted sediments confined to nearshore zones, essentially to the mouth of the rivers in association with courser sediment, though some samples from deep and with hilly surrounding topography show a high fine material content. Regions of highest energy in the lake, occurs around the periphery of the lake in the nearshore zone. It is interesting that this zone predominates in the northern and eastern shores of the lake and is absent from regions with hilly surrounding topography.

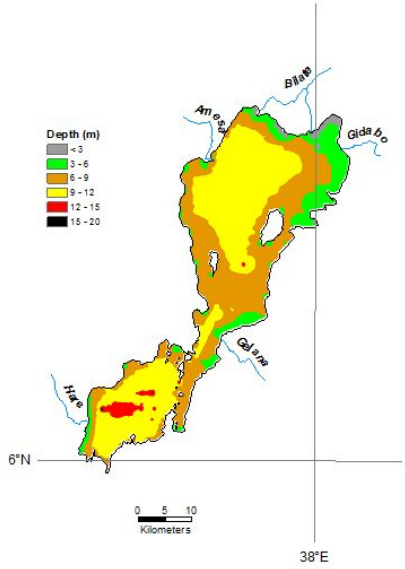

Figure 5.22: Bathymetry map of Lake Abaya.

The bulk of the remainder of the lake is composed of sediment with high fine fraction which indicates the main depositional basin and part of the nearshore zones. The changes occurring in the sediment textural characteristics from a nearshore environment through a zone of mixing associated with decreasing energy to an offshore zone is which the sediments are derived primarily from suspension. These zones representing decreasing energy from nearshore to offshore environment verified by the textural characteristics. The basin sediments are composed of fine grained, soft, sandy-silty-clay, grey black, grey, to reddish brown in colour. Exception is consolidated dark grey between the largest island in the south basin and the east shore and the sheltered zone near west shore in the north basin.

Near the shore line the sediment colour is dark grey to black except the water-sediment interface. A thin oxidized microzone of reddish brown, varying in thickness was observed at the surface of all mud samples. The black grey colour dominates near the east shores of the northern part of the south basin and the north basin, whereas the grey to brown colour is present near the west shore. The reddish brown clay at the most top surface of the recent mud increases towards the centre and south. This increasing reddish brown clay at the top suggests the fine materials derived mainly from suspension are deposited at the low energy zones. The coarsening of the grain sizes can be observed by the decrease of the reddish brown at the most top at the water sediment interface and darkening of the underlying light grey and brown to black grey onshore.

5.2.2 Sediment composition

The sediments of Lake Abaya contain variable amounts of quartz, feldspar (essentially sanidine and andesine), clay minerals, calcite, and organic and carbonate carbons, with possible traces of hematite, magnetite, pyrite and hornblende in some samples. Hematite and magnetite were often detected in several samples. The presence and absence of these different minerals is a clear function of location. This section presents some data on the horizontal heterogeneity of major chemical and mineralogical components of the lake sediments. The detailed mineralogical composition is given in Appendix A.

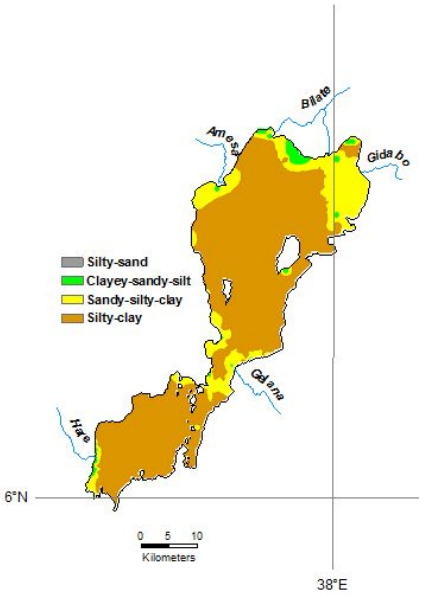

Figure 5.23: Surficial sediment distribution in Lake Abaya.

Quartz

The quartz content is found to be within the range of <1 to 40 percent. With respect to quartz concentrations in surfical sediments, the lake basin may be partitioned geographically (Figure 5.24). Percent content of quartz is high (> 20 percent) in the areas close to the mouths of the major rivers entering the lake in the north basin, except Shope River where the quartz fraction settled in the flat flood plain before reaching the lake. Although relative amounts of quartz are not significant in most Lake Abaya sediments, they are nevertheless useful indicators of sedimentation patterns.

The influence of major streams in the distribution of sediment in the north basin

is illustrated by the fact that sediments of the quartz fraction carried significant distance from the river mouth by flow current before setting. The general trend for horizontal distribution of quartz minerals is decrease to the centre of the main basins and from north to the south. Samples from the south basin contain quartz within 10 percent. It is interesting to note that the main depositional zone of sediments in the north basin contain quartz content in the range of 5 to 10 percent, whereas the south basin has less than 5 percent in the majority of samples both from onshore and offshore. In general, the quartz content of surficial sediments show decreasing tendency towards to the south. Thus, considering the quartz population in Lake Abaya, it is convenient to define the north end as the area of high concentration and the south end as the area of low concentration.

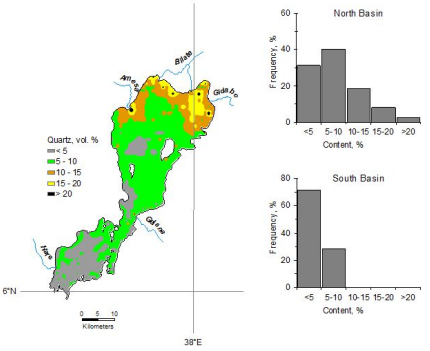

Figure 5.24: Quartz distribution in surfacial sediments of Lake Abaya.

Feldspar

One of the most abundant constituent minerals in Lake Abaya sediments is feldspar. All surficial sediments collected from Lake Abaya contain feldspar. However, there is considerable variability (Figure 5.25): relatively high concentrations associated with nearshore sediments and with stream deltas where the winnowing (erosion) action of waves or currents is not effective in preventing deposition of feldspar rich inputs. Thus, distribution of feldspar followed nearly similar pat-

terns in both north and south basins. Lake Abaya sediments contain substantial quantities of feldspar ranging from 3 to 76 percent (overall mean total feldspar of about 28 percent).

Highest feldspar contents (more than 60 percent) are observed along the west and north shorelines near the mouths of major tributaries and the lower feldspar contents occur around the centre of the main basins. The distribution structure at the area of the narrow connection of the north and south basins at the bottleneck parallels that of the nearshore zones. It is important to note that samples taken from the station close to the shoreline but within the influence of cliffs or hilly surrounds have lower feldspar content. The general feldspar concentration is less than 20 percent in the main basin, distribution in the north basin being slightly more variable than in the south basin.

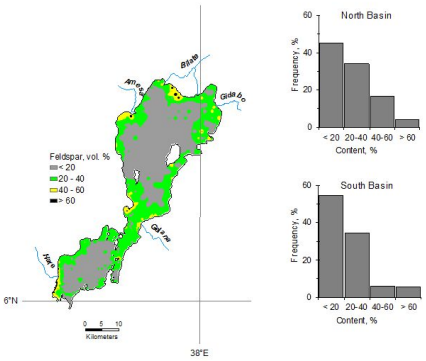

Figure 5.25: Distribution of feldspar in surficial sediments of Lake Abaya.

Clay

Total clay minerals distribution in surficial sediments of Lake Abaya is shown in Figure 5.26. Clay minerals are the most abundant mineral fractions in Lake Abaya sediments. Total clay minerals at each sampling site were calculated by subtracting quartz, total feldspar, calcite, organic matter and other traces, if any,

of hematite, magnetite, pyrite and hornblende from the total sediments. Organic matter was computed from organic carbon using a factor of 1.72 (Schoettle and Friedman, 1973). Clay content computed from quartz, carbonate, and organic carbon, however, is probably a more precise method which is more desirable for the interpretation of geochemical data (Thomas, 1968).

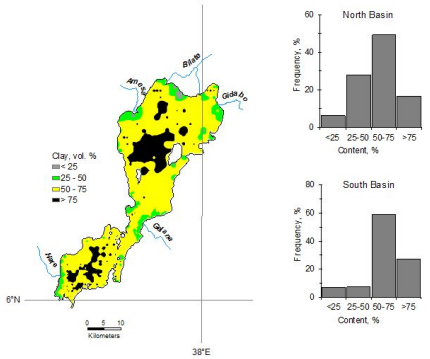

Figure 5.26: Distribution of clay in surficial sediments of Lake Abaya.

Clay mineral content ranges from 6 to 96 percent with a mean of 61 percent. Relatively low concentration of clay minerals is associated with nearshore sediments and stream deltas where the winnowing action of waves or currents is effective enough in preventing deposition of fines. Sediments with less than 25 percent of clay (hence mostly sandy) are restricted to the west shoreline and northernmost part close to the mouth of major rivers (Figure 5.26). Clay minerals show the expected general distribution pattern, with relatively low values in nearshore sediments increasing to maximum concentration at the centres of the main basins. Further noticeable patterns in clay distribution are: (1) increasing clay concentration in the nearshore sediments collected from stations surrounded by cliffs or hills; (2) generally low clay concentration at the narrow bottleneck transition and narrow passage between the largest Gidicho Island and east shore; and (3) southward increasing tendency.

Calcite

The calcite distribution in Lake Abaya is shown in Figure 5.27. Most samples contain only small quantities of calcite, and its amount ranges from less than 1 to 24 percent. Similar distribution patterns are observed in the north and south basins. Calcite is relatively more abundant in the shoreline than in the main basins sediment samples of both north and south basins. No general trend is observable, but higher calcite values occur around narrow passages such as the area of bottleneck connection and to the east of Gidicho Island. Similar amounts of calcite values observed in the west shoreline of south basin.

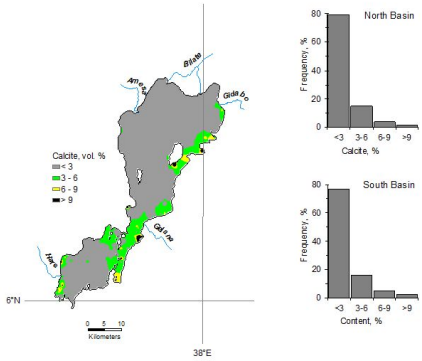

Figure 5.27: Distribution of calcite in surficial sediments of Lake Abaya.

Organic Carbon

The organic carbon distribution in surficial sediments is shown in Figure 5.28. Organic carbon is generally low throughout the lake ranging from less than 1 to 16 percent. Few values of organic carbon exceed 3 percent and most of them contain between 0.5 and 1.0 percent in both south and north basins. The highest organic carbon content was observed in the delta of Gelana River. Organic mater is more evenly distributed in the main basin and high organic carbon contents are confined to nearshore zones. It is readily observed from organic carbon

distribution (Figure 5.28) that organic muds settled more rapidly close to the input points. A decline in organic carbon to the west is observed around the area of narrow bottleneck transition. Sediments from the western part of the narrow transition were mostly depleted of organic carbon. A marked difference is apparent between the organic sediment distribution in the sediment samples from deltas of the eastern and western major tributaries. Sediment samples from the deltas of eastern major tributaries showed higher relative abundance of organic carbon. Similar amounts were observed in the northern part of the south basin.

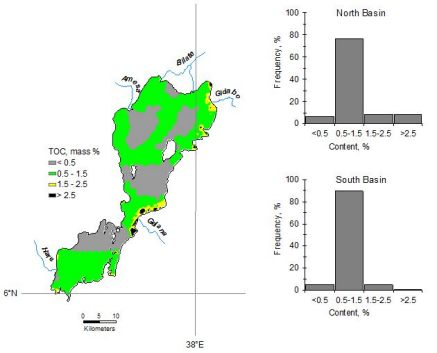

Figure 5.28: Distribution of organic carbon in surficial sediments of Lake Abaya.

Carbonate Carbon

The distribution of carbonate carbon in the surficial sediments of Lake Abaya is presented in Figure 5.29. Carbonate carbon is generally low throughout the lake ranging from 0 to 3 percent. No general trends observable but higher carbonate carbon values occur along the eastern shoreline and in the bottle neck connection in the middle. Few values of carbon exceed 1 percent and most of the sediments in Lake Abaya contain less than 0.5 percent carbonate carbon. The sediments of the narrows have increased carbonate carbon. From x-ray diffraction results, all the carbonates appear to be in the form of calcium carbonate with no siderite or dolomite resulting parallel distribution pattern with calcite.

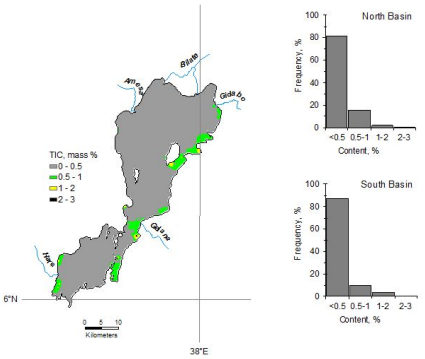

Figure 5.29: Distribution of carbonate carbon in surficial sediments of Lake Abaya.

Trace Minerals

Trace minerals detected by X-ray diffraction are principally hematite, magnetite, pyrite and hornblende. Widespread traces of hematite occurred in surficial sediments of Lake Abaya (Figure 5.30). The general distribution pattern shows increasing tendency southward. The amount of hematite observed in the north basin is mainly less than 2 percent with occasional occurrence between 2 - 4 percent. It is observed that hematite is an important constituent of samples from south basin. The distribution in the south basin does not have obvious pattern except increase towards the centre of the basin.

The distribution of magnetite in the surficial sediments of Lake Abaya is presented in Figure 5.31. This distribution, however, is quite variable over the lake basin; increasing tendency towards the mouth of main streams in the western side is evident. It is interesting to note that the maximum concentration is observed in the deepest sampling site in the south basin. Similarly, increasing concentration in the north basin was observed around the deepest zone. Another feature of magnetite distribution is that most of the samples from south basin are found to have magnetite than the counterpart samples from the north basin.

The pattern of spatial variability for concentration of pyrite has some similarity

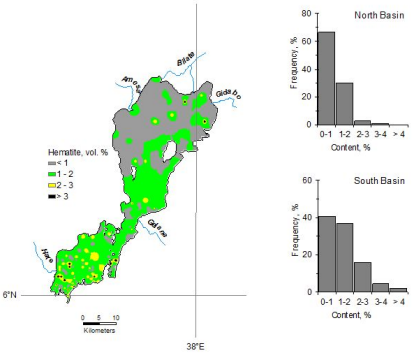

Figure 5.30: Distribution of hematite in surficial sediments of Lake Abaya.

with that of hornblende. Both minerals detected rarely and showed no obvious trend in both south and north basins. Pyrite was detected in more samples from the south basin than from the north basin. The concentration of hornblende also exhibited similar but less pronounced patterns. Larger concentration of pyrite and hornblende are found in the south basin surficial sediments than in surficial sediments of the north basin. The largest pyrite was found near the Hare and Amesa deltas. Like pyrite, the largest concentration of hornblende was also found in the Hare Delta. On the other hand, pyrite concentrations were substantially smaller (less than 5 percent) than hornblende concentration (5 to 13 percent).

5.2.3 Interrelationships between Variables

A correlation coefficient matrix summarizing the relationships between variables (minerals, water depth) is given in Figure 5.32. With 706 samples were used in the analysis, a correlation coefficient greater than 0.091 is significant at the 1 percent confidence interval. The expected high degree of relationship between water depth and clay content is obvious from Figure 5.32. A comparison of bathymetric contours with the distribution of clay minerals shows that the deeper parts in both basins of the lake are underlain by clay, whereas the shallower parts bottomed by silty sands. Exceptions to this fact are the sheltered near shore regions

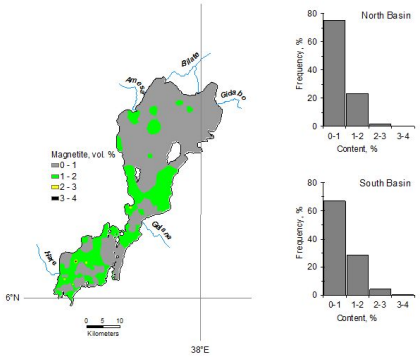

Figure 5.31: Distribution of magnetite in surficial sediments of Lake Abaya.

where reduced circulation by wind allows clay size material to deposit. Clay and feldspar show strong but inverse relationship indicating that high clay content is associated with low feldspar content. It is further demonstrated that feldspar has strong but inverse (or indirect) relationship with depth.

Examination of Figure 5.32 shows that with increasing water depth there is a decrease in feldspar, quartz, calcite and organic carbon. Another obvious relationship in Table 5.10 is direct relationship between calcite and carbonate carbon, as expected. Clay correlated inversely with quartz and calcite.

Organic carbon contents show inverse correlations to depth as discussed previously and direct correlation to calcite, and poor but significant yet inverse correlation to clay. A comparison of lake bottom morphology with organic carbon content and sediment colour shows that interrelationship exists between these variables. The thin sediment deposits of reddish-brown colour at sediment water interface in the shallow parts of the lake are dark-grey to black. In the deeper parts of the lake, sediment colours change to light grey to reddish-brown and the organic carbon content is low.

Samples from the deltas of the major tributaries contain variable mixtures of clay, quartz, feldspar and calcite and various minerals detected in traces (Figure 5.33).

	Quartz	Calcite	Feldspar	Clay	Hematite	Magnetite	Pyrite	Hornblende	TIC	Organic Carbon
Depth	−.366	−.280	−.651	.688	.206	.045	−.155	−.018	−.285	−.317
Quartz		−.129	.048	−.240	−.161	−.247	−.108	−.071	−.139	−.080
Calcite			.208	−.336	.026	.091	.150	.112	.922	.267
Feldspar				−.942	.027	.253	.222	.168	.221	.106
Clay					−.041	−.229	−.286	−.319	−.324	−.224
Hematite						.217	.028	.018	.032	−.058
Magnetite							.099	.129	.046	.020
Pyrite								.219	.183	.125
Hornblende									.081	.064
TIC										.196

Figure 5.32: Correlation coefficient Matrix

Samples from Amesa, Gidabo and Bilate River mouths have in total higher quartz contents than mouths of others. Traces of pyrite are observed in samples from Amesa and Hare deltas. Feldspar concentrations are highest along the western shoreline; while clay mineral contents are highest in the north and east rivers deltas. Along a transect from west to east there is no clear trend except a more marked increase or decrease of major minerals near shore zones.

5.2.4 Cluster Analysis

A cluster analysis, using the Ward method, resulted in six groups of sediment samples that differed primarily with respect to their relative mineralogical compositions (Figure 5.34). The main differences between the groups are reflected in the mean percent of the sediment samples (Figure 5.35). The number of samples included in the clusters range between 40 and 239, with minimum and maximum numbers corresponding to clusters 6 and 3, respectively. Feldspar and clay are generally characterized as the most variable minerals across the clusters. All samples included in Cluster 2 from North Basin have above average quartz content. Majority of samples rich in quartz are included in clusters 1 and 2, whereas those rich in calcite, feldspar and hornblende are included in clusters 5 and 6.

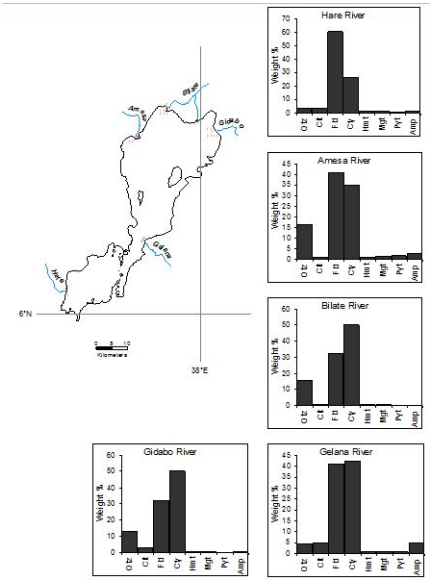

Figure 5.33: Average mineral compositions at deltas of major tributaries.

These samples are located in the deltas of tributaries, while such samples are absent from the central part of the lake basin. By contrast, clusters 3 and 4 mainly occur in samples from the central basin, or are generally characterized by highest values of clay and lowest values of feldspar, quartz, calcite and hornblende.

5.3 Water Quality

5.3.1 Water Temperature

Water temperature at fixed stations in Lake Abaya varied from 21.9°C to 30°C, with an overall average of 24.1°C (n = 571). The minimum water temperature at all fixed monitoring stations observed in late June and July 2004 field sessions when stations were visited at different times between 1000 and 1700 local

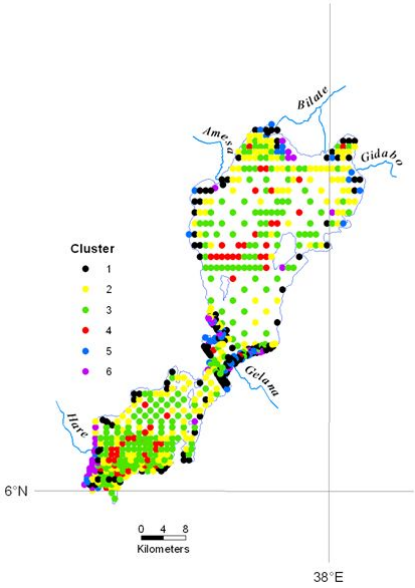

Figure 5.34: Clusters of sediment samples distinguished on the bases of relative mineralogical contents.

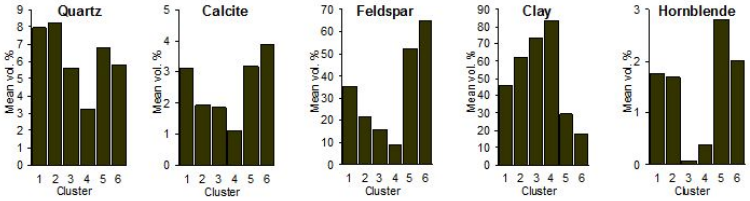

Figure 5.35: Average mineralogical contents of identified clusters.

standard time (LST), whereas the maximum temperature measured near-surface

in various months when the stations were monitored in the afternoons (Figures B1, B2 and C1, Appendixes B and C). In fact, the time of sampling of the depth profile did not necessarily capture the daily extremes. Because of the high irradiance and the low river inflow during the study period, the lake water commonly attained temperature >20°C throughout the lake. However, it is more likely that the overall cooler temperature of the lake in June and July 2004 than other months from March through October 2004 was determined by a combination of temperature of inflows as well as climatic factors.

Contour plots of temperature profiles at fixed monitoring stations shown in Figures B1 and B2 displayed at bimonthly and monthly sampling intervals for the stations located in the south and north basins, respectively. It is sown that the temperature vitiations in the water column were small. Further, the well mixed conditions from near surface to near bottom, which prevailed during most of the field sessions, are indicated by the nearly vertical isolines. Thus, given its shallow depth and prevailing diurnal wind structure, the Abaya Lake water exhibited very weak thermal stratification, amounting an average temperature differential of about a quarter of a degree per meter positive upwards.

Temperature variations occurring near-surface were confined to the top layer of about 2m thick (Figures B2 and B3). The near-surface water temperature associated with each of the depth-profile measurements indicates that the lake water was warmer in the afternoon by up to 5°C than at 1-m depth when the prevailing wind was light. This was documented by the maximum variation between near surface and 1-m depth observed on 19 May 2004 (Julian day 140) around 1500 LST at station S6 in the north basin when variable winds less than 2 ms^{-1} (and more than 70 percent of the 5-min interval records being less than 1 ms^{-1}) at Wajifo Weather Station prevailed until the sampling time.

To examine the relation between weather and temperature in the lake, the air temperature records at Wajifo Weather Station during sampling dates from the nearest stations S7 and S4 in the north and south basins, respectively, were considered. Since the depth-profiles taken only once during each sampling session were not adequate to examine closely the relation between temperature in the lake and air temperature, 5-minute interval air temperature readings were smoothed with the recent 1-hour records before taking depth profiles. The corresponding

average of air temperature records from Wajifo Weather Station were plotted with the average of near-surface and 1-m depth water temperature (Figure 5.36). It is indicated that the fluctuations in the average water temperature nearly parallels the recent 1 hour averages of 5 minute interval air temperature records, water temperature being warmer than air temperature when measurements were taken before noon.

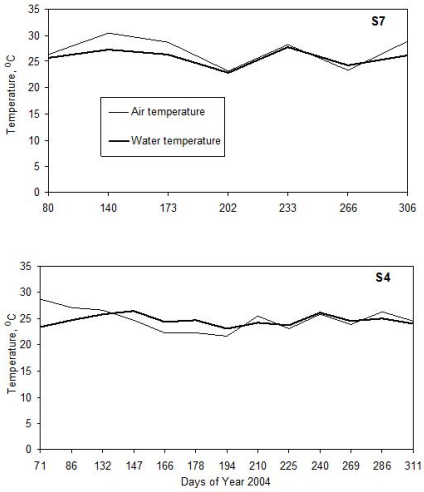

Figure 5.36: Comparisons of daily average temperature at Wajifo Weather Station and near surface water temperature at nearest fixed stations from south (S4) and north (S7) basins.

The water temperature averaged over the water column at fixed monitoring stations during the sampling days of Year 2004 and the corresponding monthly averages of air temperature records at Wajifo Weather Station were shown in Figure C1. Average temperatures ranged between 22.2 and 27.2 (n = 75). In general, temperature in Lake Abaya exhibits weak seasonal signals, the successive bi-monthly and monthly averages of depth profiles in the south and north basins, respectively, varying up to 4.8°C and 2.2°C. Further, nearly similar trend of the monthly averages between fixed monitoring stations were found. On the other

hand, the spatial variability of up to about 5oC was measured on a given sampling date between about 1000 and about 1600 LST at the same water depth. Such differences that appear to be spatial because of change in value from one station of the lake to another can be temporal due to the time taken to travel between the monitoring sites.

5.3.2 pH

The values of pH at fixed monitoring stations in Lake Abaya ranged from 8.8 to 9.3 (overall mean = 8.9, n = 571). The maximum pH value of 9.3 was observed in the north basin on Julian days 79 and 80 at stations S5 and S7. Other stations monitored on the same dates had values of 9.1 and 9.2 at stations S6 and S8, respectively. Thus, when high pH values were observed, it was common to measure them at most of the station in the lake. Bimonthly measurements of pH values exceeded 9.0 only on Julian day 147 (around the end of May) field session in the south basin. The lowest values of pH observed at stations close to the mouth of major tributaries. The depth profile data shown in Figures B7 and B8 indicate that vertically homogenous pH value occurred mostly, or that condition near the surface can be different from other measurements by 0.1 unit increment occasionally. Further, horizontal spatial structure on a given sampling session is virtually absent.

The monthly and bimonthly measurements at fixed monitoring stations were analysed for the frequency distribution of pH values. Results for March through October 2004 demonstrated that an excursion into pH value greater than 9 units was a relatively rare event (about 7% when all stations and depths combined). Another remarkable feature of the profile data is the geographical dependence of the frequency distribution pH values. The pH value of the largest percentage of the data (more than 80%) were observed to be not greater than 8.9 at stations situated close to the mouths of the major tributaries.

5.3.3 Conductivity

Water conductivity at fixed monitoring stations in Lake Abaya ranged from 861 to 1162 μScm^{-1} (overall mean = 1124 μScm^{-1}, n = 571). The minimum con-

ductivity was observed at station S2 on Julian day 286 (around mid of October), whereas the maximum conductivity observed at station S4 on Julian day 240 (around end of August). Except for one field session mentioned above, conductivity at station S2 was found to be high (>1110 μScm^{-1}). Conductivity in the south basin stations generally exceeded those of the stations in the north basin. During the study period, conductivity differentials of the depth profiles at fixed stations amount about 40-296 μScm^{-1} in the south basin, and about 30-119 μScm^{-1} in the north basin. There is no clear seasonal signal in conductivity at fixed stations other than specific and marked decline at stations close to the mouth of main tributaries. Conductivity near surface displayed lower values at stations S1 and S2 in the south basin during Julian day 286 sampling event (Figure B3).

The depth profiles structure of conductivity at fixed stations shown in Figures B3 and B4 are obscured because there is such relative constancy or noisy character in conductivity. Overall, the higher frequency (> 90 percent) of water conductivity was greater than 1100 μScm^{-1}. It is shown in Figure C2 that the average conductivity distribution is predominantly a north-to-south gradient of increasing conductivity. Time related variation of the average conductivity at fixed stations in the north basin showed gradually increasing trend, whereas stations in the south basin exhibited initially high levels decreasing until Julian day 132 (around mid May), gradually increasing until Julian day 269 (around end of September, then gradually decreasing (Figure C2).

5.3.4 Dissolved Oxygen

Dissolved oxygen in water column at fixed monitoring sites was found to be in the range of 5.4 - 7.9 mg.L^{-1} (mean = 6.8 mg.L^{-1}, n = 571). An overall analysis of the depth profile reveals that a large percentage of the data (about 75 percent) is made up of concentration of dissolved oxygen (DO) greater than 6.5 mg.L^{-1}, and concentrations less than 6.5 mg.L^{-1} did not appear before Julian day 240 (around end of August) at site S1, or even not before October at other stations (Figures B5 and B6). The minimum value of DO was observed at station S2 on Julian day 286 (around mid October) near surface and at station S9 on Julian day 306 at 0.5m and 1m depths above the lake bed, whereas the highest value obtained on Julian day 71 (March) at station S3. In general, the content of dissolved oxygen

fluctuated mostly (> 90 percent) in the range of 6-8 mg.L^{-1} in the depth-profile dataset, and occurrences of dissolved oxygen values less than 6 mg.L^{-1} were rare during the study period.

The vertical stratification is rare and slight as shown in Figures B5 and B6, the maximum gradient amounting on the order of 0.1 ppm/m increasing uniformly upward. In general, vertical variation in dissolved oxygen was insignificant; and a relatively slight stratification in DO observed in deep water. Even little variations in the vertical structure of DO are found to be confined to the top 1 m layer of the water body. There is no apparent correlation with depth in stratification, although low DO events occur primarily in the measurements at depth. Occasional profiles show uniform DO throughout the depth. General trend of slightly declining DO concentration occurred starting July, 2004.

Figure C3 shows mean values for dissolved oxygen obtained from depth profiles measured once at each site during regular field sessions around between 0830 and 1500 LST in the south basin and around between 0930 and 1730 LST in the north basin. Mean dissolved oxygen of each sampling event was found to generally high throughout all fixed sites. There was slightly different time-related variation of DO between south and north basins. In the south basin, initially high levels decreased until Julian day 132, increased on Julian day 147 and staid nearly constant at that level until Julian day 194, then decreased gradually. On the other hand, the north basin average DO values stayed constant until Julian day 173, then gradually decreased at constant rate in the remaining sampling sessions. The mean of overall profile data at each fixed station also indicates that average dissolved oxygen concentrations at fixed monitoring sites are uniformly high (Figure C3). Exception to this is the average of two measurements taken at station S9 which showed slightly lower dissolved oxygen mean.

5.3.5 Suspended Solids

Water column profile of total suspended solids (TSS) concentrations in Lake Abaya at fixed monitoring sites observed to have great variability in the range 4 - 404 mg.L^{-1} (overall mean = 77 mg.L^{-1}, n = 327) during the study period. The average concentration of the TSS from the south basin was 50 mg.L^{-1}, n = 208, and from the north basin 123 mg.L^{-1}, n = 119, whereas the maximum

concentrations were 181 mg.L^{-1} and 404 mg.L^{-1} for the stations in the south and north basins, respectively.

Suspended solids in Lake Abaya have a close geographical association with regions of inflow and stations remote from river inputs. The depth profile dataset revealed that the maximum total suspended concentration was observed at station S9, whereas the minimum concentration was observed at station S6 at a depth of 1m above the lake bed. Overall, TSS concentrations were higher at stations close to major tributaries, as expected. On the other hand, maximum range of station values observed at stations S2 and S7 in the south and north basins, respectively, whereas the minimum ranges of station values found at station S9 in the north basin and station S4 in the south basin.

Stratification in TSS is usually noisy, especially at stations located in the deeper central parts (Figures B9 and B10). Few samples taken from fixed sites S8 and S9 in the north basin displayed higher, but nearly homogenous TSS concentrations. This is no doubt due to the riverine inflow containing high proportion of fine grained particulates. It is important to note that significant concentrations of TSS found in samples taken from various depths at stations situated far away from main tributaries and central parts of the lake. This suggests that fine sediments that easily maintain in suspension account for most of the material carried by the river and are largely transported as suspended sediment.

The most remarkable feature of TSS observed during this study is more frequent occurrence of low TSS concentrations near the bed than near water surface at deeper sites. Figure 5.25 presents comparisons of TSS concentrations found at three depths (near surface, at 2 m water depth, and at 1m above the bottom) on sampling days of Year 2004. The highest frequency (about 67 percent of sampling sessions) of occurrence of higher TSS concentration near surface than near bed were found at deep and central station in the south basin (S4). At the same site, samples taken from 2m depth had more frequent (about 73 percent) occurrence of higher concentrations than samples taken 1m above the lake bed. In the central part of the north basin, stations S5 and S6 had equal frequency (50 percent) of occurrence of higher TSS concentrations near surface than near the bed.

Averages of depth profiles indicate the relative importance of inputs from differ-

ent main tributaries (Figure C4). Graphs corresponding to stations in the south basin show erratic and complicated changes of bimonthly variations in average TSS concentrations. It is interesting to note that the general trend at station S5 in the north basin parallels the averages of stations S6 and S7 upstream. Because station S7 is mainly influenced by Amessa River input, other main tributaries have a modifying effect to station S5 downstream. Further, the declining trend during the initial bimonthly sampling sessions at station S4 in the south basin nearly parallels the general trend of the nearest monthly sampling station S5 in the nearest sampling date in the north basin.

5.3.6 Dissolved Solids

Total dissolved solids (TDS) concentrations obtained from some water samples taken from fixed monitoring sites in Lake Abaya range 618 - 1206 mg.L^{-1} (mean = 872 mg.L^{-1}, n = 193). The maximum and minimum TDS concentrations depth profiles were observed in October 2004 during different field sessions at stations S4 and S9 in the south and north basins, respectively. Like TSS concentrations, no obvious vertical stratification was observed, and occurrences of higher TDS near surface than near lake bed were also common (Figures B11 and B12). The range of the TDS concentrations at fixed stations showed maximum values at S4 and S6 in the north and south basins, respectively, whereas the corresponding minimum values were found at stations S1 in the south end of the lake and at station S8 at the north end and close to the mouth of the largest tributary.

Mean TDS concentrations at fixed stations show that monthly data from north basin were more variable between sampling sessions than bimonthly data from the south basin (Figure C5). A close look at the mean data structure revealed nearly uniformly constant mean TDS concentration appeared from Julian day 132 through 225 at station S1, whereas gradually decreasing trend observed in other fixed sites in the south basin during the same time period. Exception to this is TDS starting to increase at stations S3 and S4 after sampling session on Julian day 194. This trend is followed by uniformly increasing trend in all fixed sampling sites, reaching the maximum values of about 1116 mg.L^{-1} at station S2, and 1190 mg.L^{-1} at station S4 during the rest of the sampling sessions. Although there is no systematic variation between sampling sites in the north basin,

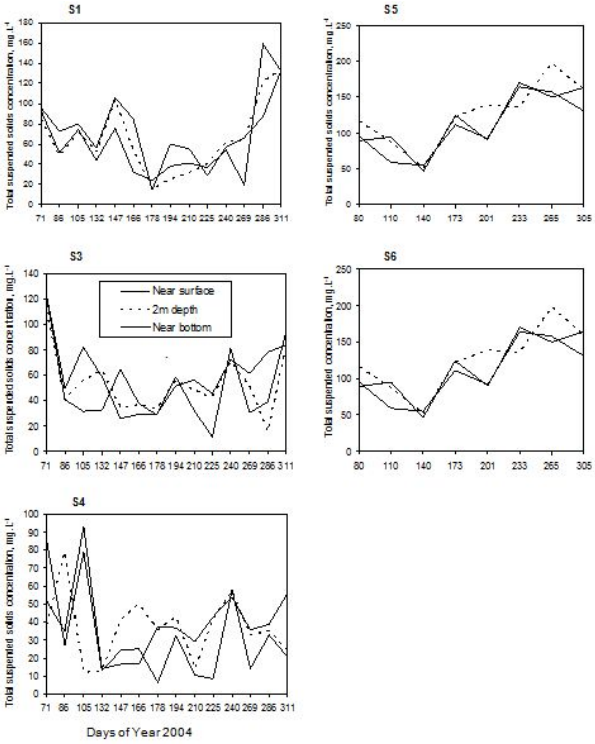

Figure 5.37: Comparisons of total suspended solids concentrations at three depths during sampling days of Year 2004.

the general variation between sessions followed similar fashion. Another spatial structure of the TDS concentration was that overall averages are higher at stations situated far away from the mouths of major tributaries.

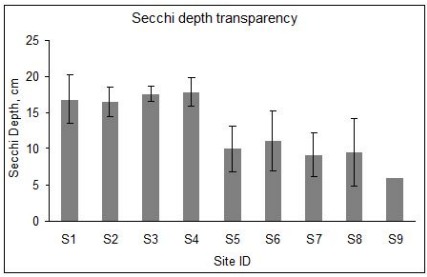

Figure 5.38: Average Secchi depth transparency (śSD) at fixed monitoring stations (see Figure 4.4).

5.3.7 Secchi Depth Distributions

Water transparency (Secchi) at fixed monitoring stations in Lake Abaya was found to be extremely low with Secchi disk depth average of 15 cm (range 5-20 cm, $n = 71$). The maximum transparency was observed at station S4 situated at the central part of the south basin, whereas the minimum Secchi value was measured at station S8 close to the mouth of the largest tributary. However, the difference in Secchi disk readings between shallow sites, which are close to the river mouths and shorelines, and central deep parts of the lake during sampling dates has been less than 5 cm. Exception is significantly lower transparency further south, at station S1. Overall data structure of the routine measurements at fixed monitoring stations is that there has been little variations between sampling sessions and no significant trend in the south basin, whereas the north basin showed decreasing transparency with time. It is clear from Figure 5.26 that station mean values in displayed increasing transparency from single measurement taken from station S9 in the northeast to stations S3 and S4 in the south basin (mean Secchi 18 cm, $n = 12$).

The mean Secchi values at fixed monitoring sites were combined with single measurements taken from some sediment sampling locations (Figure 5.39a) to estimate the mean spatial distribution of water transparency (Figure 5.39b). Comparison of individual Secchi values with their 'site mean' for the survey period indicates that most of the measurements vary within 3 cm above or below the site

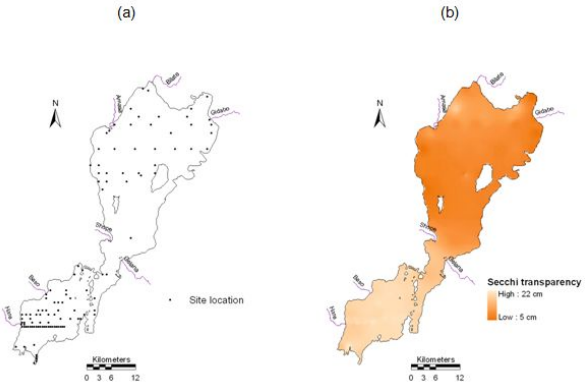

Figure 5.39: (a) Secchi depth measuring sites location, and (b) spatial distribution of Secchi Disk Transparency.

mean value. Thus, the visual impression given in Figure 5.39b, and derived from combined dataset, provides good estimate of the spatial variation of transparency throughout the lake. Figure 5.39b shows that there is a clear increasing transparency to the central parts and southwards overall. Figure 5.39b also revealed that there was better clarity at the northwest in the north basin close to the cliff and hilly surrounding boundary.

5.3.8 Interrelationship between Quality Parameters

To observe statistical differences of water quality parameters between fixed stations, an independent samples two-tailed t-test at a significance level of 0.05 was used to determine if the water column was homogenous for each parameter (Figure 5.40). Of the six quality parameters, only water temperature showed significant differences between near surface and near bottom at stations S3 and S4 in the south basin as well as when all stations combined.
A one-way ANOVA was used to assess differences between quality parameters among different fixed sampling stations (Figure 5.41). Results of one-way ANOVA revealed that only DO and TSS did not differ significantly ($P > 0.05$)

PARAMETER	S1	S3	S4	S5	S6	S7	All Stations
Temperature	0.094	0.018	0.031	0.102	0.057	0.115	0.000
Electrical Conductivity	0.603	0.646	0.452	0.818	0.640	0.870	0.990
pH	0.331	0.764	0.898	0.929	0.921	0.954	0.608
Dissolved Oxygen	0.421	0.254	0.105	0.473	0.466	0.577	0.169
Total Suspended Solids	0.530	0.352	0.333	0.711	0.761	0.968	0.964
Total Dissolved Solids	0.701	0.700	0.885	0.895	0.846	0.729	0.928

Figure 5.40: T-test Comparing Near Surface versus Near Bottom Water Quality Parameters at Each Fixed Stations and All Stations Combined.

PARAMETER	F Value	Significance Level
Temperature	9.808	0.000
Electrical Conductivity	26.909	0.000
pH	7.778	0.000
Dissolved Oxygen	1.839	0.104
Total Suspended Solids	65.683	0.000
TDS	1.392	0.229

Figure 5.41: One-Way ANOVA for Depth Profiles Combines at Stations

PARAMETER	S1 v. S3	S1 v. S4	S1 v. S5	S1 v. S6	S1 v. S7	S3 v. S4	S3 v. S5	S3 v. S6
Temperature	0.966	0.936	0.015	0.001	0.157	1.000	0.074	0.004
Electrical Conductivity	0.026	0.001	0.010	0.026	0.046	0.991	0.000	0.000
pH	0.999	0.956	0.001	0.876	0.895	0.997	0.000	0.579
Dissolved Oxygen	0.215	0.911	0.637	0.194	1.000	0.542	0.992	1.000
Total Suspended Solids	0.502	0.000	0.000	0.998	0.000	0.020	0.000	0.200
Total Dissolved Solids	1.000	0.717	1.000	0.975	0.882	0.584	1.000	0.953

Figure 5.42: Matrix of Tukey HSD Multiple Comparisons Probabilities.

from each other. Tukey's multiple comparison test was used to detect significant differences in the parameters among the fixed monitoring sites considered (Fig-

PARAMETER	S3 v. S7	S4 v. S5	S4 v. S6	S4 v. S7	S5 v. S6	S5 v. S7	S6 v. S7
Temperature	0.018	0.034	0.001	0.007	0.983	0.000	0.000
Electrical Conductivity	0.000	0.000	0.000	0.000	0.997	1.000	0.999
pH	0.968	0.000	0.199	0.995	0.024	0.000	0.326
Dissolved Oxygen	0.641	0.497	0.497	0.997	0.983	0.919	0.596
Total Suspended Solids	0.000	0.000	0.000	0.000	0.000	0.000	0.000
Total Dissolved Solids	0.882	0.992	0.992	0.266	0.967	0.904	0.559

Figure 5.43: Matrix of Tukey HSD Multiple Comparisons Probabilities.

ure 5.42). Comparisons between sites in the south basin (S1 versus S3) and (S3 versus S4) showed the least number of differences (one), while S1 and S4 in the south basin versus S5 in the north basin showed the greatest number of difference (four).

A summary of the relationship between depth-profiles of water quality parameters measured at fixed sampling stations is given in the Pearson Correlation coefficient matrix in Figure 5.43. With 571 in situ measurements of water quality parameters, 327 total suspended sediment and 200 total dissolved solids concentration values, water temperature correlated antipathetically, whereas electrical conductivity and total dissolved solids correlated sympathetically with depth. This relationship is an expression of decreasing temperature and increasing salinity with depth, as expected. On the other hand, total suspended solids correlated antipathetically with depth, describing decrease in total suspended solids with depth. This could be attributed to high proportion of fine clay particles that could maintain is suspension contained in the sediment input from upland catchments by tributary rivers. Additionally, dissolved oxygen correlated antipathetically and very similarly with total suspended and dissolved solids, and that might be explained by increased biochemical oxygen demand with concentration levels of the constituents both in suspension as well as in solution.

	Temperature	Electrical Conductivity	pH	Dissolved Oxygen	Total Suspended Solids	Total Dissolved Solids
Depth	−.318**	−.141*	.063n.s.	−.067n.s.	−.297**	.166*
Temperature		−.185**	.024n.s.	−.134**	.109n.s.	−.060n.s.
Electrical Conductivity			.097n.s.	.251**	−.391**	.347**
pH				.236**	−.144*	.059n.s.
Dissolved Oxygen					−.178**	−.385**
Total Suspended Solids						−.158*

Figure 5.44: Correlation coefficient matrix. n.s. denotes not significant, * denotes significant at the 0.05 level, ** denotes significant at the 0.01 level

6 Discussion

6.1 Meteorology

6.1.1 The Wind Fields

Analysis of wind records from two stations adjacent to the western shoreline of Lake Abaya shows that a periodic diurnal wind dominates the wind field during 53 days considered. They indicate that the western shoreline experiences a lake breeze during the day and a land wind at night. The daily occurrence of land-and-lake breeze observed in diurnal variation of wind speed and direction suggests that there were relatively light prevailing large scale synoptic flows (i.e., the western shoreline is more or less protected from the general flow pattern). The lake-breeze at both stations found to begin early in the days considered, suggesting that the general flow is reinforcing the lake-breeze (Freizzola and Fisher, 1963).

Comparisons of the time of onset of formation and speed are not in agreement at both stations. The inhomogeneous characteristic of the surface boundary layer is responsible to many of the variations in the thermal forcing involved (Kusuda and Alpert, 1983). The difference in the time of lake-breeze onset between the Fura station in the south and the Wajifo station in the north can be explained in terms of horizontal advection of diurnally cooled air by the large-scale flow (Neumann, 1977). The time of occurrence of lake-breeze at Fura is about one hour earlier than the corresponding time of occurrence at Wajifo. This time difference may represent approximately the amount of time needed for the cold air to move from south to north by prevailing southerly general flow.

The differences in the maximum wind speeds observed at both stations can be ac-

counted for by the broadness of the valley floor and water body and surrounding topography (Fisher, 1960; Kusuda and Alpert, 1983). Comparison of the wind field at two stations showed that the wind speed at Wajifo was usually greater than that at Fura, which indicates greater thermal forcing and less friction (Zhong and Takle, 1992).

The rapid rise of the average diurnal wind speed between 0700 hr and 1000 hr and relatively steady values between 1200 hr and 1600 hr clearly delineate the onset and duration of the lake-breeze (Figure 5.3). Larger speed changes, usually occurring in short periods in the morning and in late afternoon, are probably associated with the onset and cessation of convective mixing (Crawford and Hudson, 1973). The maximum speed observed during the daytime can be explained by the pronounced vertical exchange of momentum during early afternoon because of thermal convection (Yu and Warner, 1970). The near stagnations of early morning and nighttime points represent approaches to two equilibriums (Staney, 1957). Weak lake-breeze suggests that the stations are located far from appreciable reinforcing by mesoscale forcing of the nighttime mountain winds (Kusuda and Alpert, 1983).

The resultant wind direction is found to oscillate and the average rate of rotation at both stations is far from uniform over the diurnal cycle (Figures 5.4 and 5.5). The common feature at both stations was relatively rapid rotation during onset of lake-and-land breeze and a slow turning at later times. Rotation of the wind vector in the lake-land breeze is a result of an imbalance among the Coriolis, mesoscale, and large scale pressure gradients (Zhong and Takle, 1993). Thus, the difference in the rotational rates at any given time from station to station indicates that the forcings responsible for the rotation were not uniformly distributed in either time or space (Zhong and Takle, 1993).

The comparison of simultaneous wind records at Wajifo and Fura stations reveals that there is a spatially variable distribution of wind stress along the western shoreline of Lake Abaya. The difference between wind roses of two stations corresponding to the same month emphasizes the impact of the shape of the shoreline and local topography on the wind field distribution around the lake (Figures 5.6 and 5.7). On the other hand, similarities and differences between monthly wind roses at a station mark the presence of characteristic seasonal pattern.

The prevailing large-scale synoptic flow has a direct effect on the strength of the lake breeze (Johnson and O'Briens, 1973). The calmest month at Wajifo (January) is in the dry season of the suppressing northeasterly synoptic-scale winds prevailing in most of the East Africa, whereas the strongest month (June) with predominantly southerly component is in the rainy season when the southeasterly general wind pattern is more active (Figures 5.8 and 5.9). Further, the directional change of the lake breeze is slowed down during the rainy season when the lake breeze and general wind are on the same direction (Neumann, 1977). At Fura, winds during the rainy months consist of a variety of synoptic conditions that include winds from many directions (Figure 5.7). These suggest that the effect of large scale synoptic wind system on the lake-and-land breeze is more propounded in the larger and more exposed north basin than the south basin.

Wind records of 2 and 5 minutes intervals at Wajifo and Fura stations were processed to form mean monthly winds for a one year period (March 2004 - February 2005). Mean annual winds are then formed for both station by averaging all the monthly means. The annual mean winds at both stations are similar. The annual mean winds contain contributions from harmonics of diurnal cycle, but these should generally cancel in vector summations and should generally be small in comparison to the general flow pattern. These mean quantities, however, must be used with care since the wind direction distribution oscillates diurnally. The monthly and annually averaged winds at both stations suggest that the prevailing southerlies would dominate lake water circulation and associated material distribution. However, it is obvious in the original data that many of the strongest winds come from the east. These strong winds are likely to have major effect on the sediment dispersal in the transverse direction.

6.1.2 Temperature

The average diurnal variations of surface air temperature shown in Figure 5.12 by the monthly mean values of each hour of a day at Wajifo station can be attributed mainly to the absorption of solar energy (Pernter, 1914; Balland, 1933). It is apparent in the graphs of average diurnal surface air temperature march that rainy season (June - September) is characterized by fairly uniform increase in temperature after sunrise. The relatively rapid rise in air temperature between 0600 hr and

0800 hr local time in the dry season is probably brought about mainly by the relatively small amount of water vapour before the lake breeze develops fully. This rapid increase in smoothened during rainy season by relatively great amounts of water vapour available from moist soil and vegetation. The tendency of uniform and slow rise to the daily peak afterwards throughout the year suggests that the lake breeze along the western shoreline produces important effects on the diurnal variation of the air temperature.

Seasonal differences in temperature pattern occur between rainy season (June-August) and dry season at Wajifo weather station. Both, standard deviation and mean daily temperature range are larger in dry season. This might be due to the water vapour in the air, which decreases the diurnal range by decreasing the maximum temperature and increasing the minimum temperature (Balland, 1933; Court, 1951). The maximum temperature in rainy season is decreased largely (1) by the depletion of solar energy in passing through water vapour, and (2) by the evaporation of surface moisture. The minimum is increased by the absorption of ground radiation.

The effect of incoming radiation and the more instable state of the atmosphere in the early morning around onset of the lake breeze could make the wider primary modes of the frequency distribution of warming. The changes from the generally observed primary modes of the daily average interdiurnal variability could be steered by the general circulation and not by local factors. On the other hand, the seasonal characteristics of interdiurnal variability do not appear to be certain, because of the material here considered in this study is not extensive enough.

6.1.3 Atmospheric Pressure

Roden (1965) noted that the atmospheric pressure oscillation can be regarded as consisting of two parts: the regular oscillations due to the atmospheric tides, and the irregular oscillations superimposed upon them. Several investigators (e.g. Pyle, 1959) described the mechanism which links the 24-hr component to the daily heating and cooling. The primary diurnal minima in the afternoon near the time of maximum heating are explained by the fact that the daytime heating causes the air to expand upwards and also outwards into regions of less heating. The outward expansion results in a depletion of mass from the air column and

thus causes the pressure to fall slightly at valley bottom stations. On the other hand, the primary maxima are caused by the nighttime cooling and contraction that cause a corresponding pressure maximum near the dawn. It is therefore observed that there is a close agreement between observed diurnal minima and maxima and hours of maximum heating and cooling. The highest daily pressure ranges of 117.62 mb on 1 June 2004 and the lowest daily range of 4.14 mb on 10 August 2004 occurred in rainy months when the atmospheric pressure system is active.

6.2 Sedimentology

6.2.1 Texture

The textural trends observed in Lake Abaya may assist the interpretation of the transport and deposition of sediments relative to increasing or decreasing energy environments due to wave and current activity. It is well known that sediments maintain the essential characteristics of the source material modified by the agents of transportation with its final texture and composition reflecting the overall conditions existing at its point of deposition (Thomas *et al.*, 1972; Yuretich, 1979; Håkanson, 1981). Overall, surficial sediments from the north basin of Lake Abaya comprise the coarser (sandy) fines in large proportion, whereas samples from the south basin are composed mainly of silt and clay. This general pattern of the lake sediments' textural distribution is a direct function of different energy environments. It suggests that relatively higher energy environment exists in the northern basin due to relatively stronger wind stress and hydrological flow pattern (Figures 2.4 and 5.6) and shallow water depth (Figure 5.22) (Thomas *et al.*, 1972; Håkanson, 1977).

No sample was found entirely free of silt and clay fractions. The occurrence of fine materials in small amount at the deltas of major streams provided evidence that sediment settles from suspension when the inflow energy decreases. Dispersal which is caused by mechanical agitation near the stream mouths and shallow regions prevent deposition of fines (Wright, 1995; Van Maren and Hoekstra, 2005). Correspondingly, it appears that the great bulk of sand sized erosion products remain as foreset beds and topset beds at the deltas. Increase in clay fraction offshore and downstream from river inputs is explained by the fact that

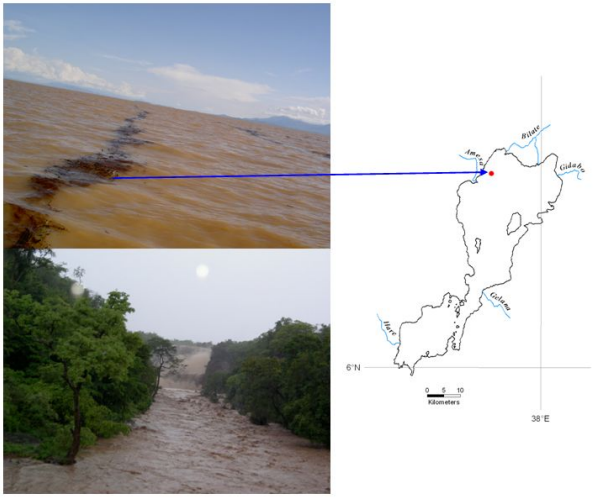

Figure 6.1: (Left top): sharp river plume on 1 May 2004 extending about 10km from Bilate River mouth; (left bottom): Amesa River flooding on 30 April 2004

deposition of fines probably occurs shortly after flocculation has overcome dispersal, so that progressively more flocculated material is deposited as water speed decreases (Holmes, 1968).

The prime cause of grain size variations of Lake Abaya lake floor sediments is water depth which, in turn, is a function of distance from shoreline. Lake floor sediments characterized by high silt and clay fraction predominate in water depths >5 m throughout the lake. Thus nearshore zone, there is a progressive deepening of the lake leading to decrease in sand and an associated increase in clay. In the deeper part of the lake the sediments consist almost entirely of fines with a minimum of discrete sand. High-energy conditions at main river mouths following flood events (Figure 6.1) would perhaps have caused more energy transmitted from river mouths to deep water carrying small fraction of sand. Most sediment is brought into the lake by floods which could be expanded several kilometres from main stream mouths during the heavy floods in rainy sea-

sons. Sharply defined paths of the river plumes extending for kilometres from the mouth of Bilate River were observed during the field work (Figure 6.1), which suggests that outflow inertia dominates the dispersal pattern of effluent during large runoff events (Wright, 1977).

6.2.2 Mineral Composition

Quartz

Basin of Lake Abaya can be divided into distinct regions with respect to the quartz content of lake floor sediments (Figure 5.24). Samples with relatively large quartz contents (>15 vol. %) are confined to comparatively narrow areas along the shoreline. This suggests that most of the quartz introduced from upland drainage is deposited in the deltas of the major rivers and dispersed along the shore. The north end of Lake Abaya close to the mouth of Bilate and Gidabo rivers is characterized by high contents of quartz with respect to the central and south basin, which can be attributed to the high quartz contents of the detrital load of both rivers. As quartz predominantly occurs in sand and silt fraction and originates from the drainage basin, its deposition concentrates on the delta regions. Correspondingly, the increase in quartz content at deltas is related to natural sorting during sedimentation with quartz content deposited at any locality being the net result of both the suspended load and the characteristics of the transporting mechanism (Thamas, 1968).

Feldspar

Also origin of feldspar in lake sediments is from the drainage basin, documented in its linear correlation to the quartz contents. Highest percentage of feldspar at deltas in the north and west of Lake Abaya suggests that feldspar is like quartz abundant in detrital loads of tributaries originating from the Western Highlands. Similarly, locally increased feldspar concentrations at the southern end of the south basin reflect the increased importance of the frequent inflow of Kulfo and Hare rivers during rainy seasons.

Clay

The abundance of clay minerals in lake floor sediments of Lake Abaya suggests that detrital loads of streams contain high percentage of fines in clay fraction. The sheltering effect of hilly surroundings to wind-induced lake circulation results in low energy zones that favour clay minerals to settle from suspension. On the other hand, funnelling effect at the narrow passages between islands and bottleneck connection may form high-energy zones, which prevent deposition of clay particles. The southward increasing clay concentrations can be explained by increased turbulence due to wind-induced waves and currents which slow down deposition of clay fraction from suspension.

Calcite

Analysis of mineral composition shows that carbonates in the lake floor sediments only occur as calcites, while Mg-calcites and dolomites lack. As carbonates lack in the drainage basin (Schütt *et al.*, 2005), the carbonates in lake floor deposits are derived from precipitation form the lake water and (or) deposition of organisms (shells, bones). The small calcite contents in most sediment samples and relatively uniform distribution in the main basin imply that calcite precipitation occurs area wide in the lake basin. On the other hand, the influence of local source areas is indicated by higher concentrations in certain near-shore localities. For example, the abundance of snail shells in the sediments from sites close to the eastern shoreline suggests that most of the calcite removal is accomplished biologically.

Organic Carbon

The low contents of organic carbon in most sediment samples reflect well mixed, oxidizing environment of the overlying water mass encouraging bacterial decomposition of organics (Yuretich, 1979). Since the organic matter in water is present in true solution, in colloidal solution, and as a suspension of organic detritus and living organisms, each of these forms plays different part in the supply of organic matter to sediments (Bordovskiy, 1965a, 1965b). In mountain rivers the proportion of organic matter totals 4-5% of the mineral salts in solution, and the greater part is detritus (Bordovskiy, 1965b). This general fact suggests that low

organic carbon contents in the lake floor deposits of the main basin can be partly explained by the small fraction of dissolved organic matter to be extracted by adsorption of suspended mineral particles and its incorporation in bottom deposits. Another reason for low organic carbon in the deposits of the lake's central zone can be attributed to the attack of detritus-feeders and bacteria during sedimentation of the organic detritus (Bordovskiy, 1965b). Organic carbon contents are increased around river mouths corresponding to organic detritus washed in with runoff. Next to this, increased concentrations of organic carbon at near shore zones can be related to increased population of habitants such as hippos and crocodiles and human activities.

Interrelationship between Variables

The direct relationship between concentration of clay in lake deposits and water depth suggest different energy environments. Variations in clay content can be attributed to variations in the degree of mixing causing decreasing energy as water depth increases as discussed previously. The inverse relationships between water depth and lake sediment's quartz contents and feldspar contents respectively can be explained by the transport mechanisms of suspended fines corresponding to grain size as discussed above (Thomas, 1969).

Although the relationship of the organic carbon content to clay content in the lake sediments is that organic carbon increases with increasing clay content (e.g. Thomas, 1969; Schoettle and Friedman, 1973; Hilton and Gibbs, 1985), it may be influenced by environmental conditions. For example, carbon loss may be incurred through oxidation during settling and (or) deposition in well oxidized bottom sediments (Thomas, 1969). This is evidenced by the fact that the reddish-brown sediment colour at the water sediment interface indicates oxidizing conditions (Thomas *et al.*, 1972; Schoettle and Friedman, 1973). Sediments containing high organic carbon content are black, indicating reducing conditions (Schoettle and Friedman, 1973).

The differences of the average mineral compositions at river deltas can be directly related to the petrological character of the source areas (Figure 5.33). Because the Western Highlands are the source area for the rivers entering Lake Abaya from the west and north, sediments of the corresponding deltas possess a strong

compositional resemblance. Similarly, the compositional character of sediments in the eastern deltas is closely controlled by the detrital load of the main tributaries.

Lack of clear trend in mineral composition along the transverse axis of the lake from west to east can be explained by nearly flat bottom topography of the main basin. The abrupt increase in depth near shore zone causes a sudden drop in energy level, which allows deposition of most of the fine load from suspension, resulting in a sharp change in depositional characteristics. Exception to this is that the sheltering effect of the surrounding hilly topography from wind forcing creates low energy zone to give rise to identical compositional trend near shore and main depositional zones.

Cluster Analysis

The geographical relevance of each cluster is inferred by comparing mean values of the mineralogical contents in the identified clusters (Figure 5.35). Samples included in Cluster 2 from North Basin with quartz content above average and located mostly offshore suggest that strong circulation in the north basin resulted effective dispersal of quartz fraction in sediment input mainly during flood events. The most variable minerals across clusters (i.e. feldspar and clay) could explain different energy zones prevailing in Lake Abaya, with higher feldspar or lower clay value corresponding to higher energy zone. The Clusters 1, 2, 5 and 6 with highest mean proportion of other minerals, which included samples mainly from deltas and near-shore localities, indicate that localized compositional character of sediments is closely controlled by the detrial load.

6.3 Water Quality

Significant changes in water quality with water depth of Lake Abaya were not observed during the study period. Lake responses to the wind forcing were documented by the vertical mixing of the water column as indicated by total suspended solids (TSS) concentration levels and profiles of water quality parameters. Lack of significant stratification effects for different variables are indicators of continuous mixing, initiated by wind driven wave motions in the environment

of Lake Abaya. Olango and Odada (1996) note that the water column of Lake Turkana is particularly well mixed above 15 m depth as a result of wind induced surface waves, with subsurface counter currents generating further mix the rest of the lake water at depth. Several other studies on the mixing of East African tropical lakes (Eccles, 1974; Spigel and Coulter; 1996; Bugendyi and Magumba, 1996; Ochumba, 1996; Halfman, 1996) show that the stratification patterns possess well defined mixed layers ranging from approximately 60 up to 200 m depending on season. These depths extend far beyond the maximum depth of Lake Abaya and suggest that the light winds predominating for the most part of a day on Lake Abaya are sufficient enough to generate waves that will keep the top layer well mixed so that fines will remain in suspension.

6.3.1 Water Quality Parameters

Secchi Depth Distribution

The attenuation of light in water is a function of the interaction of size-concentration-composition of suspended material as well as the effect of dissolved substance (Biggs, 1970). Thus, loss of water clarity in Lake Abaya, which was reflected in the lower Secchi disk depth, is due to both, high solids in suspension and high colour due to dissolved solids. Sources of suspended solids are external (introduced by freshwater run-off), marginal (shoreline erosion), or internal (supply of organic matter and skeletal material from primary production within the system) (Biggs, 1970; Halfman, 1996). Each of the input processes may operate according to a seasonal cycle, so that, at any time during the year one of these processes may dominate over the others. The effect of the Omo River sediment plume on light attenuation in Lake Turkana, with somewhat comparable sediment source mainly from the western part of Lake Abaya drainage basin, is found to be dramatic (Spigel and Coulter, 1996). This may suggests that the relative contribution of suspended sediment to light attenuation in Lake Abaya is high.

Suspended Solids

Resuspension of bed sediments by current and wave action can contribute to the turbidity at shallow depth but this factor was probably of minor importance as significant differences in Secchi disk depth between shallow and deep portions

of the lake lack. In the shallow areas of the lake, upward decreasing TSS stratification is due to gravitational settling of sediments and mobilization of bottom sediments. Particulates subject to gravitational settling are expected to accumulate towards the bottom. This does not explain the substantial and more frequent decline of TSS concentration in the lower water layers at deeper stations. It is more likely that the amount of fine material moving within the lake in the top layer is a significant fraction of the sediment that is deposited on the lake bed. High concentration of TSS near surface following the rainy periods implies that most of the sediment input by the tributaries consists of fine grain particles (Håkanson and Jansson, 1983). Thus, the fineness of the clay together with the high dissolved solids content of the water account for the persistent turbidity of Lake Abaya.

The association of TSS with average flows is evident in two respects: the geographical distribution of TSS, with higher concentrations near stations affected by major tributaries, and a tendency for declining in TSS concentration during low average flows. An increased TSS concentration in October 2004 typically is due to sediment-rich floodwater. On the other hand, the southward tendency of TSS is explained by two trends: higher concentration of TSS at station S5 in the south direction than at station S6 in the north, and generally similar average TSS concentration variations between stations S5 in the north basin and S4 at the centre of the north basin. Significantly higher concentrations of TSS or lower Secchi transparency occasionally at station S1 in the south end of Lake Abaya most likely reflect flood flow from Kulfo River, which leaves its main channel draining to Lake Chamo and enters Lake Abaya at the south end during flood events (Schütt and Thiemann, 2006).

Dissolved Oxygen

Factors potentially contributing to the oxygen budget of the lake water include primary algal photosynthesis and respiration, reaeration from the atmosphere (i.e. mixing), advection, biochemical and sediment oxygen demand, and nitrification (Wood and Talling, 1988; Losada, 2001). Nearly uniform dissolved oxygen levels with depth at all fixed stations suggest that oxygen demands created by different components of the oxygen budget were offset by enhanced productivity by

the algal community and reaeration from the atmosphere via wave activity and mixing process. On the other hand, slight fluctuation of dissolved oxygen only near surface water is indicative of the inherent relationship between dissolved oxygen and temperature; oxygen is more soluble in cold water than in warm water (Camp and Meserve, 1974). Thus, surface aeration can act as either a source or a sink of oxygen depending on the temperature and oxygen concentration of the surface layer (Losada, 2001).

Conductivity

Electric conductivity of water is a function of water temperature and the total number of dissolved ions in water (Bartram and Ballance, 1996). The overall spatial and temporal structures of the average electrical conductivity at fixed stations indicate that both freshwater inflow and evaporation play a major role in the salt budget of Lake Abaya. A decline in average conductivity at stations close to the mouths of major tributaries during high discharges might be due to dilution with freshwater with less dissolved ions, whereas an increase in conductivity levels during dry months is more likely due to the low inflow and higher irradiance, and hence increase surface water loss by evaporation. The shore line fluctuation at flat surroundings during the course dry period and after major rain events in the catchments indicated the importance of evaporation in the water balance of Lake Abaya.

Other Water Quality Parameters

Most water quality parameters are strongly affected by surface processes (Jones and Bowser, 1978; Ward and Armstrong, 1997). Solar radiation, wind, rainfall and temperature interact within the water mass to determine the structure of the water column (Bugenyi and Magumba, 1996). Fluctuations of water temperature near surface and strong correlation with air temperature are consistent with domination of surface heat flux in the tropical lakes. The vigorous vertical mixing rendered many parameters measured vertically homogeneous. A high degree of aeration is implied by nearly homogenous vertical structure of dissolved oxygen profiles. Observation of deficit dissolved oxygen near bottom at S9 indicates increased oxygen consumption in the water column and in the lake floor sedi-

ment. Although electric conductivity is considered technically as a conservative parameter (Ward and Armstrong, 1997), it has been observed to be less conservative most of the time. This can be accounted to the role of evaporation to affect the solute budget of the lake (Sonnenfeld, 1984). The effect of freshwater inflow in depressing electric conductivity is demonstrated at sites close enough to the major tributaries to respond to their inflow. Furthermore, the north-to-south trend of increasing average electric conductivity distribution can be due to decrease in fresh water inflow southwards.

The specific composition of water on any lake will depend upon the length of time that the lake has existed, the volume and composition of the inflows, the rate of evaporation from the lake's surface and the retention time of water in it (Baxter, 2002; Teklemariam, 2005). In general the highest concentrations are found in closed basin or terminal lakes, in which the retention time approaches infinity (Baxter, 2002; Legesse et al., 2004; Alemayehu et al., 2006). The dissolved solids and pH are normally high in Lake Abaya due to the geological characteristics of the basin area that is underlain during the tertiary and quaternary periods of basaltic formations and the dominance of the calcium-magnesium-bicarbonates contains of tributary rivers (Teklemariam, 2005).

7 Conclusions and Recommendations

The main subject of this thesis is estimation of the mean circulation pattern in Lake Abaya based on the spatial and temporal variability of physical parameters and sediment distribution. A one-year observation of meteorological forcing along the western shoreline suggested that land and lake breezes are important components of the prevailing wind system. The diurnal wind variations have essentially the same feature at both weather stations established at Fura in the south basin and Wajifo in the north basin. During a typical sunny day, the lake surface is calm in the morning, with winds picking up between midmorning and noon, strengthening in the afternoon and dying out in the evening. Diurnal variation of wind speed and direction was in about the same time each day, with daytime wind from lake to land being stronger than nighttime wind from land to lake, and stagnations for a short while early in the morning and in the evening. Directional preference and difference in strengths of wind components in opposite direction in diurnal basis considered as important indicators for the existence of mean currents representing large scale circulation.

Lake Abaya presents a number of special features. It mixes throughout its depth during every month of the year. It is shallow (maximum depth 24 m) and the water level fluctuates through the year quite markedly. Its drainage basin has a higher degree of spatial and temporal variability of precipitation. The concentration of precipitation into fewer months is producing greater seasonality of inflow patterns.

The most conspicuous feature of rainy season behaviour of Lake Abaya is the combination of strong winds and high flows with high sediment input into the lake. Large amounts of freshwater and fines are delivered by the tributaries during energetic discharge events. The initial fluvial sediment dispersal is mainly determined by the flow dynamics of the plume, but the subsequent dispersal will be

regulated by the mixing rates with ambient water. Major tributaries are expected to cause appreciable horizontal current in the offshore direction in the vicinity of river mouths. Prevailing winds in the north basin during the rainy season are from south-east and north-west, while the stronger winds were always coming from the south-east direction. Higher wind speeds will produce higher current speeds at all depths. The resulting mean circulation patterns are a northward alongshore and southward return flow in the main basin. Consequently, large volumes of water and sediment exchange between the north and south basins can occur after flood events of the main tributaries in the north basin following rainy seasons.

The mean currents in the shallow nearshore zone are relatively stronger than the counterpart mean currents of return flow in the deep central zone. The strong current near shore zone has considerable importance for dispersal of any effluents near shore. Owing to the natural sorting based on the characteristics of suspended load and transporting mechanism, the coarser particles settle near-shore from the water-body, while the finer particles (clay and silt) might remain in suspension for months or years. Thus, still finer particles are transported to the greater depths and southwards from input points located mainly in the north basin, and this is important to explain the horizontal extent of total suspended solids concentrations (TSS).

Southward and offshore, descending into the central basin, net water flow and associated sediment transport is indicated by an increase in TSS at the station around the centre (S6) and further south in the north basin (S5) following a rainy season. The net transport of fines in the shore region may depend on the relative strength of currents induced by alternating onshore and offshore winds on a diurnal basis. Since onshore winds are stronger than offshore wind, currents at the bottom and surface layers are quite strong and opposite in direction than in the case of offshore winds. In consequence suspended sediments are transported away from the shore by the large currents. In general, most of the fluvial sediments are deposited during calm weather and when the weak offshore wind causes insignificant bottom shear stress. These sediments, however, can later be resuspended, owing to the presence of strong onshore wind, and can be transported offshore by the strong currents near the bottom layer. It is, therefore,

apparent that repeated accumulation, erosion, and transport results in the long-term transport of sediments from nearshore to the deep portion of the basin.

Lake Abaya floor sediments are dominated by muds, showing little variability over wide areas. Decreasing percent sand (or feldspar and quartz) is negatively correlated with increasing percent of clay. In addition, percent sand decreases and percent clay increases with increasing depth. These mineralogical trends are due to hydrodynamic sorting by high-energy conditions at shallow proximal areas and declining energy as water depths increase at deep distal portions. The rapid energy decrease at stream mouths appears to allow deposition of much of the sand and silt. As the energy level further decreases out into the lake clay particles begin to flocculate and the floccules are deposited alongside the remaining sand and slit. Any major trends in mineralogy at deltas of major tributaries are likely to reflect source variation. Thus this investigation recognizes that mineral sorting trends of lake deposits, containing large amounts of detrital origins, might be used in interpretation of sediment transport patters in shallow lake basins.

Stratification of water quality parameters in a shallow water body like Lake Abaya is generally of low significance. The intense wind mixing together with shallow depth apparently result an essentially homogenous water column. In general, the Lake Abaya water is characterized by high temperature, high dissolved oxygen contents, high alkalinity, very low Secchi disk depth, high electric conductivity, and high concentration of solids in suspension. Sediment loading by river inflow and subsequent transport and mixing would have caused more or less uniform TSS concentrations at the stations close to the river mouths. It appears that the highest TSS concentration following raining months reflects the significance of increased erosion from upland catchments. More frequent occurrences of higher TSS concentrations near surface than near bed in distal portions suggest that most of the suspended load spreads though Lake Abaya as surface overflows and shallow interflows. Continuous and prolonged mixing of the top layer by wind-induced currents and wave action leads to the persistence of clay in suspension. Thus, most of the fine sediments, predominantly clay and fine silts, are distributed by near surface currents.

7.1 Conceptual model

Conceptual models describe the physical processes that are part of an environment, how they relate to each other and which processes dominate the system (Flint *et al.*, 2001). They define the general physical framework within which important components of system dynamics can be captured and details of their processes can be worked out (Flint *et al.*, 2001; Kavetski *et al.*, 2006a). An important, perhaps defining, feature of conceptual models is that their parameters are not directly measurable and must be inferred ('calibrated') from the observed data (e.g. Beven and Binley, 1992; Kavetski *et al.*, 2006a).

The current conceptual model of mean circulation of Lake Abaya water is evolved in order to account for the processes reflected in observed field data as well as for those concepts from relevant literature references that are most consistent with the measured data and observations. Recent observations and past records are relevant to the discussion of the assumed conceptual model for a typical average condition of variables. The major components of the conceptual model address the following processes: (a) inflow of freshwater and sediment; (b) outflow from the lake; (c) mixing of freshwater with ambient water and sediment dispersal; (d) mean wind forcing along the western shoreline; (e) mean circulation pattern, and (f) evaporation from lake body. A simplified schematic that highlights these components is depicted in Figure 7.1. It should be noted that this approach follows descriptions and explanations in the previous chapters, and the suggested conceptual model diagram is not to scale.

- **A.** Freshwater and sediment input at several locations around the lake vary temporally and spatially considerably, ranging from intermittent to large-volume perennial flows depending on the season and catchments characteristics. From spatial and temporal variability of TSS concentration at fixed stations close to the river mouths and mean monthly lake input and rainfall in the drainage basin, it is inferred that lake input processes are governed primarily by the distribution and timing of precipitation in the drainage basin, the physical properties of the surface soils and the processes controlling soil erosion. Lake input is represented by mean values (1970-2003) of volumetric records at gauged main tributaries (Figure 2.9). From mean annual total inflow data, more than 90% input was observed in the north

basin that correspond to net flow of water and associated sediment in suspension from north to south. The noticeable increase in Total Suspended Solids (TSS) concentration around the centre of south basin following high flow period in the north basin supports further that significant fraction of water and sediment entering at the north basin transported further to the south basin.

- **B.** Lake Abaya lacks a direct surface outlet and drains into Lake Chamo by overflowing the sill in its south end during lake level highs (Bekele, 2001; Schütt and Thiemann, 2006). With respect to the water budget of Lake Abaya, the average values for the period 1969-1996 of components suggested by Bekele (2001) are: inflow to the lake, 1902 x 106 m3/year; precipitation on the lake, 787 x 10^6 m^3/year; evaporation, 2405 x 10^6 m^3/year; and outflow 115 x 10^6 m^3/year. These values show that all water input is approximately balanced by evaporation, with outflow making minor contributions. The lake water may interact regularly with the near-surface groundwater storage in highly porous deposits in the rift floor around the lake (Makin *et al.*, 1975; Grove, 1986) depending on the seasonal fluctuations of the lake level. Therefore an arrow indicating groundwater recharge or discharge flux could be included in the mean conditions shown in the conceptual model depicted in Figure 7.1, and while deviations from this conceptual model may occur in some instances, this illustration depicts the general mean hydrodynamic response of Lake Abaya to external forcing.

- **C.** From water column profile of TSS concentration at fixed monitoring stations near the mouth of major rivers, the initial fluvial sediment dispersal is characterized by nearly well mixed water mass during dry season, whereas highly turbid buoyant plume transported offshore during maximum sediment supply for the major part of the rainy season. Additionally, it was observed during 2003-2004 field year that the Bilate River plumes were advected from two entrances at the north end to the south by well-developed coastal currents which originated from the river discharge inertia. Channelling or focused flow occurs during flood events resulting fast flow pathways, which transport sediment input further downstream. These findings confirm the fact that dispersal and mixing of reverine input

with lake water will take place depending on the energy transmitted to the lake by stream currents and varying contributions from modifying forces (Garvine and Monk, 1974; Carmack *et al.*, 1979; Blanton and Atkinson, 1983; Wright, 2006). Therefore in strong and rapidly changing currents the effluents will be dispersed more effectively (Murthy, 1972; Hilton *et al.*, 1986). Winds occurring from different directions in Lake Abaya will alter the surface plume as the inertia dissipates and enhance lateral dispersion of fresh water and sediments in the transverse direction (Warrick *et al.*, 2004). Further, textural and mineralogical compositions of surficial sediments obtained from deltas suggest spatial variability of lake input and strength of dispersal mechanisms.

- **D.** Observations of diurnal wind field along the western shoreline and profiles of water quality parameters at fixed stations during 2003-2004 suggest that wind induced currents and waves are the principal, year-round controls on the strength of water circulation within Lake Abaya. The daytime lake breeze and nighttime land breeze are sufficiently strong to influence the lake's circulation and associated sedimentation processes. The near stagnations of early morning and nighttime points would encourage sedimentation, which could be reworked further by currents and waves generated by alternating onshore and offshore winds.

  The monthly averaged wind vectors in Figure 7.2, derived from 2 and 5 minutes records at stations along the western shoreline of Lake Abaya, indicate that strong mean winds are mainly southesterly. Orientation of the major axis of elongated Lake Abaya is parallel to the regularly flowing strong winds in the uplake direction, from which it is inferred that wind forcing in the longitudinal direction plays a key role in transporting the water and sediment in suspension horizontally and mixing them vertically. However, it gets obvious in the weather data that many of the strongest winds come from the east. It is increasingly evident that these strong winds are likely to have major effect on the sediment dispersal in the transverse direction. For example, the widespread existence of quartz fraction in sediments obtained from the deep central zones in the north basin may provide further support for the effectiveness of strong episodic winds in the trans-

verse direction for much stronger dispersal of sediment.

Stronger southerly winds prevail at both stations during the rainy season when peak floods occur. This suggests that the combination of most sediment input and highly energetic conditions of external forcing in the wet season would encourage effective mixing and rapid dispersal, resulting weak TSS concentration gradients between near river mouth and central stations as well as nearly identical temporal trend of water quality parameters at fixed monitoring stations. Overall, the relatively stronger winds in the north basin would result in stronger circulation patterns than in the south, which is illustrated by spatial trend and relative frequency of mineralogical composition of bottom sediments in the two main basins (e.g. Figures 5.24-5.26). Based on reviews of the evidence for various sedimentary processes that have been inferred from seismic reflection and side scan sonar profiles from East African Lakes, Johnson (1996) notes that surface waves generated by strong winds can sort and redistribute sediments in water depths as great as 100 m.

- **E.** The monthly and annually averaged winds along the western shoreline (Figures 7.1 and 7.2) suggest that the prevailing southerlies dominate mean lake water circulation and associated material distribution. Assuming these average wind vectors correspond to the two main basins of Lake Abaya, it is possible to pose the following hypothesis for the wind driven mean circulation in Lake Abaya depicted in Figure 7.1.

  The literature suggests a general northward flow of surface waters in response to the southerly winds is accompanied by compensating flow of the lower layers southward (e.g. Gedney and Lick, 1972; Csanady, 1973; Signell *et al.*, 1990). On the average, the northerly mean currents in the nearshore zone will transport water parallel to the shoreline in the direction of the mean wind and the return flow will be downlake to the south in the main basin (Bennett, 1974; Lien and Hoopes, 1978; Pickett, 1980; Hunter and Hearn 1987; Beletsky *et al.*, 1999). The monthly mean wind vectors in the north basin are southerly for every month of the year, with a maximum mean wind run of 122.4 Km/day in June. The resulting mean flow can be two gyre circulations in the north basin (Csanady, 1967; 68;

Pickett and Dossett, 1978; Beletsky *et al.*, 1999). Some of the flow, especially near the shoreline, returns northward on the east and west sides and then eastward along the north side of the lake to re-enter the circulation pattern while the remaining water moves into the south basin through the deep channel in the west of Gidicho Island. This general structure is modified by the small passages between islands and at the bottleneck transition as well as the relative strength of the bathymetric-wind curl effects (Pickett, 1977). The hydraulic role of the narrow transitions between islands and the bottle neck connection of two main basins is increased flow rate as a result of reduction in flow width. The steep slope at the near shore zone may enhance lateral transport compared to the essentially flat floored central areas (Hunter and Hearn, 1987). Since major tributaries enter the lake in the north basin, there is a general water transport from north to south supplying mass from surplus region to deficit region. This suggests that the two main basins on the average interact by mean flow from north basin to the south as depicted in Figure 7.1. A general one gyre circulation pattern seems to be developed in the south basin due to more variable winds observed in the western shoreline (Figures 5.7 and 7.2) and the sheltering effect of the mostly hilly surrounding in the eastern boundary (Csanady, 1968; Beletsky *et al.*, 1999).

- **F.** Lake Abaya loses water presumably by evaporation. The most significant component of water balance of Lake Abaya (about 2.25 m/year or 2405 x 10^6 m^3/year) (Bekele, 2001) is lost to the atmosphere by way of evaporation driven by extensive heating. The seasonal fluctuation in lake level is 0.2 - 1.69 m (Bekele, 2001). As noted by Sigel and Coulter (1996), the large proportion of rainfall and evaporation in the balance of the African Lakes makes their levels particularly sensitive to climate change. This is evidenced further in Lake Abaya by large fluctuation of shorelines at zones of relatively gentle slopes observed during the field work program in 2003-2004. These observations suggest that evaporation during dry season exceeds temporarily the amount of freshwater input.

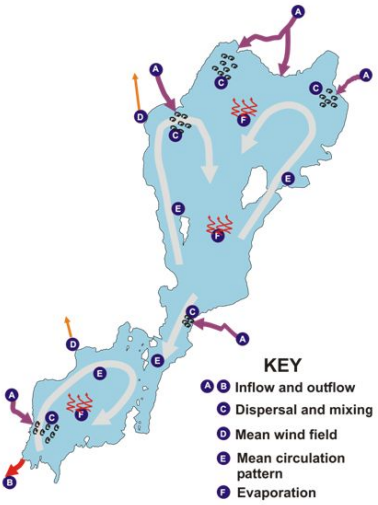

Figure 7.1: Generalized conceptual model of Lake Abaya water circulation. Arrows denote direction of flow and mean wind field, letters denote the major components described in the text.

7.2 Limitations

It should be noted that no systematic measurements of currents has been conducted to construct the mean circulation pattern assumed for Lake Abaya. The conceptual model presented in this study is preliminary in nature. It is intended to be the starting point for analysis of Lake Abaya circulation and do not reduce the critical importance of careful measurements and theoretical study for better understanding. Therefore further investigation by current measurements is necessary for direct evidence of the circulation pattern. Overall, it is intended that the suggested simplified conceptual model should be continually evolve and be improved through both theoretical and observational testing and review.

Since the wind field observed simultaneously at two stations along the western

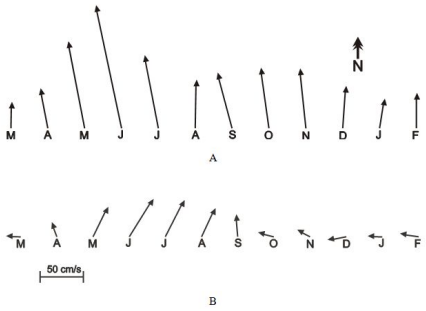

Figure 7.2: Monthly average wind vectors: A, at Wajifo Station; and B, at Fura Station (March 2003-February 2004)

shoreline is found to vary considerably, further research on the Lake Abaya land-lake breeze can profit by supplementary wind observations along the north and east boundary.

There is limitation inherent in using less than one year data record to examine inter-annual variability of water quality parameters. Therefore it is emphasized that monitoring from fixed monitoring stations must be continued for a minimum of several years to allow for trend analysis. Furthermore, large effort must be placed on the establishment of monitoring systems in an attempt to understand the physics of Lake Abaya.

8 References

Alemayehu, T., T. Ayenew, and S. Kebede (2006). Hydrogeochemical and lake level changes in the Ethiopian Rift, Journal of Hydrology, 316, 290-300.

Alpert, P., M. Kusuda, and N. Abe (1984). Anticlockwise rotation, eccentricity and tilt angle of the wind hodograph. Part II: An observational study, Journal of the Atmospheric Sciences, 41(22), 3568-3583.

Alvarez, L. G., and S. E. Jones (2002). Factors influencing suspended sediment flux in the upper Gulf of California, Estuarine, Coastal and Shelf Science, 54, 747-759.

Antenucci, J. P., J. Imberger, and A. Saggio (2000). Seasonal evolution of the basin-scale internal wave field in a large stratified lake, Limnology and Oceanography, 45(7), 1621-1638.

Ardhuin, F., T. G. Drake, and T. H. C. Herbers (2002). Observations of wave-generated vortex ripples on the North Carolina continental shelf, Journal of Geophysical Research, 107(C10), 1-14.

Arritt, R. W. (1993). Effects of the large-scale flow on characteristic features of the sea breeze, Journal of Applied Meteorology, 32(1), 116-125.

Assefa, E. (2001). Features, patterns and dynamics of land use in Hare watershed, Research Report, Arba Minch Water Technology Institute, 38 pp.

Ayalew, T. (2004). Environmental implications of changes in the levels of lakes in the Ethiopian rift since 1970, Regional Environmental Change, 4, 192-204.

Baker, J. R., D. V. Peck, and D. W. Sutton (Eds.) (1997). Environmental Monitoring and Assessment Program Surface Waters: Field Operations Manual

for Lakes. EPA/620/R-97/001. U. S. Environmental Protection Agency, Washington D.C.

Balek, J. (1977). Hydrology and Water Resources in Tropical Africa (Developments in Water Sciences 8), Elsevier Scientific Publishing Company, 208 pp.

Balland, J. C. (1933). The diurnal variation of free-air temperature and of the temperature lapse rate, Monthly Weather Review, 61(3), 61-80.

Balling, R. C., Jr., and J. L. Sutherland (1988). Diurnal and seasonal wind direction patterns within the mountain-valley terrain near Glen Canyon Dam Arizona, Journal of Applied Meteorology, 27(5), 594-598.

Barry, R. G., and R. J. Chorley (2003). Atmosphere, weather and climate, Routledge, Taylor & Francis Group, London, 421 pp.

Bartram, J., and R. Ballance (Eds.) (1996). Water quality monitoring. A practical guide to the design and monitoring of freshwater quality studies and monitoring programmes, UNDP/WHO, E & FN Spon, London, 383 pp.

Baudo, R., and M. Beltrami (2001). Chemical composition of Lake Orta sediments, Journal of Limnology, 60(2), 213-236.

Bäuerle, E., D. Ollinger, and J. Ilmberg (1998). Some meteorological, hydrological, and hydrodynamical aspects of Upper Lake Constance, Archiv für Hydrobiologie Special Issues, Advances in Limnology, 53, 31-83.

Baxter, R. M. (2002). Lake morphology and chemistry. In: Tudornacea, C., and W. D. Taylor (Eds.). Ethiopian Rift Valley Lakes, Backluys Publishers, Leiden, 45-60.

Baxter, R. M., M. V. Prosser, J. F. Talling, and R. B. Wood (1965). Stratification in tropical African lakes at moderate altitudes (1500 to 2000m), Limnology and Oceanography, 10(4), 510-520.

Bekele, S. (2001). Investigation of Water Resources Aimed at Multi-Objective Development with Respect to Limited Data Situation: The Case of Abaya-Chamo Basin, Ethiopia. Dresdener Wasserbauliche Mitteilungen, Heft 19, Selbstverlag der TU Dresden, Dresden.

Beletsky, D., and D. J. Schwab (2001). Modelling circulation and thermal structure in Lake Michigan: Annual cycle and interannual variability, Journal of Geophysical Research, 106(C9), 19,745-19,771.

Beletsky, D., S. H. Saylor, and D. J. Schwab (1999). Mean circulation in the Great Lakes, Journal of Great Lakes Research, 25(1), 78-93.

Bennett, J. R. (1974). On the dynamics of wind-driven lake currents, Journal of Physical Oceanography, 4(3), 400-414.

Bennett, J. R. (1977). A three-dimensional model of Lake Ontario's summer circulation: I. Comparison with observations, Journal of Physical Oceanography, 7(4), 591-601.

Berhe, S. M., B. Desta, M. Nicoletti, and M. Teferra (1987). Geology, geochronology and geodynamic implications of the Cenozoic magmatic province in W and SE Ethiopia, Journal of the Geological Society, London, 144(2), 213-226.

Biggs, R. B. (1970). Sources and distribution of suspended sediment in Northern Chesapeake Bay, Marine Geology, 9, 187-201.

Birchfield, G. (1972). Theoretical aspects of wind-driven currents in a sea or lake of variable depth with no horizontal mixing, Journal of Physical Oceanography, 2(4), 355-362.

Blais, J. M., and J. Kalff (1995). The influence of lake morphometry on sediment focusing, Limnology and Oceanography, 40(3), 582-588.

Blanton, J. O., and L. P. Atkinson (1983). Transport and fate of river discharge on the continental shelf of the southeastern United States, Journal of Geophysical Research, 88(C8), 4730-4738.

Blumberg, S., and B. Schütt (2006). Spatial distribution of lake sediments in the Lake Abaya bottleneck, Zbl. Geol. Paläont. Teil I, 1/2, 113-128.

Bordovskiy, O. K. (1965a). Source of organic matter in marine basins, Marine Geology, 3, 5-31.

Bordovskiy, O. K. (1965b). Accumulation of organic matter in bottom sediments, Marine Geology, 3, 33-82.

Brigham, M. E., C. J. McCullough, and P. Wilkinson (2001). Analysis of suspended-sediment concentrations and radioisotope levels in the wild rice river basin, Northwestern Minnesota, 1973-98, USGS Water-Resources Investigations Report 01-4192, 21 pp.

Buckley, R. L., and R. J. Kurzeja (1997). An observational and numerical study of the nocturnal sea breeze. Part I: Structure and Circulation, Journal of Applied Meteorology, 36(12), 1577-1598.

Bugenyi, F. W. B., and K. M. Magumba (1996). The present physicochemical ecology of Lake Victoria. In: Johnson, T. C., and E. O. Odada (Eds.) The Limnology, Climatology and Paleoclimatology of the East African Lakes, Gordon and Breach Publishers, OPA, The Netherlands, 141-154.

Camp, T. R., and R. L. Meserve (1974). Water and its impurities, Dowden, Hutchinson & Ross, Inc., 384 pp.

Carlson, G. C., Jr., and S. Hastenrath (1970). Diurnal variation of wind, pressure, and temperature in the troposphere and stratosphere over Eniwetok, Monthly Weather Review, 98(5), 408-416.

Carmack, E. C., C. B. J. Gray, C. H. Pharo, and R. J. Daley (1979). Importance of lake-river interaction on seasonal patterns in the general circulation of Kamloops Lake, British Colombia, Limnology and Oceanography, 24(4), 634-644.

Celleri, R., P. Willem, W. Buytaert, and J. Feyen (2007). Space - time rainfall variability in the Paute Basin, Ecuadorian Andes, Hydrological Processes, 21, 3316-3327.

Chang, G. C., T. D. Dickey, A. J. Williams III (2001). Sediment resuspension over a continental shelf during Hurricanes Edouard and Hortense, Journal of Geophysical Research, 106 (C5), 9517-9531.

Charnock, H. (1955). Wind stress on a water surface. Quarterly Journal of the Royal Meteorological Society, 81, 639?640.

Chatfield, C. (1989). The Analysis of Time Series: An Introduction, Chapman and Hall, London, 241 pp.

Conrad, V. (1942). The Interdiurnal variability of temperature on Mount Washington, Transactions, American Geophysical Union, 22, 279-283.

Conrad, V. (1943). Interhourly variability of temperature, Transactions, American Geophysical Union, 24, 122-125.

Coulter, G. W. (1968). Thermal stratification in the deep hypolimnion of Lake Tanganyika, Limnology and Oceanography, 13(2), 385-387.

Court, A. (1951). Temperature frequencies in the United States, Journal of Meteorology, 8(6), 367-380.

Crawford, K. C., and H. R. Hudson (1973). The diurnal wind variation in the lowest 1500 ft in central Oklahoma: June 1966-May 1967, Journal of Applied Meteorology, 12(1), 127-132.

Csanady, G. T. (1967). Large-scale motion in the Great Lakes, Journal of Geophysical Research, 72(16), 4151-4161.

Csanady, G. T. (1968). Wind-driven summer circulation in the Great Lakes, Journal of Geophysical Research, 73(8), 2579-2589.

Csanady, G. T. (1972). Response of large stratified lakes to wind, Journal of Physical Oceanography, 2(1), 3-13.

Csanady, G. T. (1973). Wind-induced barotropic motions in long lakes, Journal of Physical Oceanography, 3(4), 429-438.

Csanady, G. T. (1975). Hydrodynamics of large lakes, Annual Review of Fluid Mechanics, 7, 357-386.

Csanady, G. T. (1997). On the theories that underlie our understanding of continental shelf circulation, Journal of Oceanography, 53(3), 207-229.

Danek, L. J., and J. H. Saylor (1977). Measurements of the summer currents in Saginaw Bay, Michigan, Journal of Great Lakes Research, 3(1-2), 65-71.

Darville, R., D. K. Shellman, Jr., and R. Darvillc (1998). Intensive water quality monitoring at Caddo Lake, a Ramsar wetland in Texas and Louisiana, USA. Conference Paper: Team Wetlands Arlington, VA, 15 - 17 April 1998, 20 pp.

Davis, M. B., and M. S. Ford (1982). Sediment focusing in Mirror Lake, New Hampshire, Limnology and Oceanography, 27(1), 137-150.

Donn, W. L., P. L. Milic, and R. Brilliant (1956). Gravity waves and the tropical sea breeze, Journal of Meteorology, 13(4), 356-361.

Douglas, R. W., and B. Rippey (2000). The random redistribution of sediment by wind in a lake, Limnology and Oceanography, 45(3), 686-694.

Dyner, T. G. J. (1976). An analysis of Manley's central England temperature data: I, Quarterly Journal of the Royal Meteorological Society, 102, 871-888.

Ebinger, C. J., T. Yemane, G. WoldeGabriel, J. L. Aronson, and R. C. Walter (1993). Late Eocene-Recent volcanism and faulting in the southern main Ethiopian Rift, Journal of the Geological Society of London, 150(1), 99-108.

Eccles, D. H. (1974). An outline of the physical limnology of Lake Malawi (Lake Nyasa). Limnology and Oceanography, 19, 730-742.

Estoque, M. A. (1962). The sea breeze as a function of the prevailing synoptic situation, Journal of the Atmospheric Sciences, 19(3), 244-250.

Estoque, M. A., and J. M. Gross (1978). Diurnal wind and temperature variation over Lake Ontario, Monthly Weather Review, 106, 1742-1747.

Everitt, B. S. (1993). Cluster Analysis, Edward Arnold, London, 170 pp.

Faller, A. J. (1971). Oceanic turbulence and the Langmuir circulations, Annual Review of Ecology and Systematics, 2, 201-236.

Fisher, E. L. (1960). An observational study of the sea breeze, Journal of Meteorology, 17(6), 645-660.

Fisher, E. L. (1961). A theoretical study of the sea breeze, Journal of Meteorology, 18(2), 216-233.

Fleagle, R. G. (1950). A theory of air drainage, Journal of Meteorology, 7(3), 227-232.

Fletcher, R. D. (1945). The general circulation of the tropical and equatorial atmosphere, Journal of Meteorology, 2(3), 167-174.

Floderus, S. (1988). On the spatial distribution of wave impact at the Kattegat seabed, Geografiska annaler, 70(3), 269-272.

Fong, D. A., and M. T. Stacey (2003). Horizontal dispersion of a near bed coastal plume, Journal of Fluid Mechanics, 489, 239-267.

Fong, D. A., and W. R. Geyer (2002). The alongshore transport of freshwater in a surface-trapped river plume, Journal of Physical Oceanography, 32(3), 957-972.

Frenzel, C. W. (1962). Diurnal wind variations in central California, Journal of Applied Meteorology, 1(3), 405-412.

Frizzola, J. A., and E. L. Fisher (1963). A series of sea breeze observations in the New York City area, Journal of Applied Meteorology, 2, 722-739.

Fukuda M. K., and W. Lick (1980). The entrainment of cohesive sediments in freshwater, Journal of Geophysical Research, 85(C5), 2813-2824.

Gaedke, U., D. Ollinger, E. Bäuerle, and D. Straile (1999). The impact of the interannual variability in hydrodynamic conditions on the plankton development in Lake Constance in spring and summer, Advances in Limnology, 53, 565-585.

Garbell, M. A. (1947). Tropical and Equatorial Meteorology, Pitman Publishing Corporation, 237 pp.

Garvine, R. W., and J. D. Monk (1974). Frontal structure of a river plume, Journal of Geophysical Research, 79(5), 2251-2259.

Gebremariam, B., B. Schütt, and G. Förch (2004). Recent monitoring of suspended sediment stress, bulk water quality parameters and meteorological forcing on Lake Abaya, Lake Abaya Research Symposium proceedings - 2004, 11-20.

Gedney, R. T., and W. Lick (1972). Wind-driven currents in Lake Erie, Journal of Geophysical Research, 77(15), 2714-2723.

Gemechu, D. (1977). Aspects of Climate and Water Budget in Ethiopia, Addis Ababa University Press, 71 pp.

Gilbert, R., and J. Shaw (1981). Sedimentation in proglacial Sunwapta Lake,

Alberta, Canadian Journal of Earth Sciences, 18, 81-93.

Gleeson, T. A. (1953). Effects of various factors on valley winds, Journal of Meteorology, 10(4), 262-269.

Gorham, E. (1958). Observations on the formation and breakdown of the oxidized microzone at the mud surface in lakes, Limnology and Oceanography, 3(3), 291-298.

Gorham, E., and D. J. Swaine (1965). The influence of oxidizing and reducing conditions upon the distribution of some elements in lake sediments, Limnology and Oceanography, 10(2), 268-279.

Gossard, E. E. (1960). Spectra of atmospheric scalars, Journal of Geophysical Research, 65, 3339-3351.

Grace Analytical Lab (1994). Standard Operating Procedure for the Sampling and Analysis of Total Suspended Solids in Great Lakes Waters. Grace Analytical Lab, Chicago, 5 pp.

Grancini, G., and B. Cescon (1973). Dispersal processes of freshwaters in the Po River coastal area, Limnology and Oceanography, 18(5), 705-710.

Grant, W. D, and O. S. Madsen (1979). Combined wave and current interaction with a rough bottom, Journal of Geophysical Research, 84(C4), 1797-1807.

Grove, A. T. (1986). Geomorphology of the African rift system. In: Frostick, L. E. et al. (Eds.). Sedimentation in the African Rifts, Geological Society Special Publication, 15, 9-16.

Grove, A.T., F. A. Street, and A. S. Goudie (1975). Former lake levels and climatic change in the rift valley of southern Ethiopia, Geographic Journal, 142, 177-194.

Håkanson, L. (1977). The influence of wind, fetch, and water depth on the distribution of sediments in Lake Vänern, Sweden, Canadian Journal of Earth Sciences, 14, 397-412.

Håkanson, L. (1981). On lake bottom dynamics-the energy-topography factor, Canadian Journal of Earth Sciences, 18, 899-909.

Halcrow, W., Sir, and Partners Ltd. (1992). Reconnaissance Master Plan for the Development of Natural Resources of the Rift Valley Lakes Basin, Final report, Appendix A: Land Resource Assessment, ETH/88/001, Food and Agricultural Organization of the United Nations, , 3, 1-18.

Halfman, J. D. (1996). CTD- transmissometer profiles from Lakes Malawi and Turkana. In: Johnson, T. C., and E. O. Odada (Eds.) The Limnology, Climatology and Paleoclimatology of the East African Lakes, Gordon and Breach Publishers, OPA, The Netherlands, 169-182.

Haurwitz, B. (1947). Comments on the sea-breeze circulation, Journal of Meteorology, 4(1), 1-8.

Hawley, N. (2000). Sediment resuspension near the Keweenaw Peninsula, Lake Superior during the fall and winter 1990-1991, Journal of Great Lakes Research. 26(4), 495-505.

Hawley, N., and B. M. Lesht (1992). Sediment resuspension in Lake St. Clair, Limnology and Oceanography, 37(8), 1720-1737.

Herron, T. J., I. Tolstoy, and D. W. Kraft (1969). Atmospheric pressure background fluctuations in the mesoscale range, Journal of Geophysical Research, 74, 1321-1329.

Hilton, J. (1985). A conceptual framework for predicting the occurrence of sediment focusing and sediment redistribution in small lakes, Limnology and Oceanography, 30(6), 1131-1143.

Hilton, J., and M. M. Gibbs (1984). The horizontal distribution of major elements and organic matter in the sediment of Esthwaite Water, England, Chemical Geology, 47(1-2), 57-83.

Hilton, J., J. P. Lishman, and P. V. Allen (1986). The dominant processes of sediment distribution and focusing in a small, eutrophic, monomictic lake, Limnology and Oceanography, 31(1), 125-133.

Holmes, P. W. (1968). Sedimentary studies of late quaternary material in Windermere Lake (Great Britain), Sedimentary Geology, 2, 201-224.

Horowitz, A. (1974). The geochemistry of sediments from the Northern

Reykjanes Ridge and the Iceland-Faroes Ridge, Marine Geology, 17(2), 103-122.

Hossaina, S., B. Eyreb, and D. McConchieb (2001). Suspended sediment transport dynamics in the sub-tropical micro-tidal Richmond River estuary, Australia, Estuarine, Coastal and Shelf Science) 52, 529-541, doi:10.1006/ecss.2001.0786.

Hunter, J. R., and C. J. Hearn (1987). Lateral and vertical variations in the wind-driven circulation in long, shallow lakes, Journal of Geophysical Research, 92(C12), 13106-13113.

Hurni, H., K. Tato, and G. Zeleke (2005). The impact of changes in population, land use, and land management for surface runoff in the Upper Nile Basin area of Ethiopia, Mountain Research and Development, 25(2), 147-154.

Jackson, I. J. (1977). Climate, water and agriculture in the tropics, Longman, New York, 248 pp.

Jackson, R. T. (1971). Periodic markets in southern Ethiopia, Transactions of the Institute of British Geographers, 53, 31-42.

Jacobs, S. J. (1974). On wind-driven lake circulation, Journal of Physical Oceanography, 4(3), 392-399.

James, W. F., J. W. Barko, and M. G. Butler (2001). Shear stress and sediment resuspension in canopy- and meadow-forming submersed macrophyte communities, Technical note, ERDC TN-APCRP-EA-03, 16 pp.

Jeffreys, H. (1922). On the dynamics of wind, Quarterly Journal of the Royal Meteorological Society, 48, 29-46.

Jellison, R., R. F. Anderson, J. M. Melack, and D. Heil (1996). Organic matter accumulation in sediments of hypersaline Mono Lake during a period of changing salinity, Limnology and Oceanography, 41(7), 1539-1544.

Jenkins, G. M., and D. G. Watts (1968). Spectral Analysis and Its Applications, Holden-Day, Inc., 525 pp.

Jeong, J., and S. D. McDowell (2003). Characterization and transport of contaminated sediments in the southern central Lake Superior, Journal of Minerals

and Materials Characterization and Engineering, 2(2), 111-135.

Jin, K. R., and Z. G. Ji (2001). Calibration and verification of a spectral wind-wave model for Lake Okeechobee. Journal of Ocean Engineering, 28, 571-584.

Johns, W. D., R. E. Grim, and W. F. Bradley (1954). Quantitative estimates of clay minerals by diffraction methods, Journal of Sedimentary Petrology, 24(4), 242-251.

Johnson, A. Jr., and J. J. O'Brien (1973). A study of an Oregon sea breeze event, Journal of Applied Meteorology, 12(8), 1267-1283.

Johnson, T. C. (1996). Sedimentary processes and signals of past climatic change in the large lakes of East African Rift Valley, 367-412. In: Johnson, T. C., and E. O. Odada (Eds.) The Limnology, Climatology and Paleoclimatology of the East African Lakes, Gordon and Breach Publishers, OPA, The Netherlands.

Jones, B. F., and C. J. Bowser (1978). The mineralogy and related chemistry of lake sediments. In: Lerman, A. (ed.), Lakes: Chemistry, Geology, Physics. Springer-Verlag, New York, 179-235.

Kebede, E., Z. G.-Mariam, and I. Ahlgren (1994). The Ethiopian Rift Valley Lakes: chemical characteristics of a salinity-alkalinity series, Hydrobiologia, 288, 13-32.

Keen, C. S., and W. A. Lyons (1978). Lake/land breeze circulations on the western shore of Lake Michigan, Journal of Applied Meteorology, 17(12), 1843-1855.

Kennedy, S. K., and N. D. Smith (1977). The relationship between carbonate mineralogy and grain size in two alpine lakes, Journal of Sedimentary Petrology, 47(1), 411-418.

Killworth, P. D., and E. C. Carmack (1979). A filling-box model of river dominated lakes, Limnology and Oceanography, 24(2), 201-217.

King, R. B., and C. J. Birchall. (1975). Land systems and soils of the Southern Rift Valley, Ethiopia, Land Resources Report 5, Land Resources Division, Ministry of Overseas Development, Tolworth Tower, England.

Koçyiğit, M. B., and Ö. Koçyiğit (2004). Numerical study of wind-induced currents in enclosed homogeneous water bodies, Turkish Journal of Engineering and Environmental Sciences, 28, 207-221.

Krause, J., B. Schütt, and S. Thiemann (2004). Hare River catchment - Landscape character of a drainage basin in the southern Ethiopia Rift Valley. In: Wenclawiak, B., and S. Wilnewski (Eds.). Sedimentary Studies in Tropics and Subtropics, Weiterblindung in Siegen, 14, 16-40.

Kusuda, M., and N. Abe (1989). The contribution of horizontal advection to the diurnal variation of the wind direction of land-sea breezes: Theorz and observations, Journal of the Meteorological Society of Japan, 67(2), 177-184.

Kusuda, M., and P. Alpert (1983). Anticlockwise rotation of the wind hodograph, Part I: Theoretical study, Journal of the Atmospheric Sciences, 40, 487-499.

Laird, N. F., D. A. R. Kristovich, X. Z. Liang, R. W. Arritt, and K. Labas (2001). Lake Michigan lake breezes: Climatology, local forcing, and synoptic environment, Journal of Applied Meteorology, 40(3), 409-424.

Largier, J. L. (1993). Estuarine fronts: How important are they? Estuaries, 16(1), 1-11.

Lawrence, G. A., K. I. Ashley, and Yonemitsu (1995). Natural dispersion in a small lake, Limnology and Oceanography, 40(8), 1519-1526.

Le Turdu, C., J. Tiercelin, E. Gibert, Y. Travi, K. Lezzar, M. Decobert, B. Gensous, V. Jeudy, E. Tamrat, M. U. Mohammend, K. Martens, B. Atnafu, T. Chernet, D. Williamson, and M. Taieb (1999). The Ziway-Shala lake basin system, Main Ethiopian Rift: Influence of volcanism, tectonics, and climate forcing on basin formation and sedimentation, Palaeogeography, Palaeoclimatology, Palaeoecology, 150, 135-177.

Legesse, D., C. Vallet-Coulomb, and F. Gasse (2003). Hydrological response of a catchment to climate and land use changes in tropical Africa: case study South Central Ethiopia, Journal of Hydrology, 275, 67-85.

Legesse, D., C. Vallet-Coulomb, and F. Gasse (2004). Analysis of hydro-

logical response of a tropical terminal lake, Lake Abiyata (Main Ethiopian Rift Valley) to changes in climate and human activities, Hydrological Processes, 18, 487-504. Lemmin, U., and N. D' Adamo (1996). Summertime winds and direct cyclonic circulation: observations from Lake Geneva, Ann. Geophysicae, 14(11), 1207-1220.

Leopold, L. B. (1949). The interaction of trade wind and sea breeze, Hawaii, Journal of Meteorology, 6(5), 312-320.

Lesht, B. M., and N. Hawley (1987). Near-bottom currents and suspended sediment concentration in southeastern Lake Michigan. Journal of Great Lakes Research, 13(3), 375-386.

Lien, S. L., and J. A. Hoopes (1978). Wind-driven, steady flows in Lake Superior, Limnology and Oceanography, 23(1), 91-103.

Linacre, E., and B. Geerts (1997). Climate & weather explained, Routledge, London, 432 pp.

Liniger, H., J. Gikonyo, B. Kiteme, and U. Wiesmann (2005). Assessing and managing scarce tropical mountain water resources: the case of Mount Kenya and the semiarid upper Ewaso Ng'iro Basin, Mountain Research and Development, 25(2), 163-173.

Liu, P. C., and D. B. Ross (1980). Airborne measurement of wave growth for stable and unstable atmospheres in Lake Michigan, Journal of Physical Oceanography, 10(11), 1842-1853.

Liu, P. C., D. J. Schwab, and J. R. Bennett (1984). Comparison of a two-dimensional wave prediction model with synoptic measurements in Lake Michigan, Journal of Physical Oceanography, 14(9), 1514-1518.

Longley, R. W. (1969). The diurnal pressure wave in Western Canada, Journal of Applied Meteorology, 8(5), 754-760.

Lonsdale, P., and J. B. Southard (1974). Experimental erosion of North Pacific red clay, Marine Geology, 17, M51-M60.

Losada, J. P. (2001). A deterministic model for lake clarity; application to management of Lake Tahoe, (California-Nevada), USA, PhD thesis, Universitat

de Girona, Spain, 231 pp.

Luettich, R. A., Jr., D. R. F. Harleman, and L. Somlyódy (1990). Dynamic behaviour of suspended sediment concentrations in a shallow lake perturbed by episodic wind events, Limnology and Oceanography, 35(5), 1050-1067.

Lund-Hansen, L. C., M. Petersson, and W. Nurjaya (1999). Vertical sediment fluxes and wave-induced sediment resuspension in a shallow-water coastal lagoon, Estuaries, 22(1), 39-46.

Madsen, J. D., P. A. Chambers, W. F. James, E. W. Koch, and D. F. Westlake (2001). The interaction between water movement, sediment dynamics and submersed macrophytes, Hydrobiologia, 444(1-3), 71-84.

Makin, M., T. J. Kingham, A. E. Wadams, C. J. Birchal, and T. Teferra (1975). Development Prospects in the Southern Rift Valley, Ethiopia, Land resources study 21, Land Resources Division, Ministry of Overseas Development Survey, England, 270 pp.

Mass, C. F., W. J. Steenburgh, and D. M. Schultz (1991). Diurnal surface-pressure variations over the continental United States and the influence of sea level reduction, Monthly Weather Review, 119(12), 2814-2830.

McPherson, R. D. (1970). A numerical study of the effect of a coastal irregularity on the sea breeze, Journal of Applied Meteorology, 9(5), 767-777.

Miller, M. C., I. N. McCave, and P. D. Komar (1977). Threshold of sediment motion under unidirectional currents, Sedimentology, 24, 507-527.

Mohammed-Zaki, M. A. (1980). Time scales in wind-driven lake circulations, Journal of Geophysical Research, 85(C5), 1553-1562.

Montgomery, D. C., and G. C. Runger (1994). Applied Statistics and Probability for Engineers. John Wiley & Sons, Inc., 895 pp.

Muchane, M. W. (1996). Comparison of the isotope record in Micrite, Lake Turkana, with the historical weather record over the last century. In: Johnson, T. C., and E. O. Odada (Eds.) The Limnology, Climatology and Paleoclimatology of the East African Lakes, Gordon and Breach Publishers, OPA, The Netherlands, 431-441.

Muri, G., S. G. Wakeham, T. K. Pease, and J. Faganeli (2004). Evaluation of lipid biomarkers as indicators of changes in organic matter delivery to sediments from Lake Planina, a remote mountain lake in NW Slovenia, Organic Geochemistry, 35, 1083-1093.

Murthy, C. R. (1972). Complex diffusion processes in coastal currents of a lake, Journal of Physical Oceanography, 2, 80-90.

Nelson, C. S. (1983). Bottom sediments of Lake Rotoma, New Zealand Journal of Marine and Freshwater Research, 17, 185-204.

Neumann, J. (1977). On the rotation rate of the direction of sea and land breezes, Journal of the Atmospheric Sciences, 34(12), 1913-1917.

Nicholson, S. E. (1966). A review of climate dynamics and climate variability in Eastern Africa. In: Johnson, T. C., and E. O. Odada (Eds.) The Limnology, Climatology and Paleoclimatology of the East African Lakes, Gordon and Breach Publishers, OPA, The Netherlands, 25-56.

Nieuwolt, S. (1977). Tropical Climatology: An Introduction to the Climate of Low Latitude, John Wiley & Sons, Ltd., 207 pp.

Ochumba, P. B. O. (1996). Measurement of water currents, temperature, dissolved oxygen and winds on the Kenyan Lake Victoria. In: Johnson, T. C., and E. O. Odada (Eds.) The Limnology, Climatology and Paleoclimatology of the East African Lakes, Gordon and Breach Publishers, OPA, The Netherlands, 155-167.

Odada, E. O., D. O. Olago, F. Bugenyi, K. Kulindwa, J. Karimumuryango, K. West, M. Ntiba, S. Wandiga, P. A. Obudho, and P. Achola (2003). Environmental assessment of the East African Rift Valley lakes, Aquatic Sciences - Research Across Boundaries, 65(3), 254-271.

Olago, D. O., and E. O. Odada (1996). Some aspects of the physical and chemical dynamics of a large rift lake: The Lake Turkana north basin, northwest Kenya. In: Johnson, T. C., and E. O. Odada (Eds.) The Limnology, Climatology and Paleoclimatology of the East African Lakes, Gordon and Breach Publishers, OPA, The Netherlands, 413-430.

Paerl, H. W., R. C. Richards, R. L. Leonard, and C. R. Goldman (1975). Sea-

sonal nitrate cycling as evidence for complete vertical mixing in Lake Tahoe, California-Nevada, Limnology and Oceanography, 20(1), 1-8.

Pan, H., R. Avissar, and D. B. Haidvogel (2002). Summer circulation and temperature structure of Lake Kinneret, Journal of Physical Oceanography, 32(1), 295-313.

Peeters, F., A. Wuest, G. Piepke, and D. M. Imboden (1996). Horizontal mixing in lakes, Journal of Geophysical Research, 101(C8), 18,361-18,375.

Pennington, W., and T. G. Tutin (1974). Seston and sediment formation in five lake district lakes, The Journal of Ecology, 62(1), 215-251, doi:10.2307/2258890.

Petenko, I. V., and S. Argentini (2001). The daily behaviour of pressure and its influence on the wind regime in East Antarctica during the winters of 1993 and 1994, Journal of Applied Meteorology, 40(7), 1255-1264.

Petterssen, S. (1969). Introduction to meteorology, McGraw Hill Inc., 333 pp.

Petticrew, E. L., and J. Kalff (1991). Predictions of surficial sediment composition in the littoral zone of lakes, Limnology and Oceanography, 36(2), 384-392.

Pickett, R. L. (1976). Lake Ontario circulation in November, Limnology and Oceanography, 21(4), 608-611.

Pickett, R. L. (1977). The observed winter circulation of Lake Ontario, Journal of Physical Oceanography, 7, 152-156.

Pickett, R. L. (1980). Observed and predicted Great Lakes winter circulations, Journal of Physical Oceanography, 10(7), 1140-1145.

Pickett, R. L., and D. A. Dossett (1979). Mirex and the circulation of Lake Ontario, Journal of Physical Oceanography, 9, 441-445.

Piñones, A., A. Valle-Levinson, D. A. Narváez, C. A. Vargas, S. A. Navarrete, G. Yuras, and J. C. Castilla (2005). Wind-induced diurnal variability in river plume motion, Estuarine, Coastal and Shelf Science, 65(3), 513-525.

Pyle, R. L. (1959). The diurnal pressure oscillation on a heated mountain island, Journal of Meteorology, 16(5), 467-482.

Rao, D. B. (1967). Response of a lake to a time-dependent wind stress, Journal of Geophysical Research, 72, 1697-1708.

Ravens T. M., O. Kocsis, A. Wuest, and N. Granin (2000). Small-scale turbulence and vertical mixing in Lake Baikal, Limnology and Oceanography, 45(1), 159-173.

Reckhow, K. H., and S. C. Chapra (1983). Engineering Approach for Lake Management, Volume 1: Data analysis and Empirical Modelling, Butterworth Publishers, 340 pp.

Riehl, H. (1979). Climate and weather in the tropics, Academic press inc. (London) PLD, 611 pp.

Roden, G. I. (1962). On sea-surface temperature, cloudiness and wind variations in the Tropical Atlantic, Journal of the Atmospheric Sciences, 19, 66-80.

Roden, G. I. (1965). On atmospheric pressure oscillations along the Pacific coast of North America, 1873-1963, Journal of the Atmospheric Sciences, 22(3), 280-295.

Rosenthal, S. L. (1960). Some estimates of the power spectra of large-scale distribution in low latitudes, Journal of Meteorology, 17(1), 259-263.

Rosenthal, S. L. (1960). The aperiodic diurnal range of temperature over the North Atlantic Ocean, Journal of Meteorology, 17(1), 78-83.

Rosenthal, S. L. (1960). The interdiurnal variability of surface-air temperature over the North Atlantic Ocean, Journal of Meteorology, 17(1), 1-7.

Rosenthal, S. L., and W. A. Baum (1956). Diurnal variation of surface pressure over the North Atlantic Ocean, Monthly Weather Review, 84(11), 379-387.

Rozanski, K., L. Araguas-Araguas, and R. Gonfiantini (1996). Isotop patterns of precipitation in the East African Region. In: Johnson, T. C., and E. O. Odada (Eds.) The Limnology, Climatology and Paleoclimatology of the East African Lakes, Gordon and Breach Publishers, OPA, The Netherlands, 79-93.

Ryan, D. A., A. D. Heap, L. Radke, and D. T. Heggie (2003). Conceptual Models of Australia's Estuaries and Coastal Waterways Applications for Coastal

Resource Management, Geoscience Australia Record 2003/09, 135 pp.

Sanford, L. P., S. E. Suttles, and J. P. Halka (2001). Reconsidering the physics of the Chesapeake Bay estuarine turbidity maximum, Estuaries, 24(5), 655-669.

Savijärvi, H. (1997). Diurnal winds around Lake Tanganyika, , Quarterly Journal of the Royal Meteorological Society, 123, 091-918.

Saylor, J. H., and G. S. Miller (1976). Winter currents in Lake Huron, Environmental Protection Agency Report No: EPA-905/4-75-004, 107 pp.

Saylor, J. H., and G. S. Miller (1987). Studies of large scale currents in Lake Erie, 1979-80, Journal of Great Lakes Research, 13(4), 487-514.

Schmidt, F. H. (1947). An elementary theory of the land- and sea-breeze circulation, Journal of Meteorology, 4(1), 9-20.

Schnurrenberger, D., J. Russell, and K. Kelts (2003). Classification of lacustrine sediments based on sedimentary components, Journal of Paleoliminology, 29, 141-154.

Schoettle, M., and G. M. Friedman (1973). Organic carbon in sediments of Lake George, New York: Relation to morphology of lake bottom, grain size of sediments, and man's activities, Bulletin of the Geological Society of America, 84, 191-198.

Schrader, D. L., and R. R. Holmes, Jr. (2000). Suspended-sediment budget, flow distribution, and lake circulation for the fox chain of lakes in lake and counties, Illinois, 1997-99, U.S. Geological Survey Water-Resources Investigations Report 00-4115, 23 pp.

Schröder, R. (1984). An attempt to estimate the fish stock and the sustainable yield of Lake Ziway and Lake Abaya, Ethiopian Rift Valley, Arch. Hydrobiol./Suppl., 69(3), 411-441.

Schütt, B., and S. Thiemann (2004). Modern water lever and sediment accumulation changes of Lake Abaya, southern Ethiopia - A case study from the Bilate River delta, northern lake area, Sustainable management of headwater resources: Research from Africa and India, 137-154.

Schütt, B., and S. Thiemann (2006) Kulfo River, South-Ethiopia as a regulator of lake level changes in the Lake Abaya-Lake Chamo System, Zbl. Geol. Paläont. Teil I, 2004, 129-143.

Schütt, B., S. Thiemann, and B. Weneclawiak (2005). Deposition of modern fluvio-lacustrine sediments in Lake Abaya, south Ethiopia - A case study from the delta areas of Bilate River and Gidabo River, northern basin, Z. Geomorph, N. F., 138, 131-151.

Schwab, D. J., and D. Beletsky (2003). Relative effects of wind stress curl, topography, and stratification on large-scale circulation in Lake Michigan, Journal of Geophysical Research, 108(C2), 3044, doi:10.1029/2001JC001066.

Schwab, D. J., W. P. O'Connor, and G. L. Mellor (1995). On the net cyclonic circulation in large stratified lakes, Journal of Physical Oceanography, 25(6), 1516-1520.

SEBA HYDROMETRIE (1999). SEBA-TERM User Manual SWE 370. Kaufbeuren, Germany, 48 pp.

SEBA HYDROMETRIE (2004). Digital Multiparameterprobe MPS-D User Manual MPS 512. Kaufbeuren, Germany, 32 pp.

SEBA HYDROMETRIE (2004). Quality Dipper User Manual KLQ 524. Kaufbeuren, Germany, 39 pp.

Sheng, Y. P., and W. Lick (1979). The transport and resuspension of sediments in a shallow lake, Journal of Geophysical Research, 84(C4), 1809-1826.

Shotbolt, L. A., A. D. Thomas, and S. M. Hutchinson (2005). The use of reservoir sediments as environmental archives of catchment inputs and atmospheric pollution, Progress in Physical Geography, 29(3), 337-361.

Signell, R. P., R. C. Beardsley, H. C. Graber, and A. Capotondi (1990). Effect of wave-current interaction on wind-driven circulation in narrow, shallow embayments, Journal of Geophysical Research, 95(C6), 9671-9678.

Simpson, J. E. (1996). Diurnal changes in sea-breeze direction, Journal of Applied Meteorology, 35(7), 1166-1169.

Smith, N. D. (1978). Sedimentation processes and patterns in a glacier-fed lake with low sediment input, Canadian Journal of Earth Sciences, 15, 741-756.

Spar, J. (1950). On the theory of annual pressure variation, Journal of Meteorology, 7(3), 167-180.

Spigel, R. H., and G. W. Coulter (1996). Comparison of hydrology and physical limnology of the East African Great Lakes: Tanganyika, Malawi, Victoria, Kivu and Turkana (with reference to some North American Great Lakes), 103 - 139. In: Johnson, T. C., and E. O. Odada (Eds.) The Limnology, Climatology and Paleoclimatology of the East African Lakes, Gordon and Breach Publishers, OPA, The Netherlands.

Spigel, R. H., and J. Imberger (1980). The classification of mixed-layer dynamics in lakes of small to medium size, Journal of Physical Oceanography, 10( ), 1104-1121.

Spreen, W. C. (1956). Empirically determined distribution of hourly temperatures, Journal of Meteorology, 13(4), 351-355.

Staley, D. O. (1957). The low-level sea breeze of Northwest Washington, Journal of Meteorology, 14(5), 458-470.

Stocker, R., and J. Imberger (2003). Horizontal transport and dispersion in the surface layer of a medium-sized lake, Limnology and Oceanography, 48(3), 971-982.

Sumner, G., V. Homar and C. Ramis (2001). Precipitation seasonality in eastern and southern coastal Spain, International Journal of Climatology, 21, 219-247.

Sundborg, Å. (1992). Lake and reservoir sedimentation and prediction and interpretation, Geografiska Annaler. Series A, Physical Geography, 74 (2-3), 93-100.

Teeter, A. M., B. H. Johnson, C. Berger, G. Stelling, N. W. Scheffner, M. H. Garcia, and T.M. Parchure (2001). Hydrodynamic and sediment transport modelling with emphasis on shallow-water, vegetated areas (lakes, reservoirs, estuaries and lagoons), Hydrobiologia, 444(1-3), 1-23.

Teklemariam, A. (2005). Water quality monitoring in Lake Abaya and Chamo regions - Ethiopia. PhD thesis, Universität Siegen, 307 pp.

Teklemariam, M. and K. Beyene (2005). Geothermal exploration and development of Ethiopia, Proceedings World Geothermal Congress 2005, Antalya, Turkey, 24-29 April 2005.

Thiemann, S. D. (2006). Detection and assessment of erosion and soil erosion risk in the wetland of the Bilate River, South Ethiopian Rift Valley, PhD Thesis, Freie Univesität Berlin, pp 236.

Thomas, R. L. (1969). A note on the relationship of grain size, clay content, quartz and organic carbon in some Lake Erie and Lake Ontario sediments, Journal of Sediment Petrology, 39, 803-809.

Thomas, R. L., A. L. W. Kemp, and C. F. M. Lewis (1972). Distribution, composition and characteristics of the surficial sediments of Lake Ontario, Journal of Sedimentary Research, 42(1), 66-84.

Thompson, O. E., P. A. Arkin, and W. D. Bonner (1976). Diurnal variations of the summertime wind and force field at three midwestern locations, Monthly Weather Review, 104(8), 1012-1022.

Tudornacea, C., and W. D. Taylor (2002). Introduction. In: Tudornacea, C., and W. D. Taylor (Eds.). Ethiopian Rift Valley Lakes, Backluys Publishers, Leiden, 1-12.

U.S. Environmental Protection Agency (EPA) (1994). General Field Sampling Guidelines. SOP#: 2001. Washington, DC.

U.S. Environmental Protection Agency (EPA) (2000). Guidance for Data Quality Objectives Process (EPA QA/G-4). EPA/600/R-96/055. Washington, DC.

U.S. Environmental Protection Agency (EPA) (2002). Guidance for Quality Assurance Project Plans (EPA QA/G-5). EPA/240/R-02/009. Washington, DC.

Vallet-Coulomb, C., D. Legesse, F. Gasse, T. Travi, and T. Chernet (2001). Lake evaporation estimates in tropical Africa, Journal of Hydrology, 245, 1-18.

Van Duin, E. H. S., G. Blom, F. J. Los, R. Maffione, R. Zimmerman, C. F. Cerco, M. Dortch, and E. P. H. Best (2001). Modeling underwater light climate in relation to sedimentation, resuspension, water quality and autotrophic growth, Hydrobiologia, 444(1-3), 25-42.

Van Maren, D. S., and P. Hoekstra (2005). Dispersal of suspended sediments in the turbid and highly stratified Red River plume, Continental Shelf Research, 25(4), 503-519.

Viner, A. B., and L. Kemp (1983). The effect of vertical mixing on the phytoplankton of Lake Rotongaio (July 1979 - January 1981) New Zealand Journal of Marine and Freshwater Research, 17, 407-422.

Visher, S. S. (1946). Average daily temperature range in the United States, Bulletin of the American Meteorological Society, 27, 594-597.

Walin, G. (1972). On the hydrographic response to transient meteorological disturbances, Tellus 24, 169-186.

Wallance, J. M., and F. R. Hartranft (1969). Diurnal wind variations, surface to 30 km, Monthly Weather Review, 97(6), 446-455.

Walsh, P. D., and D. M. Lawler (1981). Rainfall seasonality: description, spatial patterns, and change through time, Weather, 36, 201-208.

Wang, Y., K. Hutter, and E. Bäuerle (2001). Barotropic response in a lake to wind-forcing, Annales Geophysicae, 19,367-388.

Ward, G. H., and N. E. Armstrong (1997). Current status and historical trends of ambient water, sediment, fish and shellfish tissue quality in the Corpus Christi Bay National Estuary, Summary Report, Corpus Christi Bay National Estuary Program, CCBNEP-13, 270 pp.

Warrick, J. A., L. A. K. Mertes, L. Washburn, and D. A. Siegel (2004). A conceptual model for river water and sediment dispersal in the Santa Barbara Channel, California, Continental Shelf Research, 24(17), 2029-2043.

Weber, M. R. (1978). Average diurnal wind variation in the southern lower Michigan, Journal of Applied Meteorology, 17, 1182-1189.

Webster, T., and C. Lemckert (2002). Sediment resuspension within a microtidal estuary/embayment and the implication to channel management, Journal of Coastal Research, Special Issue 36, 753-759.

Wescott, W. A., C. K. Morley, and F. M. Karanja (1996). Tectonic controls on the development of rift-basin lakes and their sedimentary character: examples from the East African Rift System. In: Johnson, T. C., and E. O. Odada (Eds.) The Limnology, Climatology and Paleoclimatology of the East African Lakes, Gordon and Breach Publishers, OPA, The Netherlands, 3-21.

Winant, C. D. (1980). Coastal circulation and wind-induced currents, Annual Review of Fluid Mechanics, 12, 271-301.

Winant, C. D. (2004). Three-dimensional wind-driven flow in an elongated, rotating basin, Journal of Physical Oceanography, 34(2), 462-476.

WoldeGabriel, G. (2002). The main Ethiopian rift system: An overview on volcanic, tectonic, rifting, and sedimentation processes. In: Tudorancera, C., and W. D. Taylor (Eds.). Ethiopian Rift Valley Lakes, Backhuys Publishers, 13-43.

WoldeGabriel, G., G. Heiken, T. D. White, B. Asfaw, W. K. Hart, and P. R. Renne (2000). Volcanism, tectonism, sedimentation, and the paleoanthropological record in the Ethiopian Rift System. In: McCoy, F. W., and G. Heiken (Eds.). Volcanic Hazards and Disasters in Human Antiquity, Boulder, Colorado, Geophysical Society of America Special Paper 345, 83-99.

Woldu, Z, and M. Tadesse (1990). The vegetation in the lakes region of the rift valley of Ethiopia and the possiblility of its recoveries. SINET, Ethiopian Journal of Science, 13, 97-120.

Wood, R. B., and J. F. Talling (1988). Chemical and algal relationships in a salinity series of Ethiopian inland waters, Hydrobiologia, 158, 29-67.

Wood, R. B., M. V. Prosser, and R. M. Baxter (1978). Optical characteristics of the Rift Valley Lakes, Ethiopia, Senet: Ethiopian Journal of Science, 1, 73-85.

Wood, T. M., G. J. Fuhrer, and J. L. Morace (1996). Relation between selected water-quality variables and lake level in upper Klamath and agency lakes, Oregon, U.S. Geological Survey Water-Resources Investigations Report

96-4079, 57 pp.

Wright, L. D. (1977). Sediment transport and deposition at river mouths: A synthesis, Geological Society of America Bulletin, 88 (6), 857-868.

Wright, L. D., and C. A. Nittrouer (1995). Dispersal of river sediments in coastal seas: Six contrasting cases, Estuaries, 18(3), 494-508.

Yu, T. W., and N. K. Wagner (1970). Diurnal variation of onshore wind speed near a coastline, Journal of Applied Meteorology, 9(5), 760-766.

Yuretich, R. F. (1979). Modern sediments and sedimentary processes in Lake Rudolf (Lake Turkana) eastern Rift Valley, Kenya, Sedimentology, 26(3), 313-331.

Yuretich, R. F. (1982). Possible influences upon lake development in the east African rift valleys, Journal of Geology, 90, 329-337.

Yuretich, R. F. (1986). Controls on the composition of modern sediments, Lake Trukana, Kenya. In: Frostick, L. E. et al. (Eds.). Sedimentation in the African Rifts, Geological Society Special Publication, 25, 141-152.

Zhong, S., and E. S. Takle (1992). An observational study of sea- and land-breeze circulation in an area of complex coastal heating, Journal of Applied Meteorology, 31(12), 1426-1431.

Zhong, S., and E. S. Takle (1993). Effects of large-scale winds on the sea-land-breeze circulations in an area of complex coastal heating, Journal of Applied Meteorology, 32, 1181-1195.

9 Appendix

Appendix A. *Mineralogical composition of surficial sediments in Lake Abaya (vol. %)*

SampleID	Easting	Northing	Quartz	Calcite	Feldspar	Clay	Hematite	Magnetite	Pyrite	Hornblende
BG0101	348359	676308	3	7	40	45	1	0	5	0
BG0103	349222	675811	8	2	32	56	1	0	0	0
BG0105	350095	675355	4	4	33	55	3	1	0	0
BG0107	350963	674869	4	2	24	53	1	1	0	14
BG0109	351831	674399	4	1	25	66	0	4	0	0
BG0111	352714	673909	5	2	19	71	2	1	0	0
BG0113	353571	673426	7	1	21	69	2	0	0	0
BG0115	354450	672947	2	2	22	72	1	1	0	0
BG0117	355327	672472	0	1	10	85	2	1	0	0
BG0119	356211	671981	0	1	11	86	2	1	0	0
BG0121	357080	671514	4	1	15	77	3	0	0	0
BG0123	357947	671013	4	1	14	69	1	1	0	9
BG0125	358834	670556	1	2	9	86	1	1	0	0
BG0129	360623	669575	6	3	20	69	2	1	0	0
BG0201	345462	665517	1	5	51	35	1	0	1	6
BG0203	346346	664968	4	2	68	17	2	1	6	0
BG0205	347181	664449	3	2	42	50	1	1	1	0
BG0301	345719	665939	3	7	73	14	2	1	0	0
BG0303	346641	665451	3	3	28	64	1	1	0	0
BG0305	347499	664980	3	3	32	60	1	1	0	0
BG0401	345500	666000	3	3	66	22	2	3	1	0
BG0403	346500	666000	2	10	26	57	2	0	2	0
BG0405	347500	666000	4	3	26	56	1	0	1	8
BG0407	348500	666000	5	2	31	59	0	0	3	0
BG0409	349500	666000	3	2	12	81	2	1	0	0
BG0411	350500	666000	3	1	9	87	0	0	0	0
BG0413	351500	666000	6	3	24	62	3	2	0	0
BG0415	352500	666000	7	2	27	58	5	1	0	0
BG0501	346000	666500	6	3	61	26	1	1	2	0
BG0503	347000	666500	3	7	19	64	4	1	3	0
BG0505	348000	666500	2	1	15	79	0	0	1	0
BG0507	349000	666500	4	1	14	79	1	1	0	0
BG0509	350000	666500	4	1	20	71	1	1	2	0
BG0511	351000	666500	1	1	11	77	0	1	1	7
BG0513	352000	666500	4	1	8	85	1	1	0	0
BG0515	353000	666500	7	2	24	61	1	2	4	0
BG0601	346000	667000	2	8	66	20	1	2	1	0
BG0603	347000	667000	2	10	66	18	1	2	1	0
BG0605	348000	667000	8	2	34	52	2	1	0	0
BG0607	349000	667000	3	2	15	68	1	1	0	10
BG0609	350000	667000	4	2	16	77	1	0	0	0
BG0611	351000	667000	3	1	10	82	2	1	0	0

Appendix A. *Mineralogical composition of surficial sediments in Lake Abaya (vol. %)*

SampleID	Easting	Northing	Quartz	Calcite	Feldspar	Clay	Hematite	Magnetite	Pyrite	Hornblende
BG0613	352000	667000	4	1	13	78	3	0	0	0
BG0615	353000	667000	2	2	10	84	2	0	0	0
BG0617	354000	667000	1	2	22	71	0	1	2	0
BG0619	355500	667000	2	3	33	59	0	1	3	0
BG0621	356500	667000	3	2	14	78	1	0	2	0
BG0623	357500	667000	2	3	26	68	1	1	0	0
BG0625	359000	667000	2	4	37	49	1	1	1	5
BG0701	346000	667500	2	3	66	24	1	2	2	0
BG0703	347000	667500	4	5	56	25	2	1	2	5
BG0705	348000	667500	2	4	9	82	1	1	0	0
BG0707	349000	667500	2	2	14	80	2	1	0	0
BG0709	350000	667509	7	2	19	56	2	0	0	14
BG0711	351000	667500	1	2	23	68	3	3	0	0
BG0713	352000	667500	5	1	12	79	1	1	0	0
BG0715	353000	667500	2	1	7	88	0	0	1	0
BG0717	354000	667500	5	1	19	72	3	0	0	0
BG0719	355500	667500	3	3	26	65	1	1	0	0
BG0721	356500	667500	6	3	19	68	1	1	2	0
BG0723	357500	667500	4	2	18	60	2	0	4	10
BG0725	358500	667500	5	2	35	50	3	1	2	0
BG0727	359500	667500	6	2	33	53	3	2	0	0
BG0801	346500	668000	3	4	68	15	1	2	1	6
BG0803	347500	668000	2	11	11	67	1	1	0	8
BG0805	348500	668000	5	2	19	72	2	1	0	0
BG0807	349500	668000	10	1	19	50	9	3	7	0
BG0809	350500	668000	2	1	10	83	2	1	0	0
BG0811	351500	668000	4	1	21	72	3	0	0	0
BG0813	352500	668000	3	1	15	80	1	0	0	0
BG0815	353500	668000	0	2	19	77	1	1	0	0
BG0817	354500	668000	5	2	12	79	1	1	0	0
BG0819	356000	668000	3	2	9	83	1	1	0	0
BG0821	357000	668000	1	3	16	76	2	2	0	0
BG0823	358000	668000	2	1	7	88	2	0	0	0
BG0825	359000	668000	1	2	17	77	1	1	0	0
BG0827	360000	668000	7	2	41	44	2	2	2	0
BG0901	346500	668500	3	3	64	22	2	1	1	4
BG0903	347500	668500	3	8	56	24	1	2	0	6
BG0905	348500	668500	4	2	25	66	2	1	0	0
BG0907	349500	668500	8	2	23	60	0	2	4	0
BG0909	350500	668500	2	2	21	72	2	1	0	0
BG0911	351500	668500	4	2	20	72	1	1	0	0

Appendix A. *Mineralogical composition of surficial sediments in Lake Abaya (vol. %)*

SampleID	Easting	Northing	Quartz	Calcite	Feldspar	Clay	Hematite	Magnetite	Pyrite	Hornblende
BG0913	352500	668500	1	2	17	76	3	1	0	0
BG0915	353500	668500	5	2	9	79	2	0	2	0
BG0917	354500	668500	4	3	15	76	1	1	0	0
BG0919	355500	668500	5	3	23	63	2	2	2	0
BG0921	356500	668500	5	2	16	75	2	1	0	0
BG0923	357500	668500	6	2	19	70	3	0	0	0
BG0925	358500	668500	7	2	14	74	1	1	2	0
BG0927	359500	668500	7	2	20	67	2	1	0	0
BG0929	360500	668500	4	3	24	66	1	1	1	0
BG1001	346500	663500	2	4	29	64	0	1	0	0
BG1003	350000	663500	1	1	16	75	4	2	0	0
BG1101	346500	664000	5	3	63	14	2	3	0	11
BG1103	347500	664000	7	2	46	39	1	1	4	0
BG1105	349000	664000	1	2	7	87	1	1	0	0
BG1107	350000	664000	3	2	15	69	0	2	0	10
BG1109	351000	664000	3	3	22	68	3	1	0	0
BG1201	345000	664500	2	2	67	25	1	1	1	0
BG1203	346000	664500	2	2	49	42	1	2	2	0
BG1205	347000	664500	2	2	42	46	1	2	0	6
BG1207	348000	664500	4	10	12	72	1	1	0	0
BG1209	349000	664500	1	3	20	75	0	1	0	0
BG1211	350000	664500	5	2	13	79	1	1	0	0
BG1213	351000	664500	1	3	14	63	1	1	0	16
BG1301	345500	665000	3	2	58	27	1	1	3	5
BG1303	346500	665000	4	0	46	46	1	1	2	0
BG1305	347500	665000	3	1	28	66	1	1	0	0
BG1307	348500	665000	3	1	17	77	1	1	0	0
BG1309	349500	665000	4	1	20	73	1	1	0	0
BG1311	350500	665000	4	1	23	67	4	2	0	0
BG1313	351500	665000	6	2	30	58	2	2	0	0
BG1401	345500	665500	3	4	58	31	1	0	3	0
BG1403	346500	665500	3	6	24	65	0	2	0	0
BG1411	350500	665500	5	2	31	59	1	1	0	0
BG1413	351500	665500	5	2	17	76	1	0	0	0
BG1501	346500	669000	3	5	68	20	1	2	1	0
BG1503	347500	669000	8	6	40	39	5	2	0	0
BG1505	348500	669000	0	1	16	58	4	3	0	17
BG1507	349500	669000	3	1	10	82	2	1	1	0
BG1509	350500	669000	1	1	8	87	1	2	0	0
BG1511	351500	669000	3	1	17	77	2	1	0	0
BG1405	347500	665500	4	4	30	57	1	1	3	0

Appendix A. *Mineralogical composition of surficial sediments in Lake Abaya (vol. %)*

SampleID	Easting	Northing	Quartz	Calcite	Feldspar	Clay	Hematite	Magnetite	Pyrite	Hornblende
BG1407	348500	665500	4	3	14	75	1	1	2	0
BG1409	349500	665500	6	4	33	53	3	1	0	0
BG1513	352500	669000	1	1	20	77	0	1	0	0
BG1515	353500	669000	6	1	24	64	2	0	2	0
BG1517	354500	669000	5	2	21	69	2	1	0	0
BG1519	355500	669000	5	2	17	73	1	2	0	0
BG1521	356500	669000	5	2	6	84	3	1	0	0
BG1523	357500	669000	5	3	21	71	0	1	0	0
BG1525	358500	669000	9	2	21	62	4	1	0	0
BG1527	359500	669000	5	2	20	69	2	2	0	0
BG1529	363000	669000	5	7	30	56	1	1	0	0
BG1531	364000	669000	7	7	38	43	2	1	3	0
BG1601	347000	670000	3	2	60	27	1	1	2	4
BG1603	348000	670000	4	1	17	75	2	0	0	0
BG1605	349000	670000	5	2	12	81	1	0	0	0
BG1607	350000	670000	1	1	13	83	0	1	0	0
BG1609	351000	670000	2	1	10	84	2	1	0	0
BG1611	352000	670000	4	1	16	75	3	1	0	0
BG1613	353000	670000	1	1	21	64	1	2	0	10
BG1615	354000	670000	2	2	25	69	1	1	0	0
BG1617	355000	670000	5	2	12	78	2	1	0	0
BG1619	356000	670000	2	2	8	86	1	1	0	0
BG1621	357000	670000	4	2	16	76	2	1	0	0
BG1623	358000	670000	4	2	18	72	3	1	0	0
BG1625	359000	670000	2	2	22	70	2	2	0	0
BG1627	360000	670000	1	2	22	71	2	1	0	0
BG1629	363000	670000	3	9	37	47	1	2	2	0
BG1631	364000	670000	4	8	10	70	1	0	1	6
BG1701	347000	671000	4	2	58	28	1	2	2	3
BG1703	348000	671000	7	2	27	33	3	2	8	17
BG1705	349000	671000	3	1	16	77	0	2	0	0
BG1707	350000	671000	4	2	11	82	1	1	0	0
BG1709	351000	671000	2	1	10	84	1	2	0	0
BG1711	352000	671000	2	2	17	77	2	0	0	0
BG1713	353000	671000	5	2	18	73	1	1	0	0
BG1715	354000	671000	3	2	14	78	2	1	0	0
BG1717	355000	671000	3	1	13	80	2	1	0	0
BG1719	356000	671000	3	1	12	81	1	0	0	0
BG1721	357000	671000	5	2	22	69	0	1	0	0
BG1723	358000	671000	1	2	13	81	0	1	1	0
BG1725	359000	671000	5	2	18	73	2	1	0	0

Appendix A. *Mineralogical composition of surficial sediments in Lake Abaya (vol. %)*

SampleID	Easting	Northing	Quartz	Calcite	Feldspar	Clay	Hematite	Magnetite	Pyrite	Hornblende
BG1727	360000	671000	5	3	18	71	2	1	0	0
BG1729	361000	671000	4	3	20	70	2	1	0	0
BG1731	363500	671000	10	7	19	63	0	1	0	0
BG1733	364500	671000	4	8	11	74	2	1	0	0
BG1801	347000	672000	3	3	64	24	1	1	1	3
BG1803	348000	672000	7	2	25	62	3	1	0	0
BG1805	349000	672000	3	1	12	82	1	1	0	0
BG1807	350000	672000	5	1	14	78	1	1	0	0
BG1809	351000	672000	8	1	19	65	4	2	0	0
BG1811	352000	672000	2	2	8	84	0	1	3	0
BG1813	353000	672000	4	2	20	71	2	1	0	0
BG1815	354000	672000	7	2	19	71	1	0	0	0
BG1817	355000	672000	5	2	17	73	3	1	0	0
BG1819	356000	672000	3	2	15	77	1	1	1	0
BG1821	357000	672000	2	1	14	79	2	2	0	0
BG1823	358000	672000	2	1	6	91	0	0	0	0
BG1825	359000	672000	3	2	9	83	2	1	0	0
BG1827	360000	672000	5	2	15	75	2	0	0	0
BG1829	361000	672000	1	2	18	73	3	2	0	0
BG1833	364500	672000	4	5	13	78	0	0	0	0
BG1901	347000	672998	5	3	76	13	1	1	1	0
BG1903	348000	672998	6	2	14	75	1	2	0	0
BG1905	349000	672998	5	2	19	71	3	0	0	0
BG1907	350000	672998	6	2	18	70	2	1	0	0
BG1909	351000	672998	5	2	23	64	4	2	0	0
BG1911	352000	672998	6	2	12	72	2	1	4	0
BG1913	353000	673000	3	2	9	85	1	0	0	0
BG1915	354000	673000	3	2	5	89	2	0	0	0
BG1917	355000	673000	1	2	19	77	0	1	0	0
BG1919	356000	673000	2	2	16	76	3	1	0	0
BG1921	357000	673000	4	2	15	76	2	1	0	0
BG1923	358000	673000	4	2	19	72	2	1	0	0
BG1925	359000	673000	1	2	23	70	2	1	0	0
BG1927	360000	673000	8	2	22	65	2	1	0	0
BG1929	361000	673000	5	3	17	71	2	1	1	0
BG1931	362000	673000	5	4	21	68	1	1	0	0
BG1933	363500	672999	8	5	23	60	4	1	0	0
BG1935	364500	672999	7	5	20	53	1	0	3	10
BG2001	347000	674000	4	6	25	63	0	1	0	0
BG2003	349000	674000	5	3	11	78	0	0	2	0
BG2005	351000	674000	5	1	15	77	1	1	0	0

Appendix A. *Mineralogical composition of surficial sediments in Lake Abaya (vol. %)*

SampleID	Easting	Northing	Quartz	Calcite	Feldspar	Clay	Hematite	Magnetite	Pyrite	Hornblende
BG2007	353000	674000	3	1	16	78	0	1	0	0
BG2009	355000	674000	2	1	14	77	3	3	0	0
BG2011	357000	674000	4	2	18	58	2	1	4	12
BG2013	359000	674000	1	2	14	79	2	2	0	0
BG2015	361000	674000	7	3	22	67	1	1	0	0
BG2017	363000	674000	2	5	21	70	2	1	0	0
BG2019	365000	674000	8	5	35	47	4	1	0	0
BG2101	347000	675000	3	12	55	27	1	1	1	0
BG2103	349000	675000	5	2	19	71	2	1	0	0
BG2105	351000	675000	3	2	19	75	0	1	0	0
BG2107	353000	675000	1	2	17	75	3	2	0	0
BG2109	355000	675000	8	4	19	67	1	1	0	0
BG2111	357000	675000	3	2	10	82	2	1	0	0
BG2113	359000	675000	3	2	12	79	3	1	0	0
BG2115	361000	675000	6	3	13	77	1	0	0	0
BG2117	363000	675000	7	3	18	71	0	1	0	0
BG2119	365000	675000	6	2	10	80	1	1	0	0
BG2201	347000	676000	3	3	28	63	3	0	0	0
BG2203	349000	676000	9	1	30	57	1	1	0	0
BG2205	351000	676000	5	2	17	64	1	1	2	8
BG2207	353000	676000	2	2	16	63	2	1	0	14
BG2209	355000	676000	4	2	18	73	1	1	1	0
BG2211	357000	676000	5	2	11	78	2	2	0	0
BG2213	359000	676000	7	2	19	68	2	1	0	0
BG2215	361000	676000	3	4	17	73	2	1	0	0
BG2217	363000	676000	6	4	21	55	2	0	2	10
BG2219	365000	676000	1	11	74	11	1	1	1	0
BG2301	352000	676998	6	1	24	67	1	1	0	0
BG2303	354000	676998	3	3	18	75	0	1	0	0
BG2305	356000	677000	1	3	19	73	3	1	0	0
BG2307	358000	677000	3	2	12	80	2	1	0	0
BG2309	360000	677000	7	2	7	81	2	1	0	0
BG2311	362000	677000	3	1	13	80	2	1	0	0
BG2313	364000	676998	5	2	22	69	2	0	0	0
BG2315	366000	676998	6	3	32	52	1	1	5	0
BG2401	353000	678000	7	1	29	61	1	1	0	0
BG2403	355000	678000	3	0	23	71	2	1	0	0
BG2405	357000	678000	3	1	18	76	1	1	0	0
BG2407	359000	678000	5	2	18	72	2	1	0	0
BG2409	361000	678000	7	1	25	66	1	0	0	0
BG2411	363000	678000	5	1	21	58	1	1	3	10

Appendix A. *Mineralogical composition of surficial sediments in Lake Abaya (vol. %)*

SampleID	Easting	Northing	Quartz	Calcite	Feldspar	Clay	Hematite	Magnetite	Pyrite	Hornblende
BG2413	365000	678000	9	3	18	59	1	1	0	9
BG2414	366000	678000	7	4	26	61	1	1	0	0
BG2501	354000	679000	8	1	28	59	2	1	1	0
BG2503	356000	679000	3	1	12	83	1	0	0	0
BG2505	358000	679000	1	0	18	79	0	2	0	0
BG2507	360000	679000	2	2	16	78	1	1	0	0
BG2509	362000	679000	5	4	20	68	2	1	0	0
BG2511	365000	679000	4	8	17	69	1	1	0	0
BG2513	367000	679000	4	2	30	62	1	1	0	0
BG2601	354000	680000	7	1	30	54	1	1	1	5
BG2602	355000	680000	6	1	25	65	1	1	1	0
BG2604	357000	680000	5	2	19	71	2	1	0	0
BG2606	359000	680000	5	2	17	72	1	1	2	0
BG2608	361000	680000	4	3	12	78	2	0	1	0
BG2610	363000	680000	6	2	13	78	0	1	0	0
BG2611	365000	680000	8	2	25	61	1	1	2	0
BG2613	367000	680000	7	5	34	51	2	1	0	0
BG2614	368000	680000	7	4	28	59	1	1	0	0
BG2701	354000	681000	3	1	33	59	1	1	2	0
BG2702	355000	681000	6	2	42	45	3	2	0	0
BG2703	356000	681000	4	2	19	73	2	0	0	0
BG2704	357000	681000	3	2	19	73	1	1	1	0
BG2705	358000	681000	7	2	21	65	3	2	0	0
BG2706	359000	681000	8	4	19	65	2	2	0	0
BG2707	360000	681000	5	3	16	64	1	0	2	9
BG2709	362000	681000	6	4	18	71	0	1	0	0
BG2712	366000	681000	7	2	25	64	1	1	0	0
BG2714	368000	681000	6	6	22	54	1	2	3	6
BG2715	369000	681000	4	2	18	74	0	1	1	0
BG2801	360000	682000	7	4	31	43	1	2	0	12
BG2802	361000	682000	8	4	19	64	2	1	2	0
BG2804	363000	682000	8	4	26	58	3	1	0	0
BG2807	367000	682000	6	3	21	67	2	1	0	0
BG2809	369000	682000	7	5	22	63	1	2	0	0
BG2901	360000	683000	8	3	33	54	0	1	1	0
BG2904	364000	683000	7	2	26	63	1	1	0	0
BG2906	366000	683000	7	3	34	53	1	2	0	0
BG2908	368000	683000	9	4	26	59	1	1	0	0
BG3001	361000	684000	7	4	20	67	1	1	0	0
BG3002	362000	684000	6	6	27	59	1	1	0	0
BG3003	363000	684000	3	2	24	66	1	1	3	0
BG3005	367000	684000	9	3	26	60	1	1	0	0

Appendix A. *Mineralogical composition of surficial sediments in Lake Abaya (vol. %)*

SampleID	Easting	Northing	Quartz	Calcite	Feldspar	Clay	Hematite	Magnetite	Pyrite	Hornblende
BG3101	361000	685000	6	3	32	57	1	1	0	0
BG5801	350500	662000	5	3	20	70	1	1	0	0
BG6001	350000	663000	4	2	16	75	2	1	0	0
SBAFS01	345500	665000	2	1	59	34	1	1	2	0
SBAFS02	346800	670600	1	1	72	20	2	2	2	0
SBAFS03	347500	670600	8	5	39	42	1	1	4	0
SBAFS04	356000	674000	1	1	4	72	19	2	1	0
BG3201	379000	730000	13	1	55	30	0	1	0	0
BG3301	376000	729000	19	1	40	38	1	1	0	0
BG3302	377000	729000	21	1	44	31	2	1	0	0
BG3303	378000	729000	18	0	32	48	2	0	0	0
BG3304	379000	729000	19	0	29	51	1	0	0	0
BG3305	380000	729000	19	0	35	45	1	0	0	0
BG3401	375000	728000	11	0	19	69	1	0	0	0
BG3402	376000	728000	14	0	20	64	1	1	0	0
BG3403	377000	728000	18	0	20	60	1	1	0	0
BG3404	378000	728000	12	0	57	30	1	0	0	0
BG3501	375000	727000	17	0	23	59	0	1	0	0
BG3502	376000	727000	15	1	14	69	0	1	0	0
BG3503	377000	727000	17	1	20	60	1	1	0	0
BG3504	378000	727000	15	0	19	66	0	0	0	0
BG3505	379000	727000	15	0	22	62	1	0	0	0
BG3506	380000	727000	16	0	34	50	0	0	0	0
BG3507	381000	727000	17	1	68	11	0	0	0	3
BG3508	392000	727000	18	0	28	53	0	1	0	0
BG3509	393000	727000	22	0	31	47	0	0	0	0
BG3510	394000	727000	13	2	36	47	1	1	0	0
BG3601	374000	726000	15	1	13	71	1	1	0	0
BG3602	375000	726000	6	0	10	83	0	0	0	0
BG3603	376000	726000	8	1	9	81	1	0	0	0
BG3604	377000	726000	5	1	11	81	0	0	1	0
BG3605	378000	726000	14	1	12	72	1	0	0	0
BG3606	379000	726000	12	1	20	67	0	0	0	0
BG3607	380000	726000	8	1	10	81	0	0	0	0
BG3608	381000	726000	13	1	61	25	0	0	0	0
BG3610	391000	726000	7	2	10	80	0	0	0	0
BG3611	392000	726000	7	0	9	83	0	0	0	0
BG3612	393000	726000	8	0	10	82	0	0	0	0
BG3613	394000	726000	16	0	25	58	0	1	0	0
BG3701	373000	725000	9	1	26	63	0	1	0	0
BG3702	374000	725000	8	1	13	78	0	0	0	0
BG3703	375000	725000	10	1	17	70	1	1	0	0

Appendix A. *Mineralogical composition of surficial sediments in Lake Abaya (vol. %)*

SampleID	Easting	Northing	Quartz	Calcite	Feldspar	Clay	Hematite	Magnetite	Pyrite	Hornblende
BG3704	376000	725000	9	1	21	67	1	1	0	0
BG3705	377000	725000	15	0	17	67	0	1	0	0
BG3706	378000	725000	14	1	17	67	0	1	0	0
BG3707	379000	725000	12	1	17	69	1	1	0	0
BG3708	380000	725000	14	1	50	33	2	0	0	0
BG3709	381000	725000	12	1	59	27	1	0	0	0
BG3710	382000	725000	18	0	69	13	0	0	0	0
BG3712	390000	725000	16	1	34	48	0	1	0	0
BG3713	391000	725000	15	0	21	62	1	1	0	0
BG3714	392000	725000	16	0	17	65	1	1	0	0
BG3715	393000	725000	15	0	19	65	0	1	0	0
BG3801	373000	724000	14	1	26	50	0	1	1	7
BG3802	374000	724000	13	1	23	62	1	0	0	0
BG3803	375000	724000	15	1	19	65	0	0	0	0
BG3804	376000	724000	8	1	15	68	1	1	0	6
BG3805	377000	724000	8	1	13	78	0	0	0	0
BG3806	378000	724000	10	1	16	73	0	0	0	0
BG3807	379000	724000	11	1	20	66	1	1	0	0
BG3808	380000	724000	15	1	18	63	2	1	0	0
BG3809	381000	724000	9	1	11	77	1	1	0	0
BG3810	382000	724000	19	1	59	20	1	0	0	0
BG3811	383000	724000	22	1	66	11	0	0	0	0
BG3813	389000	724000	14	0	32	53	0	1	0	0
BG3814	390000	724000	16	1	55	26	1	1	0	0
BG3815	391000	724000	26	0	26	44	3	1	0	0
BG3816	392000	724000	18	2	23	55	2	0	0	0
BG3817	393000	724000	11	1	41	46	0	1	0	0
BG3901	372000	722000	13	1	20	64	1	0	1	0
BG3902	373000	722000	13	1	18	66	1	0	1	0
BG3903	374000	722000	12	1	14	72	1	0	0	0
BG3904	375000	722000	8	1	15	75	0	1	0	0
BG3905	376000	722000	9	0	10	76	0	1	0	3
BG3906	377000	722000	7	0	9	83	0	1	0	0
BG3907	378000	722000	6	0	9	83	1	1	0	0
BG3908	379000	722000	9	0	11	79	0	1	0	0
BG3909	380000	722000	6	0	24	69	0	1	0	0
BG3910	381000	722000	9	0	17	61	2	1	0	10
BG3911	382000	722000	11	0	13	74	1	1	0	0
BG3912	383000	722000	14	0	19	64	1	2	0	0
BG3913	384000	722000	13	0	15	70	1	1	0	0
BG3914	385000	722000	12	0	16	71	0	1	0	0
BG3915	386000	722000	13	0	20	62	4	1	0	0

Appendix A. *Mineralogical composition of surficial sediments in Lake Abaya (vol. %)*

SampleID	Easting	Northing	Quartz	Calcite	Feldspar	Clay	Hematite	Magnetite	Pyrite	Hornblende
BG3916	387000	722000	12	0	16	62	0	0	3	7
BG3917	388000	722000	16	0	16	58	1	0	0	7
BG3918	389000	722000	15	0	18	62	1	1	3	0
BG3919	390000	722000	19	0	19	59	2	1	0	0
BG3920	391000	722000	13	1	13	72	1	0	0	0
BG3921	392000	722000	16	1	21	60	1	1	0	0
BG3922	393000	722000	10	3	21	65	1	0	0	0
NBAFS05	374000	692000	7	0	15	74	3	1	0	0
NBAFS07	368700	718500	10	0	75	6	1	1	1	6
NBAFS08	378300	728500	14	0	37	47	1	1	0	0
NBAFS09	393500	721300	13	6	50	29	1	1	0	0
AMS01	370202	719065	27	4	31	34	2	2	0	0
BG4124	388000	718000	15	1	18	65	1	0	0	0
BG4128	392000	718000	18	1	20	60	0	1	0	0
BG4129	393000	718000	12	1	18	66	1	0	1	0
BG4130	394000	718000	27	2	29	40	1	1	0	0
BG4131	395000	718000	14	6	53	26	1	0	0	0
BG4201	365000	716000	7	1	36	54	0	1	0	0
BG4202	366000	716000	10	1	30	58	1	1	0	0
BG4203	367000	716000	13	1	18	67	0	1	0	0
BG4204	368000	716000	12	1	13	66	1	1	0	6
BG4206	370000	716000	8	0	14	77	0	1	0	0
AMS02	370148	719136	21	1	31	44	1	2	0	0
BG4001	370000	720000	11	1	43	37	1	0	3	4
BG4002	371000	720000	20	0	34	28	1	1	7	9
BG4003	372000	720000	12	0	19	68	1	0	0	0
BG4004	373000	720000	11	0	18	67	1	1	1	0
BG4006	375000	720000	9	0	20	69	0	2	0	0
BG4009	378000	720000	8	1	11	79	1	0	0	0
BG4013	382000	720000	6	1	15	78	0	1	0	0
BG4014	383000	720000	12	0	22	65	1	0	0	0
BG4015	384000	720000	6	0	9	83	1	0	0	0
BG4017	386000	720000	18	1	22	57	0	2	0	0
BG4021	390000	720000	16	1	21	60	1	1	0	0
BG4022	391000	720000	16	1	15	67	1	1	0	0
BG4023	392000	720000	19	1	25	54	1	0	0	0
BG4024	393000	720000	14	1	54	30	0	1	0	0
BG4025	394000	720000	9	1	27	61	0	1	1	0
BG4026	395000	720000	10	7	27	51	1	0	0	4
BG4101	365000	718000	7	3	49	36	1	0	0	4
BG4102	366000	718000	9	1	44	44	1	1	0	0

Appendix A. *Mineralogical composition of surficial sediments in Lake Abaya (vol. %)*

SampleID	Easting	Northing	Quartz	Calcite	Feldspar	Clay	Hematite	Magnetite	Pyrite	Hornblende
BG4103	367000	718000	11	1	41	45	1	1	0	0
BG4104	368000	718000	15	1	32	50	0	1	0	0
BG4108	372000	718000	13	0	25	61	1	0	0	0
BG4112	376000	718000	6	1	9	82	1	1	0	0
BG4114	378000	718000	9	1	19	71	0	1	0	0
BG4115	379000	718000	4	1	10	79	0	0	0	5
BG4116	380000	718000	13	1	21	63	1	1	0	0
BG4117	381000	718000	10	1	19	65	1	0	0	3
BG4118	382000	718000	11	1	22	63	3	0	0	0
BG4121	385000	718000	9	1	21	69	0	0	0	0
BG4210	374000	716000	11	1	14	73	0	1	0	0
BG4212	377000	716000	11	1	19	65	3	1	0	0
BG4213	380000	716000	7	1	18	73	0	1	0	0
BG4214	381000	716000	10	1	17	71	1	1	0	0
BG4215	382000	716000	7	1	14	77	1	0	0	0
BG4219	386000	716000	8	1	15	76	0	0	0	0
BG4222	389000	716000	18	2	21	56	2	1	0	0
BG4224	391000	716000	13	1	18	65	1	0	2	0
BG4225	392000	716000	9	1	16	69	4	1	0	0
BG4226	393000	716000	11	1	18	68	1	1	0	0
BG4227	394000	716000	11	1	19	62	0	0	0	6
BG4301	365000	714000	5	5	42	40	1	1	2	4
BG4302	366000	714000	8	1	23	67	1	0	0	0
BG4303	367000	714000	13	1	18	63	1	1	3	0
BG4304	368000	714000	7	1	15	75	1	1	0	0
BG4308	372000	714000	6	0	16	76	1	1	0	0
BG4312	376000	714000	9	1	17	71	0	2	0	0
BG4313	377000	714000	9	2	16	72	0	1	0	0
BG4314	378000	714000	8	1	14	75	1	1	0	0
BG4315	379000	714000	6	1	13	79	1	1	0	0
BG4316	380000	714000	10	1	14	74	1	0	0	0
BG4317	381000	714000	9	1	16	73	0	1	0	0
BG4320	384000	714000	5	2	9	83	1	0	0	0
BG4324	388000	714000	13	2	16	67	1	1	0	0
BG4326	390000	714000	18	3	63	16	0	0	0	0
BG4327	391000	714000	11	2	22	63	1	1	0	0
BG4328	392000	714000	11	1	17	64	1	1	0	5
BG4329	393000	714000	11	1	15	71	1	0	0	0
BG4401	365000	712000	9	3	20	65	2	1	0	0
BG4402	366000	712000	5	1	11	81	1	1	1	0
BG4403	367000	712000	4	1	17	77	0	1	0	0
BG4404	368000	712000	7	1	16	74	1	1	0	0

Appendix A. *Mineralogical composition of surficial sediments in Lake Abaya (vol. %)*

SampleID	Easting	Northing	Quartz	Calcite	Feldspar	Clay	Hematite	Magnetite	Pyrite	Hornblende
BG4406	370000	712000	6	0	23	71	0	0	0	0
BG4410	374000	712000	5	1	18	75	0	1	0	0
BG4413	377000	712000	5	1	16	78	0	1	0	0
BG4414	378000	712000	4	1	13	81	1	0	0	0
BG4415	379000	712000	3	1	11	84	1	0	0	0
BG4416	380000	712000	4	1	8	87	1	0	0	0
BG4418	382000	712000	8	1	12	70	1	1	1	6
BG4422	386000	712000	10	2	17	68	2	1	0	0
BG4425	389000	712000	11	4	45	39	1	0	0	0
BG4426	390000	712000	9	7	13	70	0	1	0	0
BG4427	391000	712000	9	6	18	65	1	0	0	0
BG4428	392000	712000	9	9	54	29	0	0	0	0
BG4501	364000	710000	1	1	60	33	1	2	2	0
BG4502	365000	710000	6	2	35	54	1	1	0	0
BG4503	366000	710000	9	1	22	67	0	1	0	0
BG4504	367000	710000	7	1	14	78	1	0	0	0
BG4506	369000	710000	7	0	12	76	2	1	2	0
BG4509	372000	710000	5	1	15	77	1	1	0	0
BG4513	376000	710000	4	0	9	84	1	0	1	0
BG4514	377000	710000	8	1	12	78	1	1	0	0
BG4515	378000	710000	9	1	12	76	2	0	0	0
BG4516	379000	710000	12	1	20	65	2	0	0	0
BG4517	380000	710000	10	2	16	70	1	1	0	0
BG4519	384000	710000	7	2	11	78	2	1	0	0
BG4520	385000	710000	6	2	15	76	0	1	0	0
BG4521	386000	710000	9	2	16	71	1	0	0	0
BG4522	387000	710000	7	3	11	78	1	0	0	0
BG4601	365000	708000	5	2	42	46	1	2	2	0
BG4602	366000	708000	15	1	29	50	0	1	2	0
BG4603	367000	708000	8	1	15	75	0	0	1	0
BG4604	368000	708000	10	1	21	67	0	1	0	0
BG4606	370000	708000	3	1	10	85	0	1	0	0
BG4609	373000	708000	2	0	3	94	0	0	0	0
BG4610	374000	708000	4	1	7	87	2	1	0	0
BG4611	375000	708000	5	1	14	78	1	1	0	0
BG4612	376000	708000	6	1	14	78	2	0	0	0
BG4614	378000	708000	5	1	10	82	1	1	0	0
BG4616	380000	708000	6	2	14	77	0	1	0	0
BG4617	384000	708000	11	3	18	67	0	0	1	0
BG4619	386000	708000	8	5	23	59	1	1	2	0
BG4620	387000	708000	5	4	14	74	1	1	2	0
BG4621	388000	708000	10	5	22	60	2	1	0	0

Appendix A. *Mineralogical composition of surficial sediments in Lake Abaya (vol. %)*

SampleID	Easting	Northing	Quartz	Calcite	Feldspar	Clay	Hematite	Magnetite	Pyrite	Hornblende
BG4622	389000	708000	5	11	27	54	0	0	2	0
BG4701	366000	706000	6	0	37	50	1	0	1	4
BG4702	367000	706000	7	1	13	78	1	0	1	0
BG4703	368000	706000	5	0	8	86	1	1	0	0
BG4704	369000	706000	1	0	3	96	0	0	0	0
BG4705	370000	706000	2	0	8	83	1	0	0	5
BG4706	371000	706000	5	0	9	83	0	0	2	0
BG4707	372000	706000	4	0	10	84	1	0	0	0
BG4708	373000	706000	4	0	7	83	1	0	0	4
BG4709	374000	706000	1	0	16	80	1	2	0	0
BG4710	375000	706000	8	0	14	75	2	1	0	0
BG4711	376000	706000	5	0	18	76	0	1	0	0
BG4712	377000	706000	3	0	5	92	0	0	0	0
BG4713	378000	706000	4	0	6	89	1	0	0	0
BG4714	379000	706000	10	5	20	62	2	1	0	0
BG4715	384000	706000	5	9	40	42	0	1	3	0
BG4801	367000	704000	7	2	19	72	0	1	0	0
BG4802	368000	704000	6	0	14	79	0	1	0	0
BG4803	369000	704000	10	1	18	69	1	1	0	0
BG4804	370000	704000	10	1	18	69	1	1	0	0
BG4805	371000	704000	8	1	16	72	3	0	0	0
BG4806	372000	704000	5	1	18	76	0	0	0	0
BG4807	373000	704000	5	0	19	75	0	1	0	0
BG4808	374000	704000	7	1	18	71	3	0	0	0
BG4809	375000	704000	6	1	16	75	1	0	0	0
BG4810	376000	704000	8	0	13	77	1	1	0	0
BG4811	377000	704000	5	1	11	80	0	1	2	0
BG4812	378000	704000	6	1	6	86	1	0	0	0
BG4813	381000	704000	12	15	59	14	0	0	0	0
BG4814	382000	704000	8	3	14	72	2	1	0	0
BG4815	383000	704000	7	4	15	71	2	1	0	0
BG4902	368000	702000	7	0	17	74	0	2	0	0
BG4904	372000	702000	8	1	7	82	1	1	0	0
BG4908	376000	702000	7	1	11	76	1	1	3	0
BG4912	380000	702000	7	2	13	73	1	2	2	0
BG5007	374000	700000	7	2	21	69	1	0	0	0
BG5011	378000	700000	7	2	19	69	1	2	0	0
BG5014	381000	700000	8	2	43	37	1	1	1	7
BG5101	368000	698000	6	1	18	72	1	1	1	0
BG5105	372000	698000	9	1	20	68	2	0	0	0
BG5109	376000	698000	10	1	21	65	2	1	0	0
BG5113	380000	698000	6	3	24	65	1	1	0	0

Appendix A. *Mineralogical composition of surficial sediments in Lake Abaya (vol. %)*

SampleID	Easting	Northing	Quartz	Calcite	Feldspar	Clay	Hematite	Magnetite	Pyrite	Hornblende
BG5202	370000	696000	9	1	16	72	1	1	0	0
BG5206	374000	696000	7	1	16	74	1	1	0	0
BG5210	378000	696000	9	2	19	52	1	1	3	13
BG5303	372000	694000	10	0	10	78	1	1	0	0
BG5307	376000	694000	8	2	15	63	1	2	0	9
BG5311	380000	694000	6	2	26	55	1	1	3	6
BG5407	378000	692000	9	2	12	73	2	2	0	0
BG5502	374000	690000	8	2	22	66	1	1	0	0
BG5504	376000	690000	8	5	21	64	1	1	0	0
ALT002	366908	691259	5	15	46	23	2	2	0	7
ALT004	367579	690242	3	1	65	18	2	2	0	10
ALT007	368453	688997	4	1	11	83	0	1	0	0
ALT011	369576	687342	1	3	25	69	1	1	0	0
ALT015	370564	685914	7	5	42	44	1	1	0	0
ALT018	371003	685292	7	5	30	56	1	1	0	0
ALT022	373887	688169	11	3	35	43	1	1	0	6
ALT027	372789	689749	6	3	20	69	1	0	0	0
ALT030	371933	690961	7	1	20	72	0	0	0	0
ALT034	370799	692579	2	0	40	55	2	1	0	0
ALT037	369950	693817	2	1	19	73	1	1	2	0
ALT041	368807	695469	1	1	49	46	1	2	0	0
ALT044	367957	696691	6	1	23	68	1	1	0	0
ALT048	367829	695938	2	1	29	65	1	1	0	0
ALT051	368671	694702	1	1	25	71	1	1	0	0
ALT056	367820	695085	4	1	37	55	2	1	0	0
ALT060	369256	693069	4	1	43	48	1	2	1	0
ALT063	370416	691435	1	1	13	83	1	0	0	2
ALT067	371845	689412	8	4	32	53	1	2	0	0
ALT071	372264	687182	4	12	32	50	1	1	0	0
ALT075	367468	694896	2	1	63	22	1	2	2	7
ALT078	369832	690467	1	1	31	58	1	1	0	7
ALT081	368356	690754	0	2	66	27	1	2	2	0
ALT084	366753	689667	6	1	38	42	1	2	2	8
ALT089	367440	689539	6	1	44	47	1	2	0	0
ALT093	370000	691162	3	1	41	50	4	1	0	0
ALT097	370124	688237	7	1	23	67	1	1	0	0
ALT101	371393	686372	9	4	44	41	1	1	0	0
ALT102	370498	684562	6	4	47	37	1	1	3	0
ALT103	370147	685043	8	7	34	49	2	2	0	0
ALT104	369699	685632	5	7	35	51	1	1	0	0
ALT105	369096	686431	3	5	13	78	1	0	0	0
ALT106	368502	687235	5	3	16	75	0	0	0	0

Appendix A. *Mineralogical composition of surficial sediments in Lake Abaya (vol. %)*

SampleID	Easting	Northing	Quartz	Calcite	Feldspar	Clay	Hematite	Magnetite	Pyrite	Hornblende
ALT107	367895	688031	9	2	31	56	1	1	0	0
ALT108	367597	688429	8	2	30	57	1	2	0	0
ALT109	367299	688829	8	2	34	54	1	1	0	0
ALT110	366993	689226	3	0	34	58	1	2	2	0
ALT111	367675	686710	7	8	52	32	1	1	0	0
ALT112	367968	686307	6	4	19	70	1	0	0	0
ALT113	368247	685903	6	3	17	72	1	1	0	0
ALT114	368523	685463	7	5	17	68	2	1	0	0
ALT115	368800	685064	0	5	16	78	1	1	0	0
ALT116	369079	684639	10	6	43	39	2	1	0	0
ALT117	369359	684240	20	3	34	40	0	0	0	3
ALT118	369627	683835	5	2	34	53	1	0	0	5
ALT119	369908	683410	6	3	28	57	3	2	0	0
ALT120	370188	682982	4	8	29	45	1	1	4	9
ALT121	370464	682573	4	24	21	44	1	1	5	0
ALT122	370743	682157	3	19	14	50	1	1	3	8
ALT123	370924	681893	4	23	33	28	0	3	0	9
ALT124	370881	682902	5	5	25	61	1	1	2	0
ALT125	370607	683284	1	5	34	57	2	1	0	0
ALT126	370265	683728	2	5	36	54	1	1	0	0
ALT127	370099	684161	8	5	30	46	2	2	0	8
ALT128	370825	684807	6	6	34	50	1	1	3	0
ALT129	370488	685270	10	5	54	24	1	1	0	6
ALT130	371340	685773	5	3	62	20	2	1	0	7
ALT131	371068	686148	3	7	38	49	1	1	0	3
ALT132	370791	686554	4	5	42	38	1	1	2	7
ALT133	367399	685362	8	2	62	24	2	2	0	0
ALT134	367641	685001	6	4	24	64	1	1	0	0
ALT144	369302	689478	4	1	14	81	0	1	0	0
ALT145	369859	688640	2	3	24	70	2	0	0	0
ALT146	370398	687804	4	5	22	67	1	1	0	0
ALT147	376307	688509	20	2	41	34	0	0	0	3
ALT148	376267	688824	4	6	59	20	1	1	2	7
ALT149	376191	689154	16	3	46	31	0	0	0	4
ALT150	376180	689416	9	3	40	43	2	1	2	0
ALT151	375452	689225	3	3	36	56	1	1	2	0
ALT152	374761	689169	13	2	36	40	1	1	0	8
ALT153	374926	688872	6	3	58	27	1	1	3	0
ALT154	375242	688617	0	1	33	59	0	1	0	6
ALT155	375518	688408	8	1	31	51	1	1	1	6
ALT156	374953	688112	6	4	50	33	1	1	0	5
ALT157	374734	688297	8	5	65	20	1	1	0	0

Appendix A. *Mineralogical composition of surficial sediments in Lake Abaya (vol. %)*

SampleID	Easting	Northing	Quartz	Calcite	Feldspar	Clay	Hematite	Magnetite	Pyrite	Hornblende
ALT158	374386	688555	9	3	50	35	1	1	1	0
ALT159	374047	688904	3	3	20	66	1	1	0	6
ALT160	374588	687934	16	2	45	36	0	0	1	0
ALT161	374454	688087	10	2	41	46	1	0	0	0
ALT162	374186	688263	6	2	43	44	2	1	2	0
ALT163	373817	688635	2	1	16	79	1	0	1	0
ALT164	373320	688463	5	1	45	43	2	1	3	0
ALT165	373662	688153	9	2	37	41	1	2	0	8
ALT166	373929	687758	1	1	15	82	0	0	0	0
ALT167	373541	687331	6	5	49	36	1	1	2	0
ALT168	373336	687658	22	4	35	38	1	1	0	0
ALT169	373220	687941	1	1	9	88	0	0	0	0
ALT170	372819	687709	5	4	38	45	1	1	0	6
ALT171	373020	687459	6	4	41	40	2	1	0	6
ALT172	373141	687271	21	12	36	25	1	1	0	4
ALT173	372709	687025	2	4	30	61	1	1	2	0
ALT174	372462	687367	9	4	47	38	1	1	0	0
ALT175	372148	687839	4	3	50	35	1	1	0	6
ALT176	371619	687458	5	4	38	51	1	1	0	0
ALT177	372013	687078	6	4	31	50	1	1	0	7
ALT178	372224	686791	0	2	38	58	2	0	0	0
ALT179	372360	686508	4	0	24	70	1	1	0	0
ALT180	371658	686564	4	5	47	35	1	1	1	6
ALT181	371494	686853	5	7	49	31	1	1	0	6
ALT182	371323	687161	40	2	33	21	1	0	0	3
ALT183	371072	687655	6	4	35	52	1	1	0	0
ALT184	370107	685775	3	6	13	77	1	0	0	0
ALT185	369722	684691	4	4	19	72	1	0	0	0
ALT186	375778	688783	5	4	49	36	0	1	0	5
ALT187	376972	688609	3	8	56	25	1	1	1	5
ALT188	376882	689127	3	0	16	75	0	0	1	3
ALT189	376776	689662	7	4	30	54	3	2	0	0
ALT190	377276	689844	5	5	17	71	1	1	0	0
ALT191	377409	689322	8	4	28	53	0	0	0	7
ALT192	377497	688755	10	6	61	20	2	2	0	0
ALT193	378030	689001	1	7	40	50	2	2	0	0
ALT194	377906	689521	9	8	33	40	1	2	0	7
ALT195	377793	690070	3	4	17	73	1	1	1	0
ALT196	378549	689754	5	6	34	52	2	1	0	0
ALT197	378739	689298	3	2	42	50	2	2	0	0
ALT198	379221	689662	6	4	42	46	1	1	0	0
ALT199	379132	690007	7	5	27	58	1	1	0	0

Appendix A. *Mineralogical composition of surficial sediments in Lake Abaya (vol. %)*

SampleID	Easting	Northing	Quartz	Calcite	Feldspar	Clay	Hematite	Magnetite	Pyrite	Hornblende
ALT200	379677	690091	3	4	26	66	1	1	0	0
ALT201	368387	693624	2	1	36	55	1	1	1	3
ALT202	369269	693837	2	0	34	61	2	1	0	0
ALT203	369551	693425	8	0	34	56	1	1	0	0
ALT204	369870	692998	3	0	32	62	1	1	1	0
ALT205	370153	692507	3	0	47	34	2	2	0	12
ALT206	370481	692001	3	0	39	50	2	1	0	5
ALT207	370860	691466	5	0	36	49	2	1	0	7
ALT208	371242	690986	8	0	25	65	1	1	0	0
ALT209	370641	691022	5	0	25	61	2	1	0	6
ALT210	370399	690728	4	0	30	56	1	1	0	8
ALT211	369400	690155	5	0	25	68	1	1	0	0
ALT212	370127	690031	4	1	27	66	1	1	0	0
ALT213	369655	690012	5	0	27	66	1	1	0	0
ALT214	369237	690401	1	0	30	67	1	1	0	0
ALT215	368505	690566	2	1	57	33	2	3	2	0
ALT216	367764	690694	1	0	57	32	2	2	1	5
ALT217	368930	690853	3	0	54	34	2	1	1	5
ALT218	368754	691146	1	0	59	36	2	1	1	0
ALT219	369393	691130	3	0	47	40	1	2	0	7
ALT220	369830	691401	2	0	58	36	2	2	0	0
ALT221	370114	691867	0	0	53	34	2	2	1	8
ALT222	369755	691999	2	0	59	29	2	2	0	6
ALT223	369649	692470	1	0	40	57	1	1	0	0
ALT224	369528	692072	2	0	69	25	1	2	1	0
ALT225	369123	692676	1	0	45	49	2	2	1	0
ALT226	369451	692874	3	1	54	32	2	2	0	6
ALT227	369694	693223	3	0	28	67	1	1	0	0
ALT228	369405	693682	1	0	26	71	1	1	0	0
ALT229	369095	693292	2	0	52	43	1	2	0	0
ALT230	368889	693111	2	0	40	53	1	2	2	0
ALT231	368806	693739	2	1	40	52	1	2	2	0
ALT232	369089	694075	4	0	27	67	1	1	0	0
ALT233	368791	694538	5	1	32	59	2	1	0	0
ALT234	368521	694130	2	0	58	27	2	1	3	7
ALT235	368114	693963	2	1	63	29	2	1	2	0
ALT236	367866	694263	2	0	51	37	1	1	2	6
ALT237	368208	694532	2	0	64	30	2	2	0	0
ALT238	367908	694928	4	0	31	63	1	1	0	0
ALT239	367560	694693	3	2	69	20	2	3	1	0

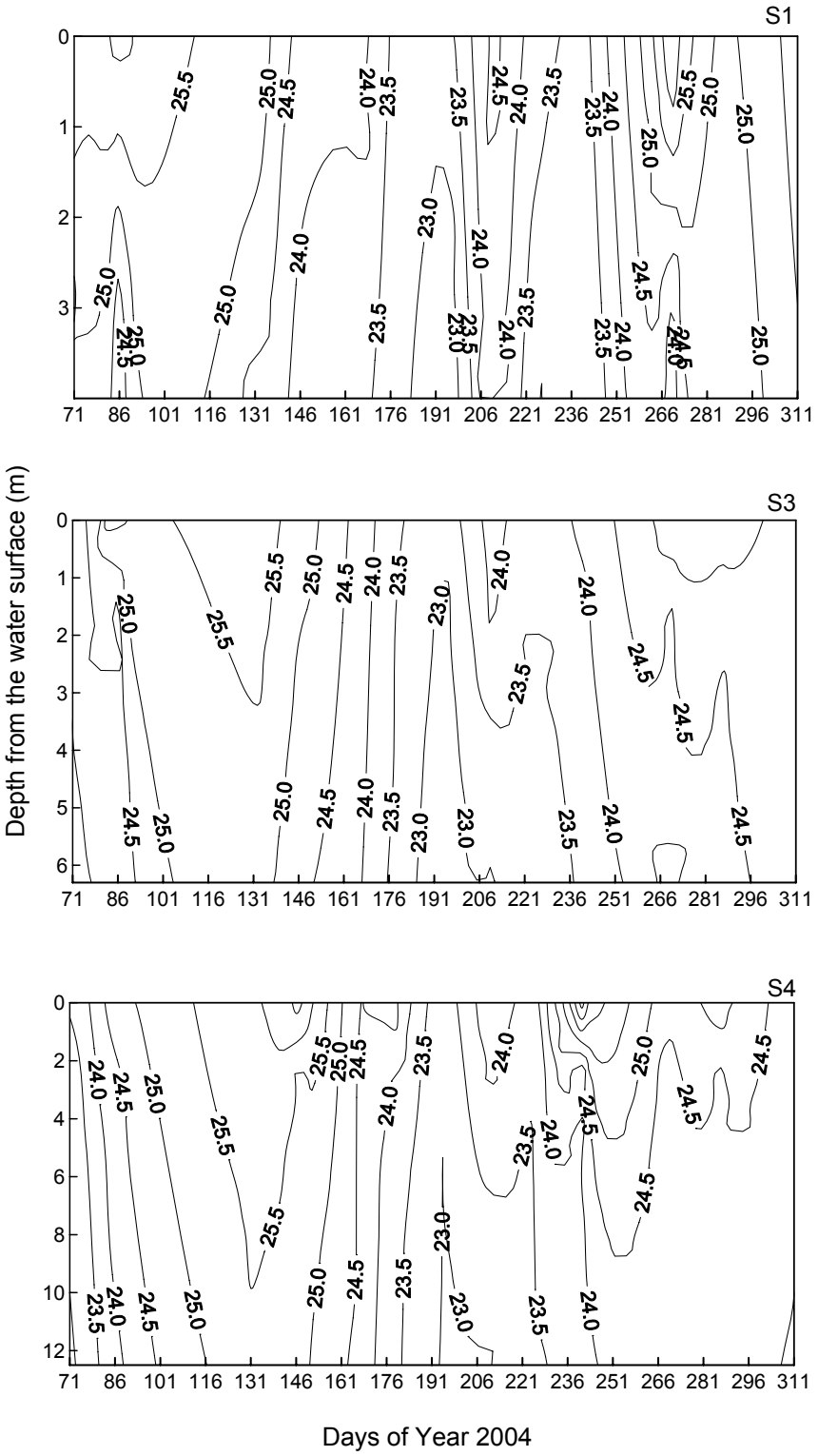

Figure B1. *Temperature (^{o}C) fields measured bimonthly at fixed monitoring stations in the south basin.*

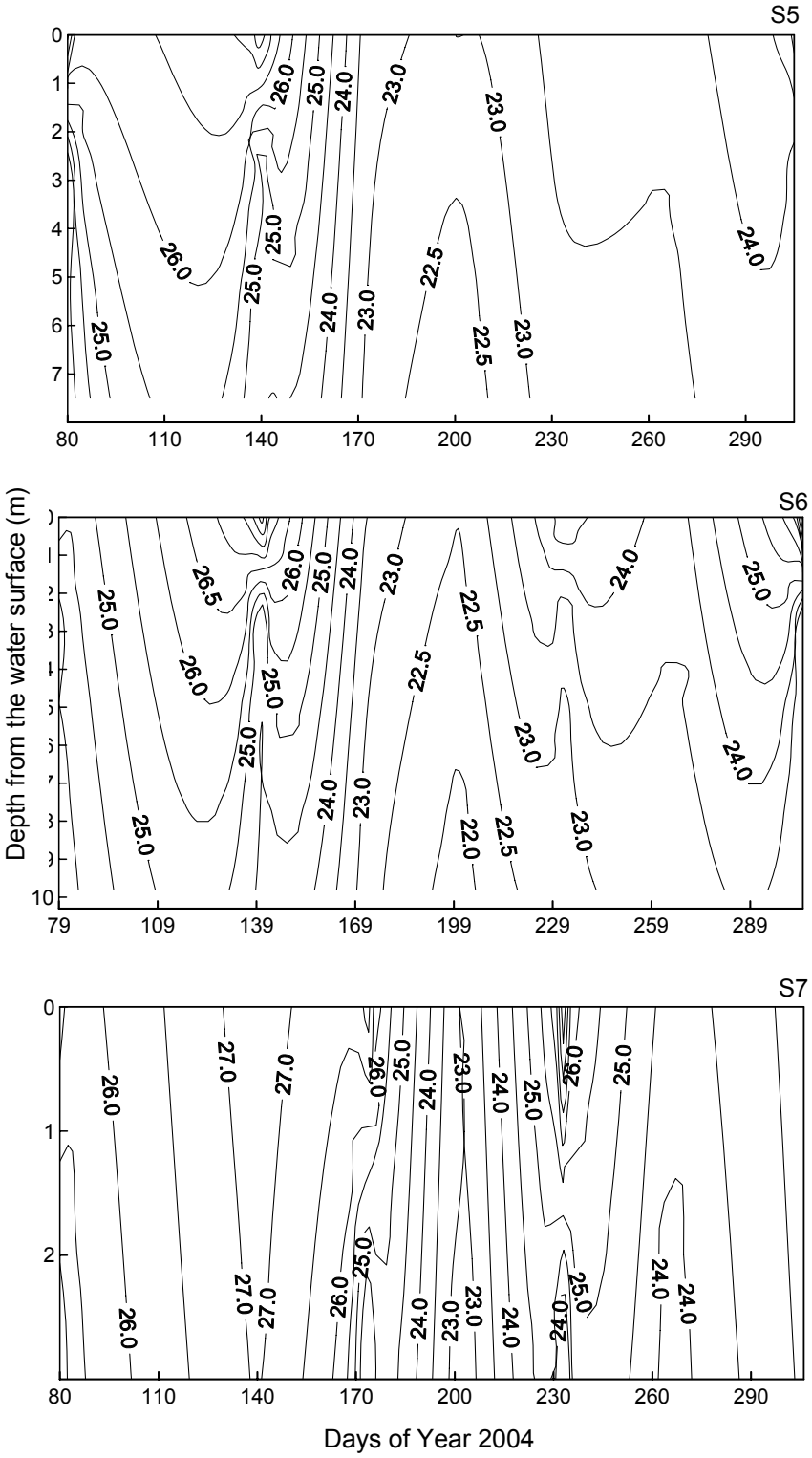

Figure B2. *Temperature (^{o}C) fields measured monthly at fixed monitoring stations in the north basin.*

Appendix B. *Contour plots of water quality parameters showing depth profiles at fixed monitoring stations vs. Julian days of sampling*

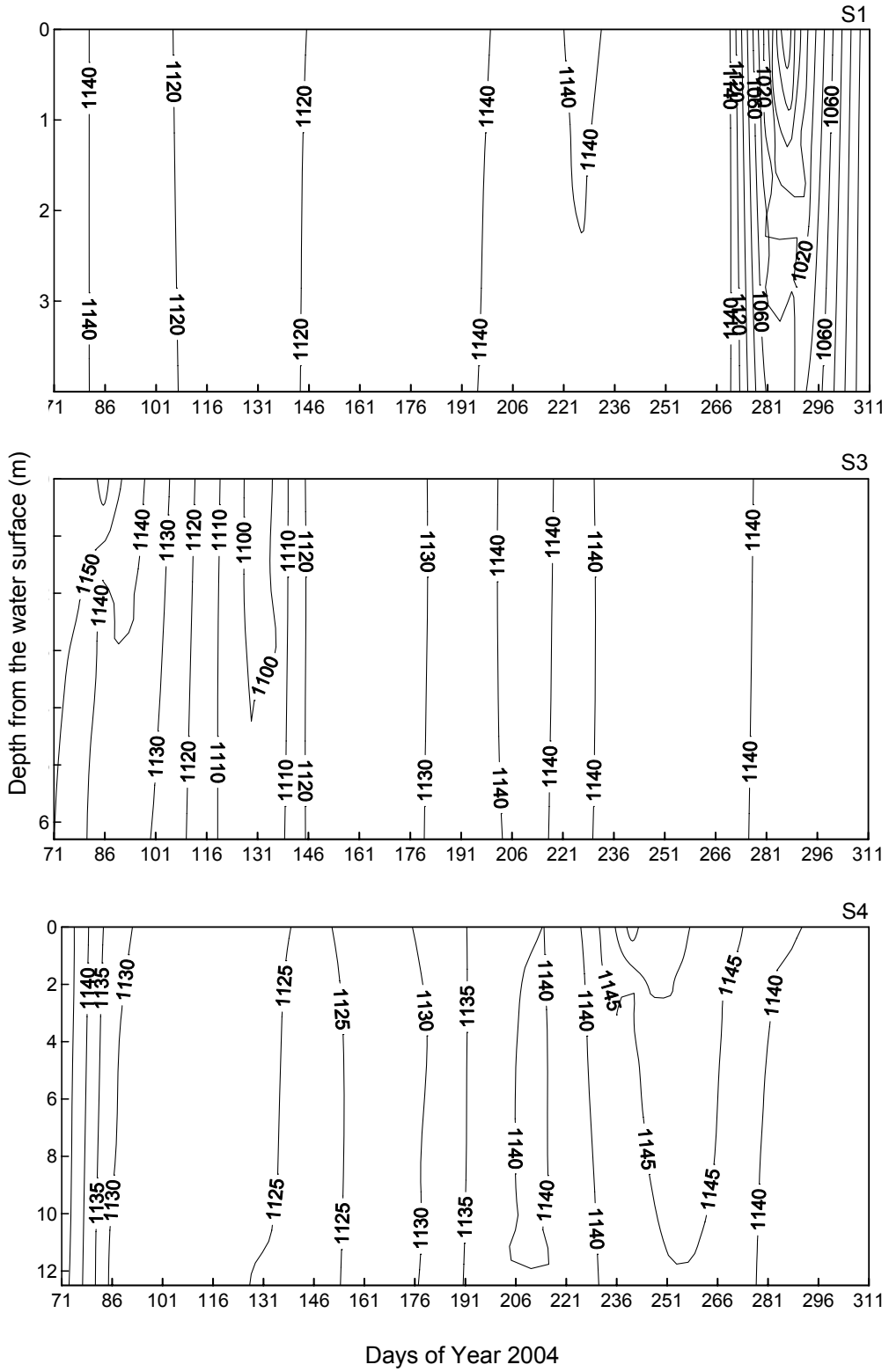

Figure B3. *Electrical conductivity (μS/cm) fields measured bimonthly at fixed monitoring stations in the south basin.*

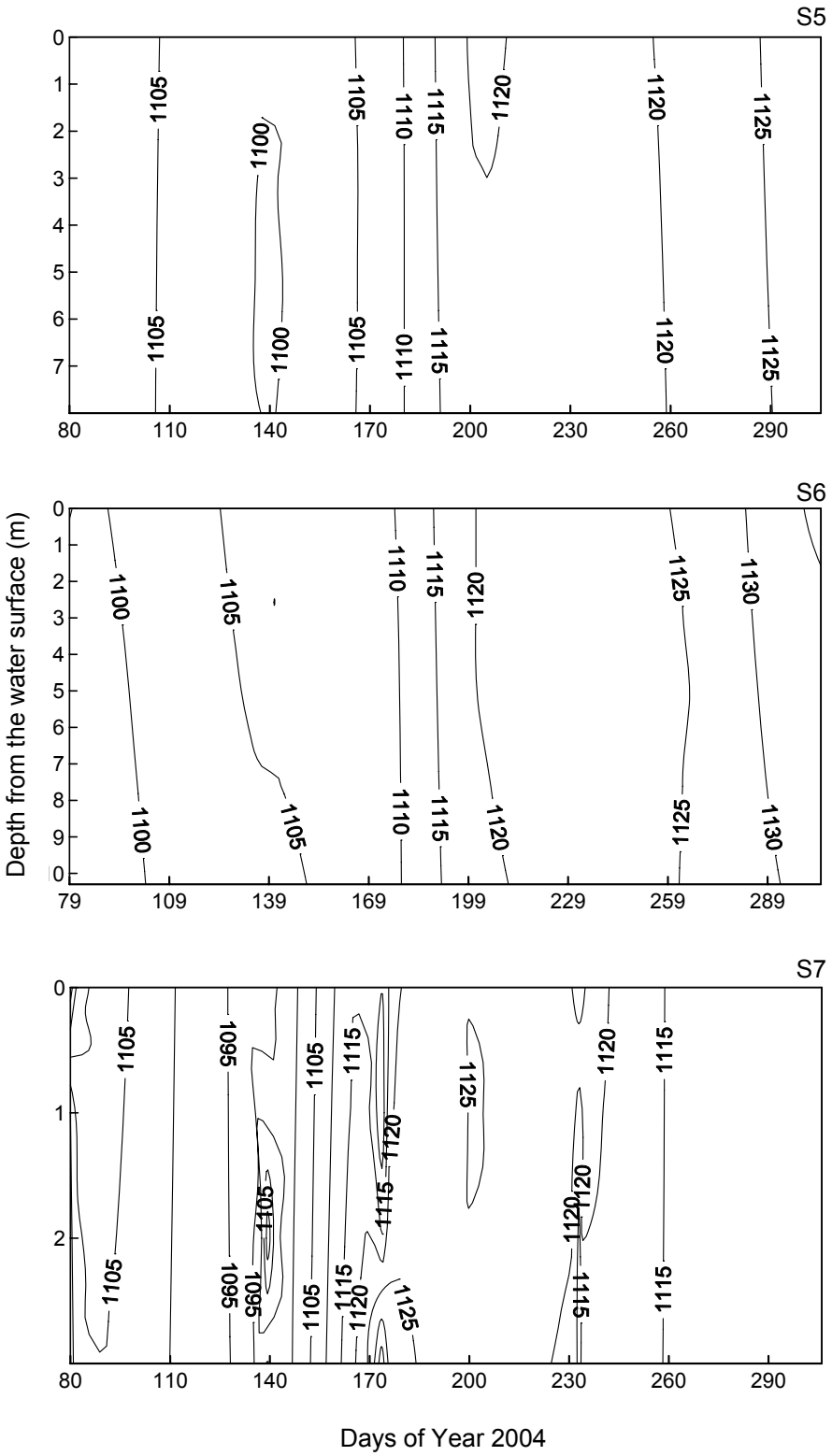

Figure B4. *Electrical conductivity (µS/cm) profiles measured monthly at fixed monitoring stations in the north basin.*

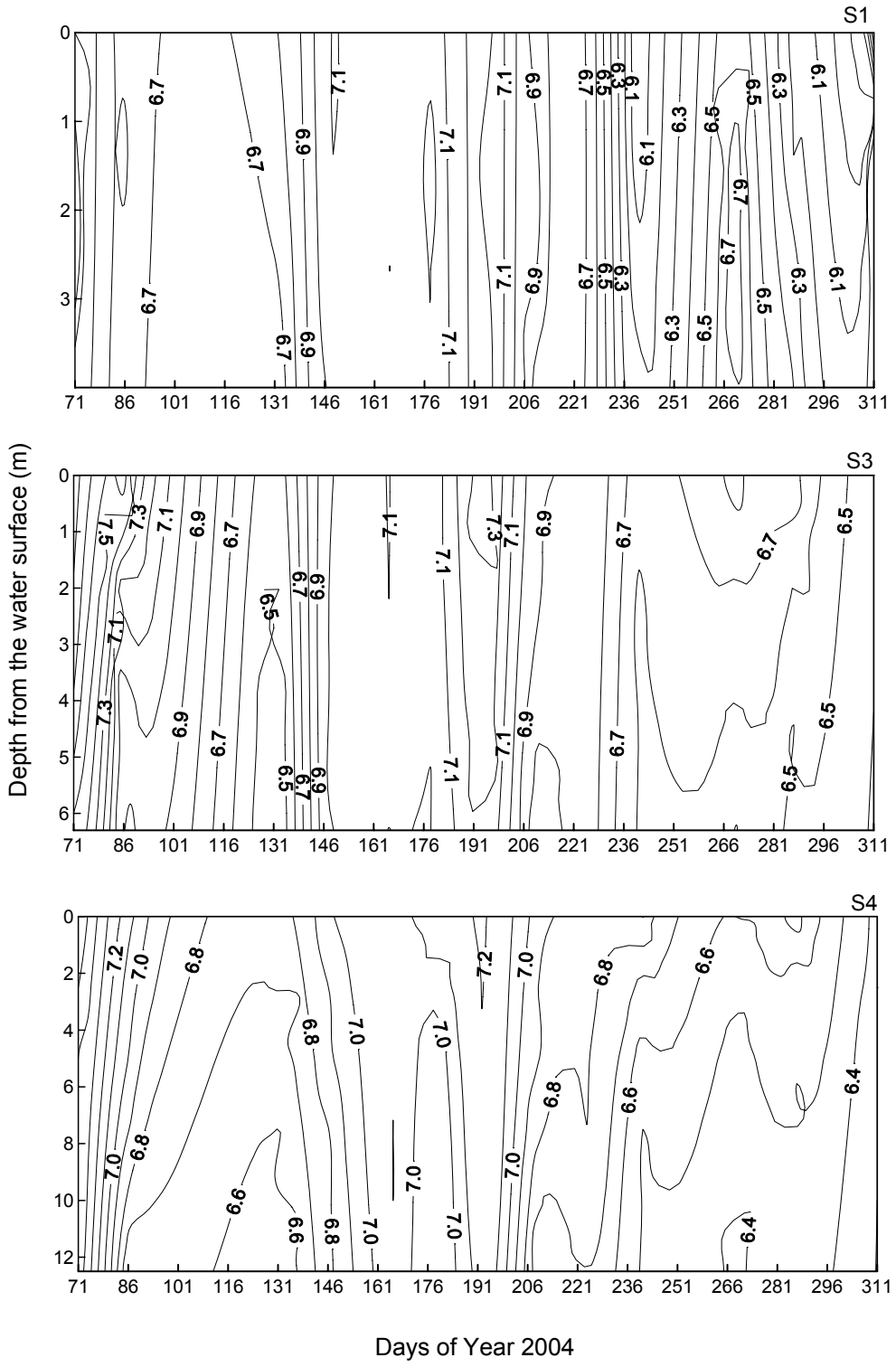

Figure B5. *Dissolved oxygen (mgL^{-1}) fields measured bimonthly at fixed monitoring stations in the south basin.*

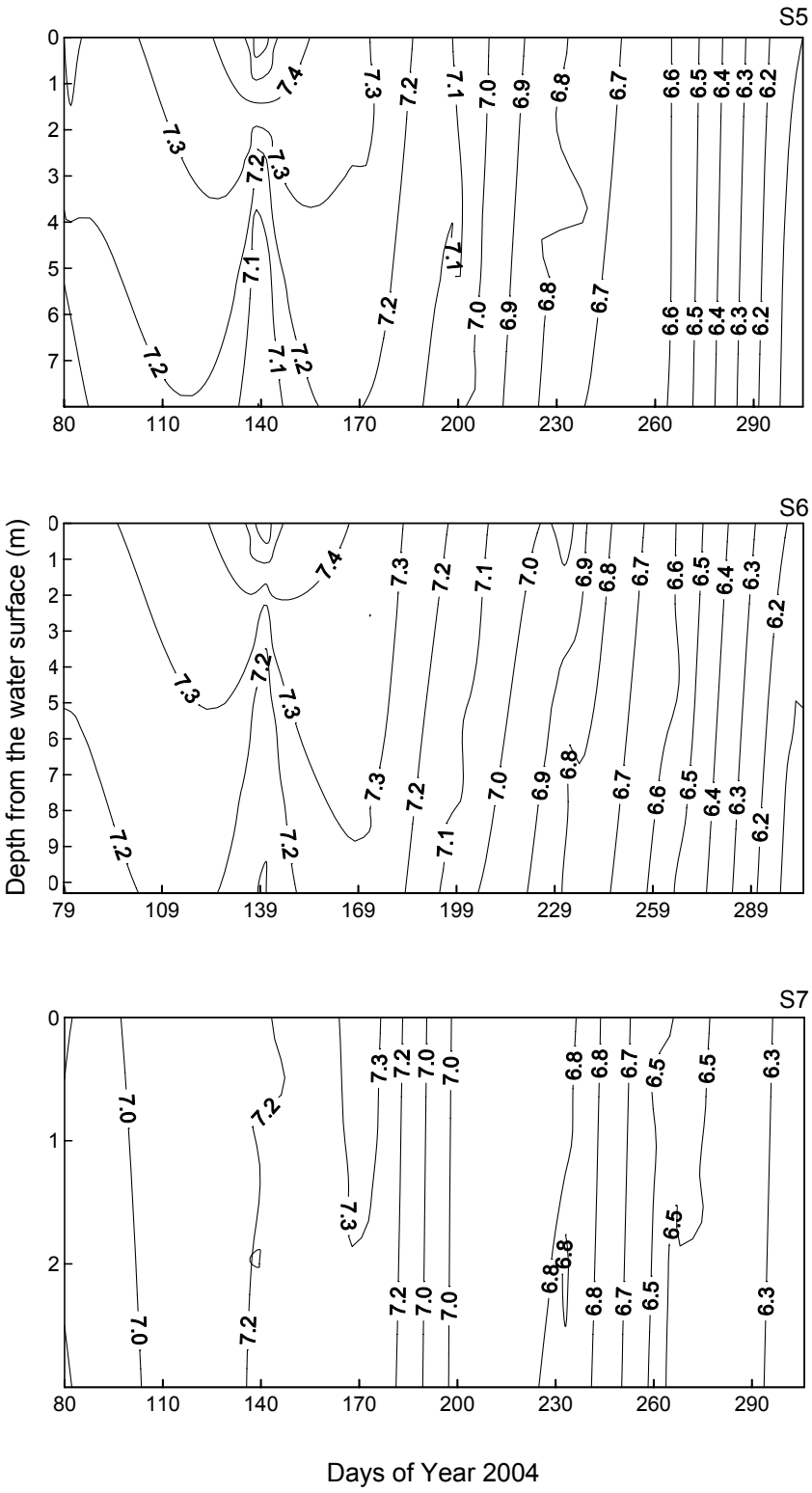

Figure B6. *Dissolved oxygen (mgL^{-1}) fields measured monthly at fixed monitoring stations in the north basin.*

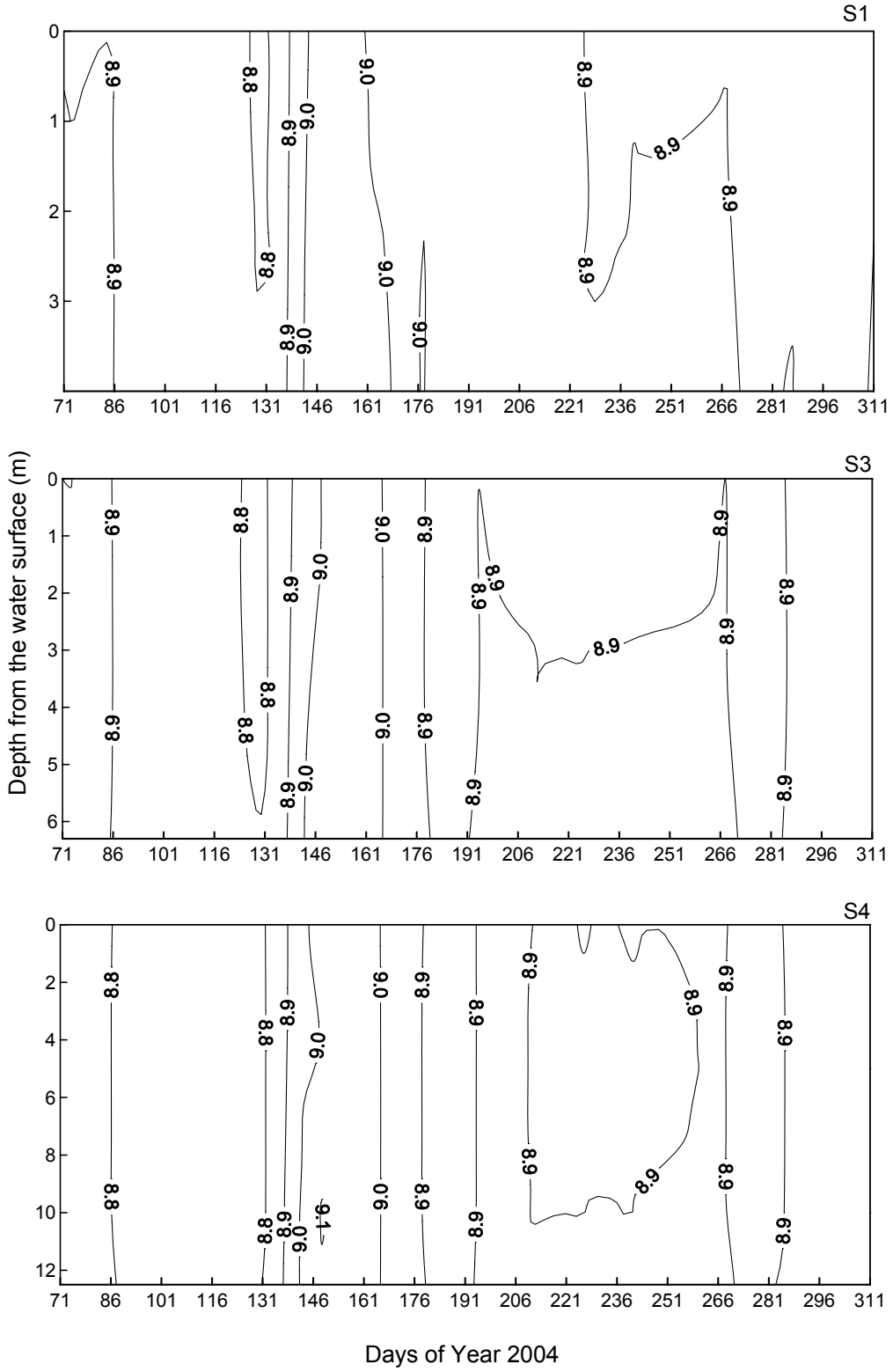

Figure B7. *pH profiles measured bimonthly at fixed monitoring stations in the south basin.*

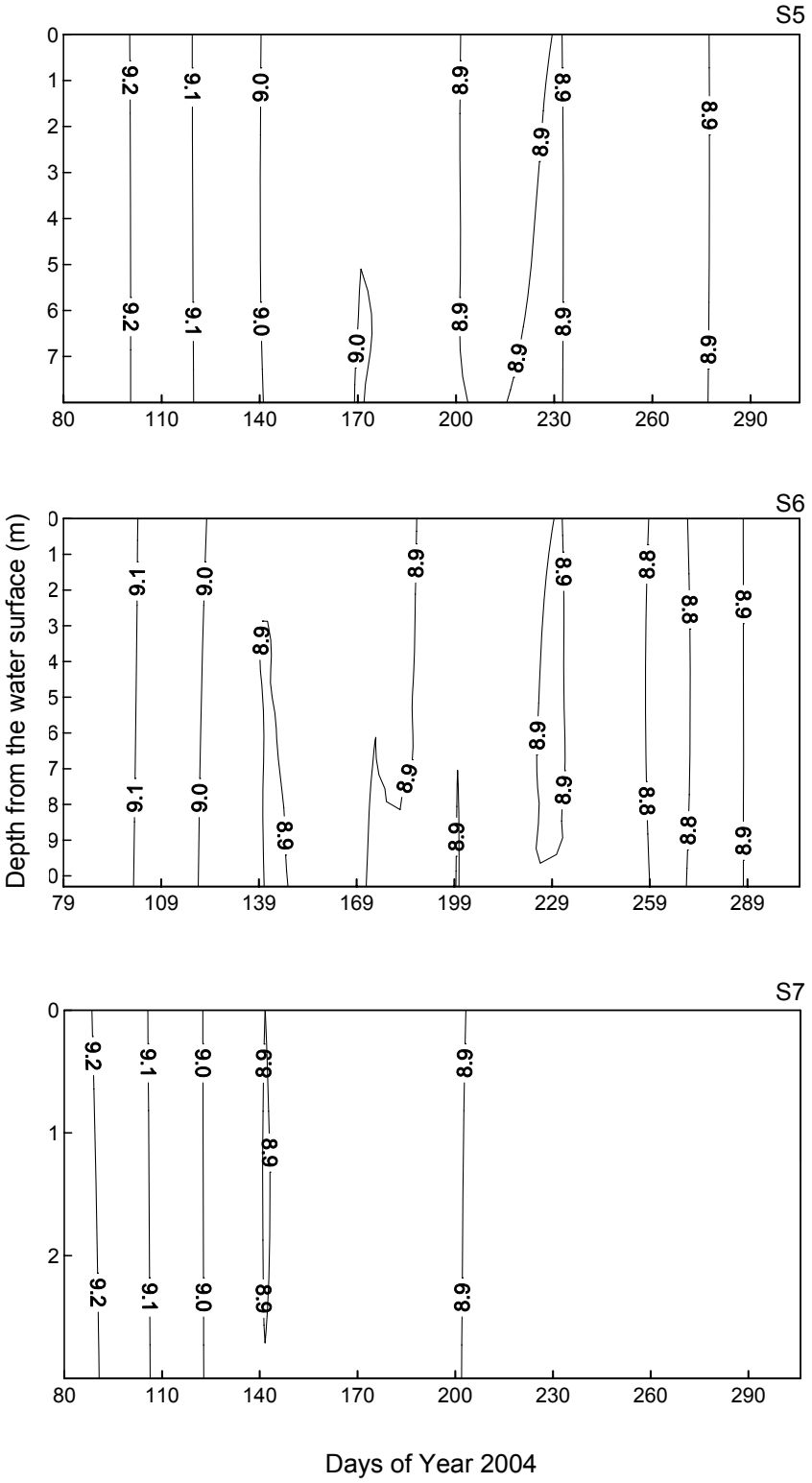

Figure B8. *pH profiles measured monthly at fixed monitoring stations in the north basin.*

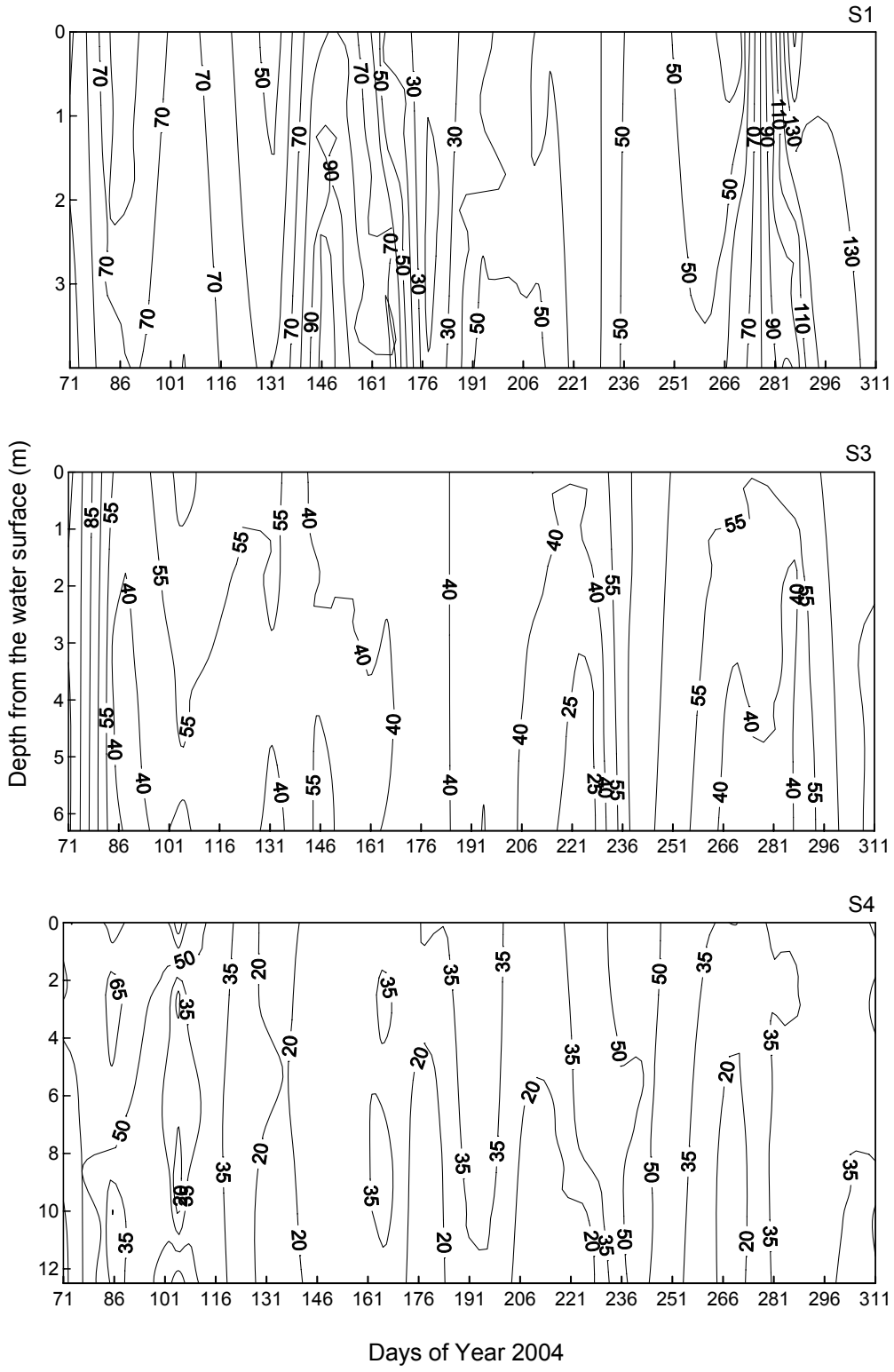

Figure B9. *Total suspended solids concentration (mgL^{-1}) fields measured bimonthly at fixed monitoring stations in the south basin.*

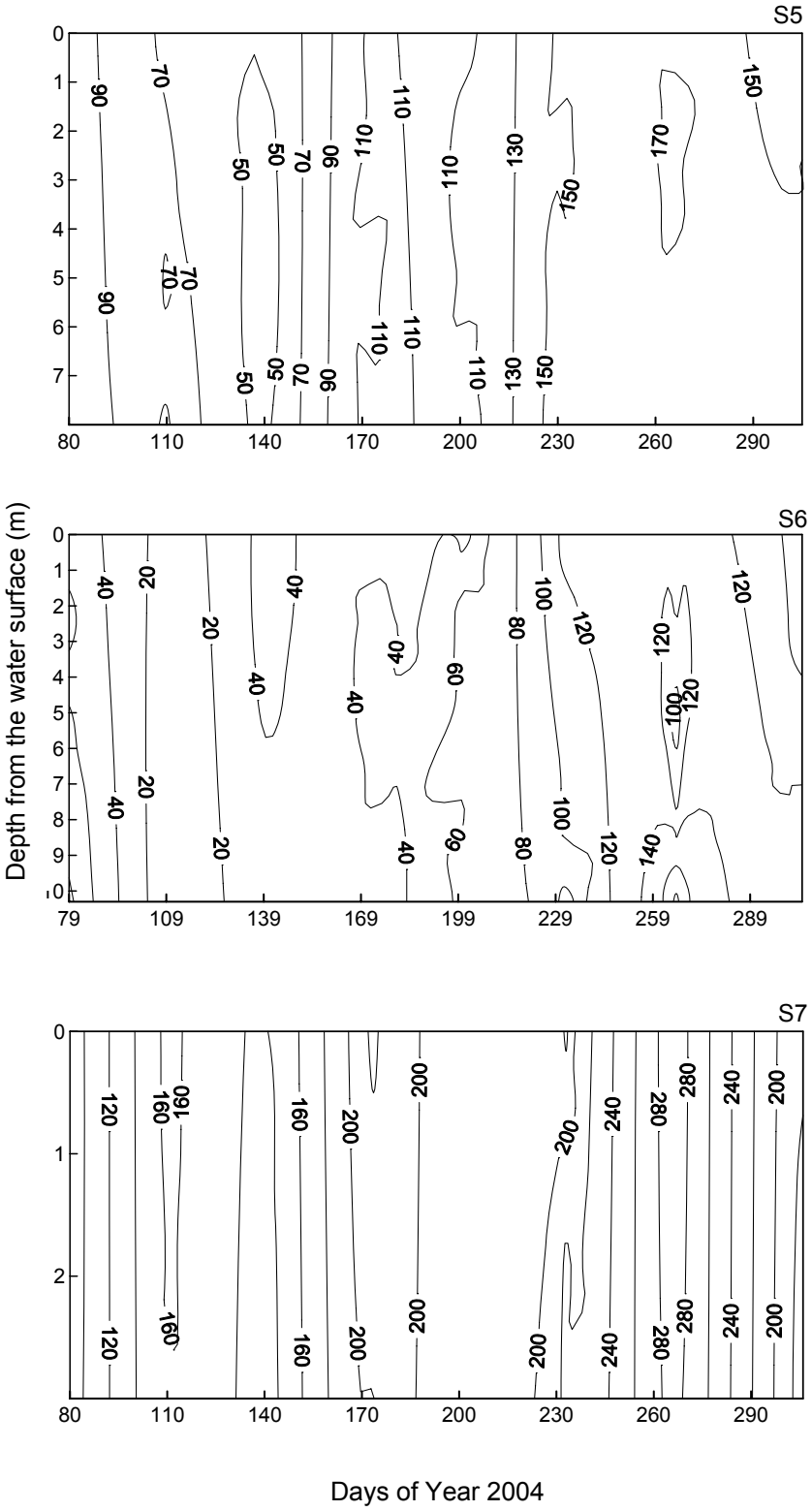

Figure B10. *Total suspended solids concentration (mgL^{-1}) fields measured monthly at fixed monitoring stations in the north basin.*

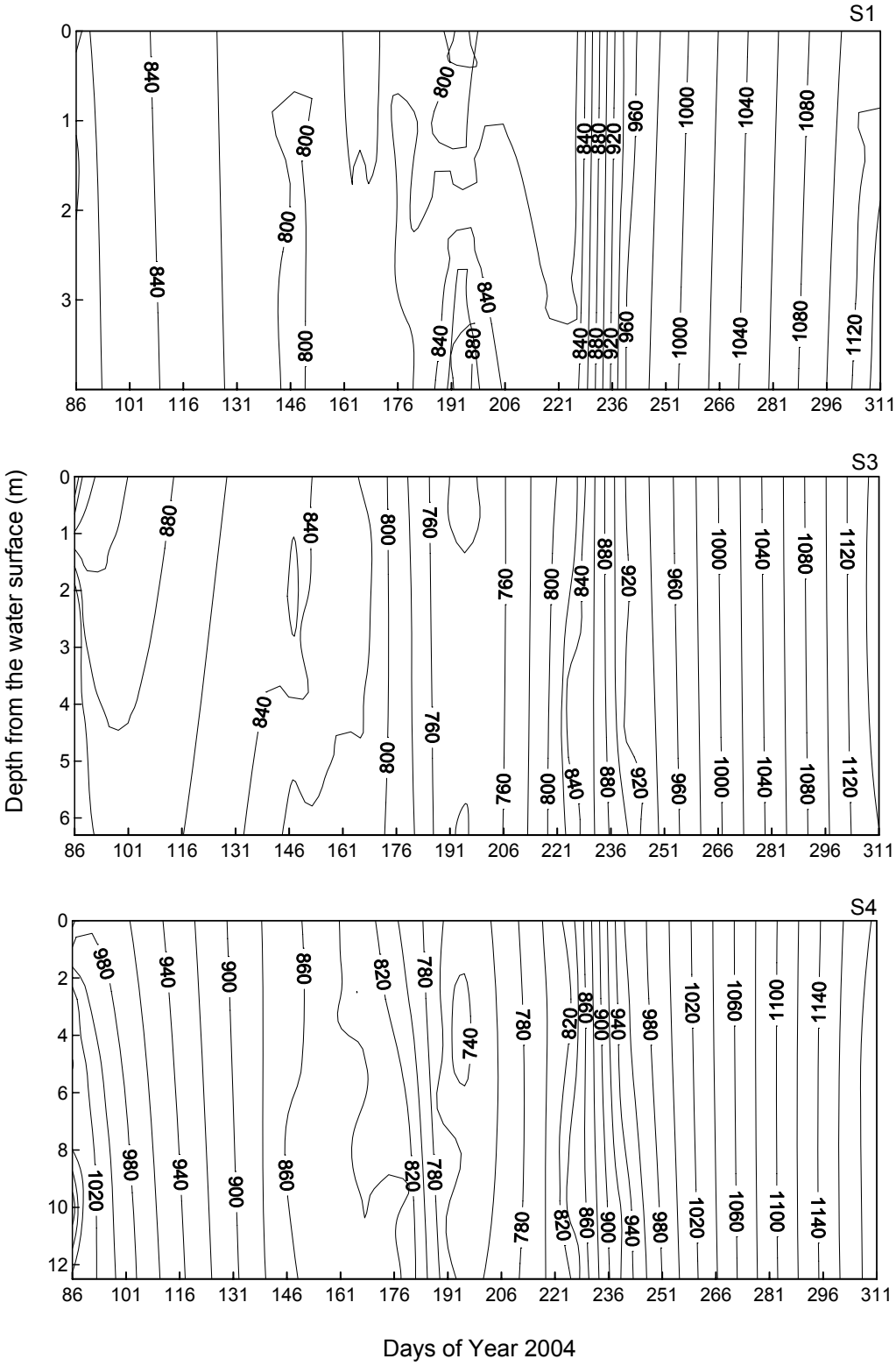

Figure B11. *Total dissolved solids concentration (mgL^{-1}) fields measured bimonthly at fixed monitoring stations in the south basin.*

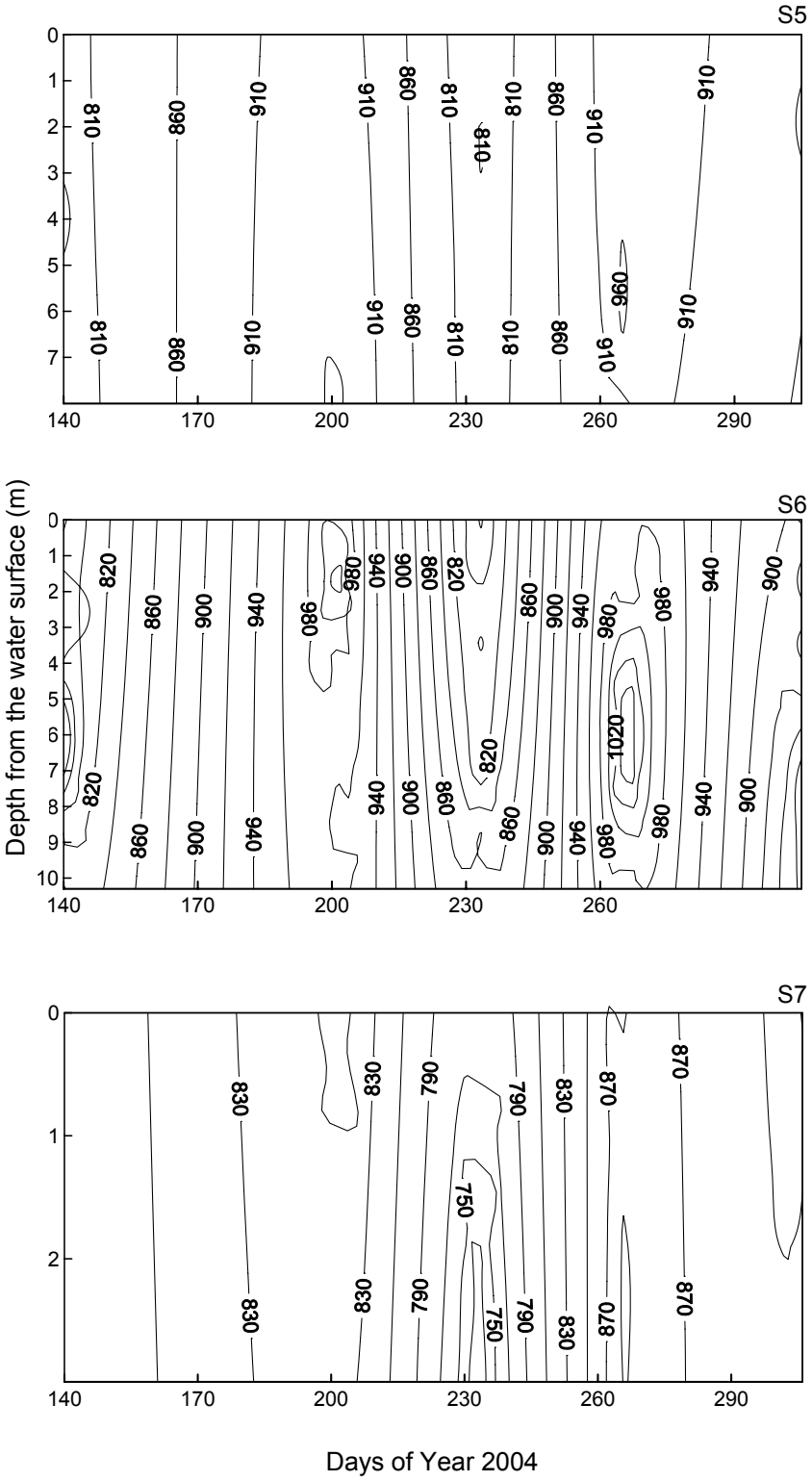

Figure B12. *Total dissolved solids concentration (mg.L^{-1}) fields measured monthly at fixed monitoring stations in the north basin.*

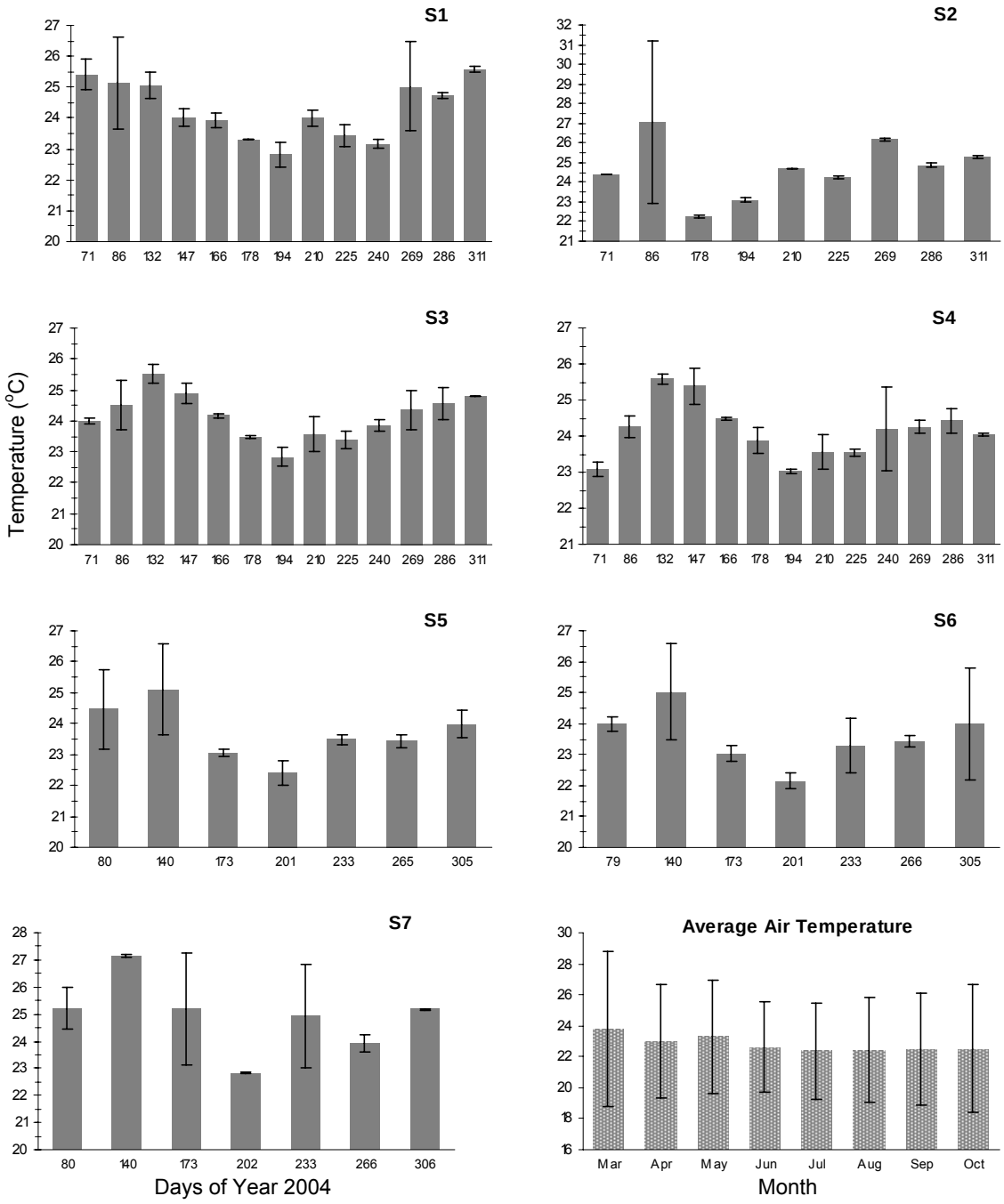

Figure C1. *Average water temperature (°C) at fixed monitoring stations and monthly average temperature at Wajifo Weather Station during the study period. Error bars indicate ±1 SD of depth profile measurements.*

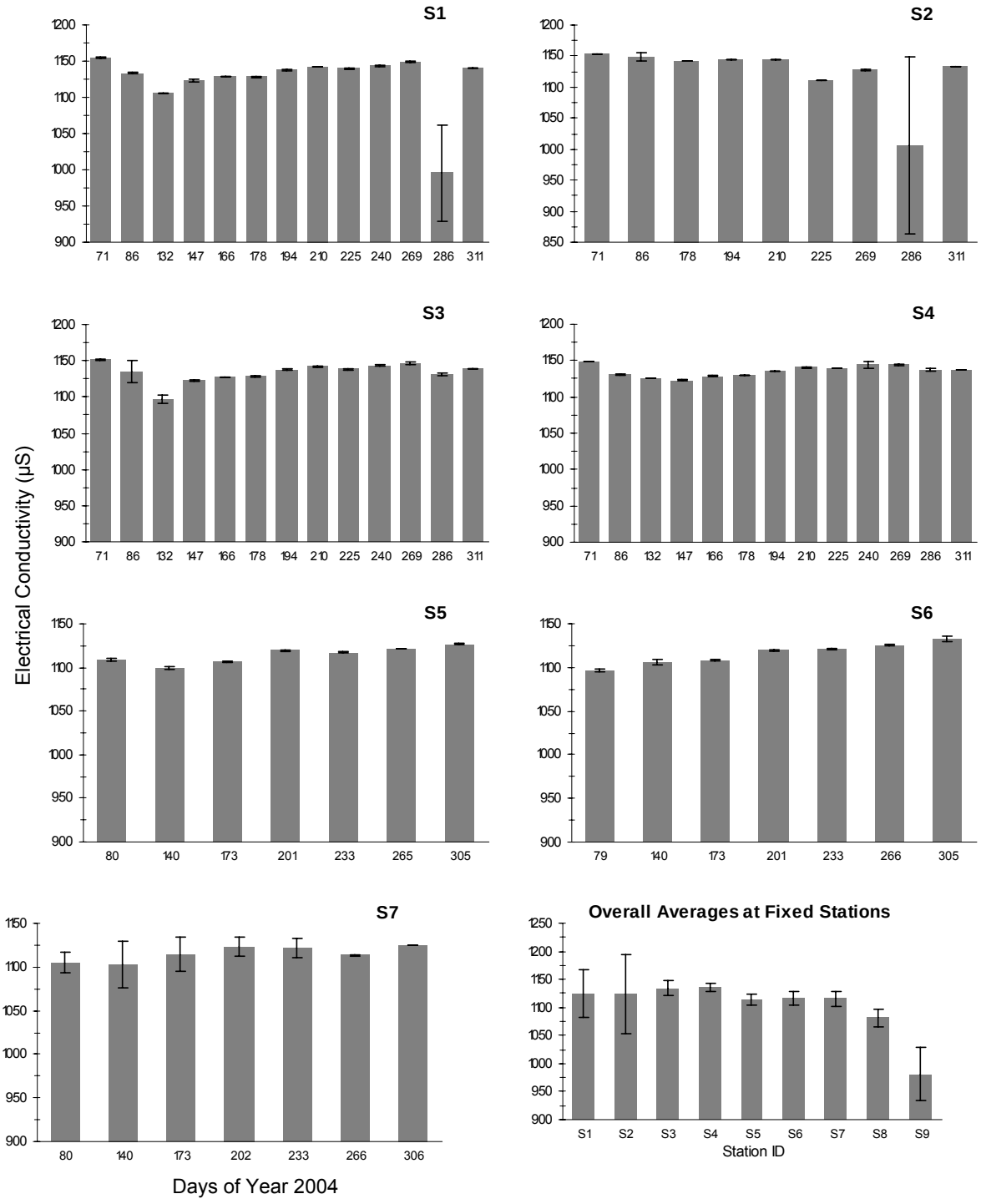

Figure C2. *Average electrical conductivity ($\mu S.cm^{-1}$) at fixed monitoring stations. Error bars indicate ±1 SD of depth profile measurements.*

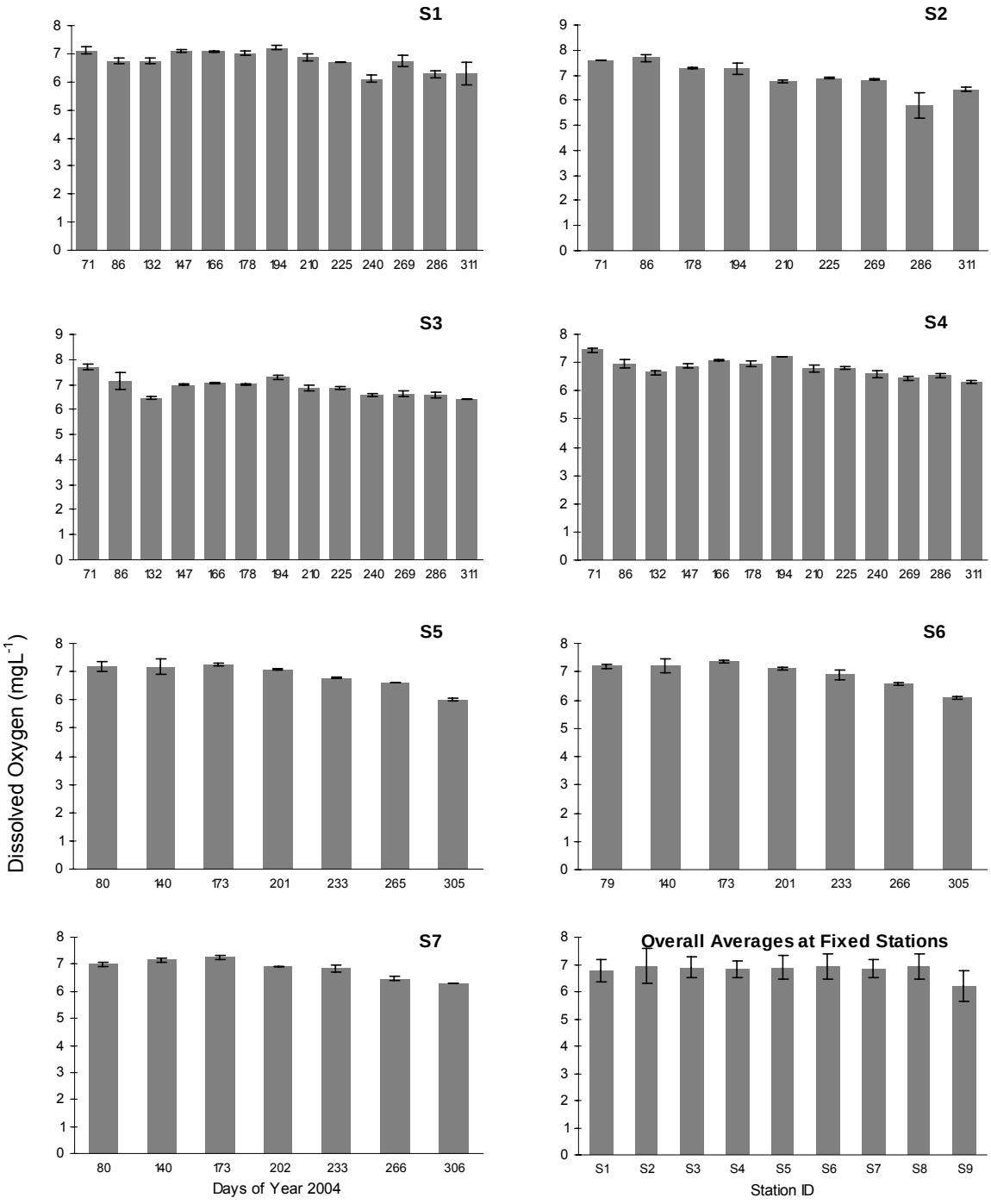

Figure C3. *Average dissolved oxygen (mg.L^{-1}) concentration at fixed monitoring stations. Error bars indicate ±1 SD of depth profile measurements.*

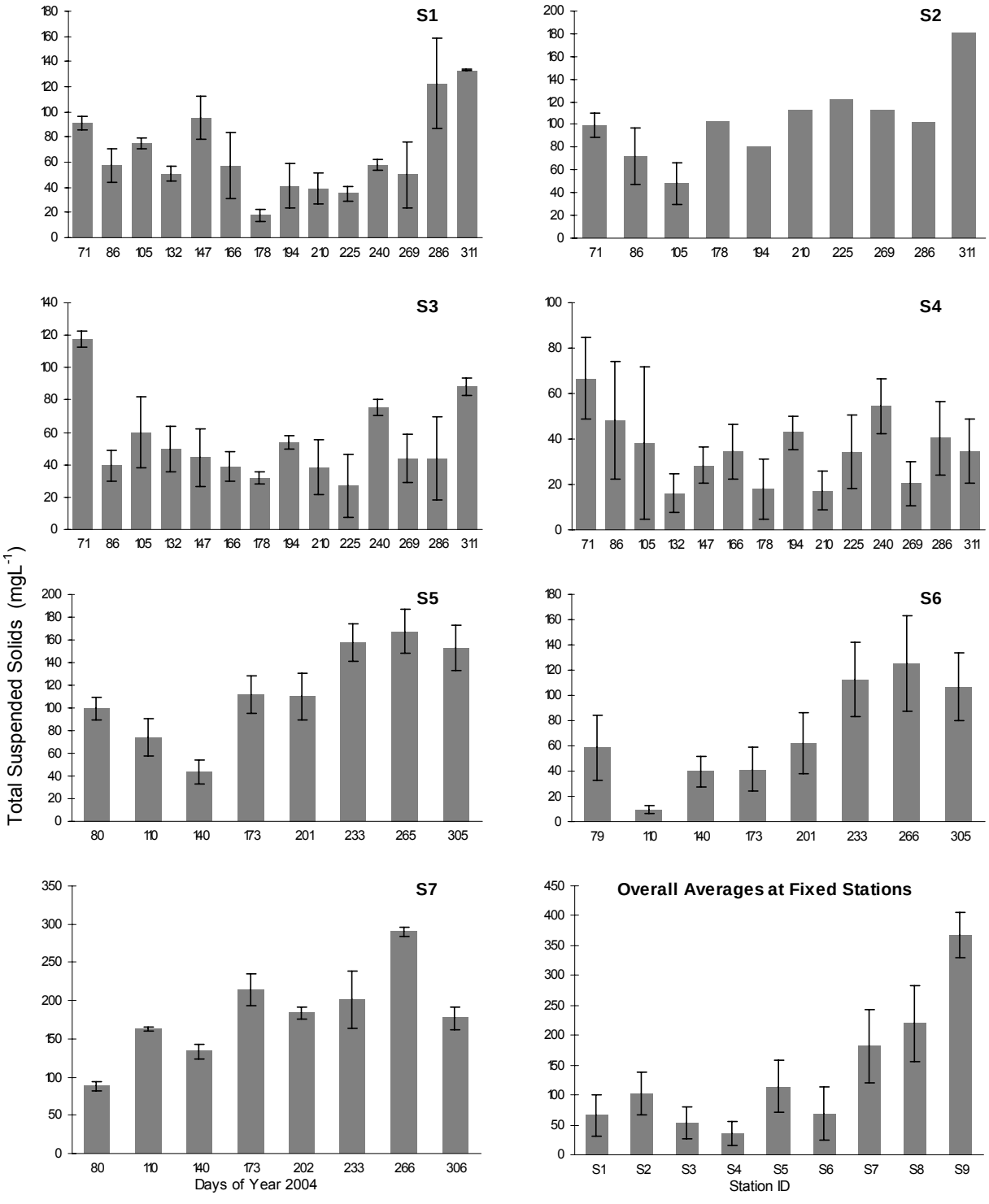

Figure C4. *Average total dissolved solids (mg.L^{-1}) concentration at fixed monitoring stations. Error bars indicate ±1 SD of depth profile measurements.*

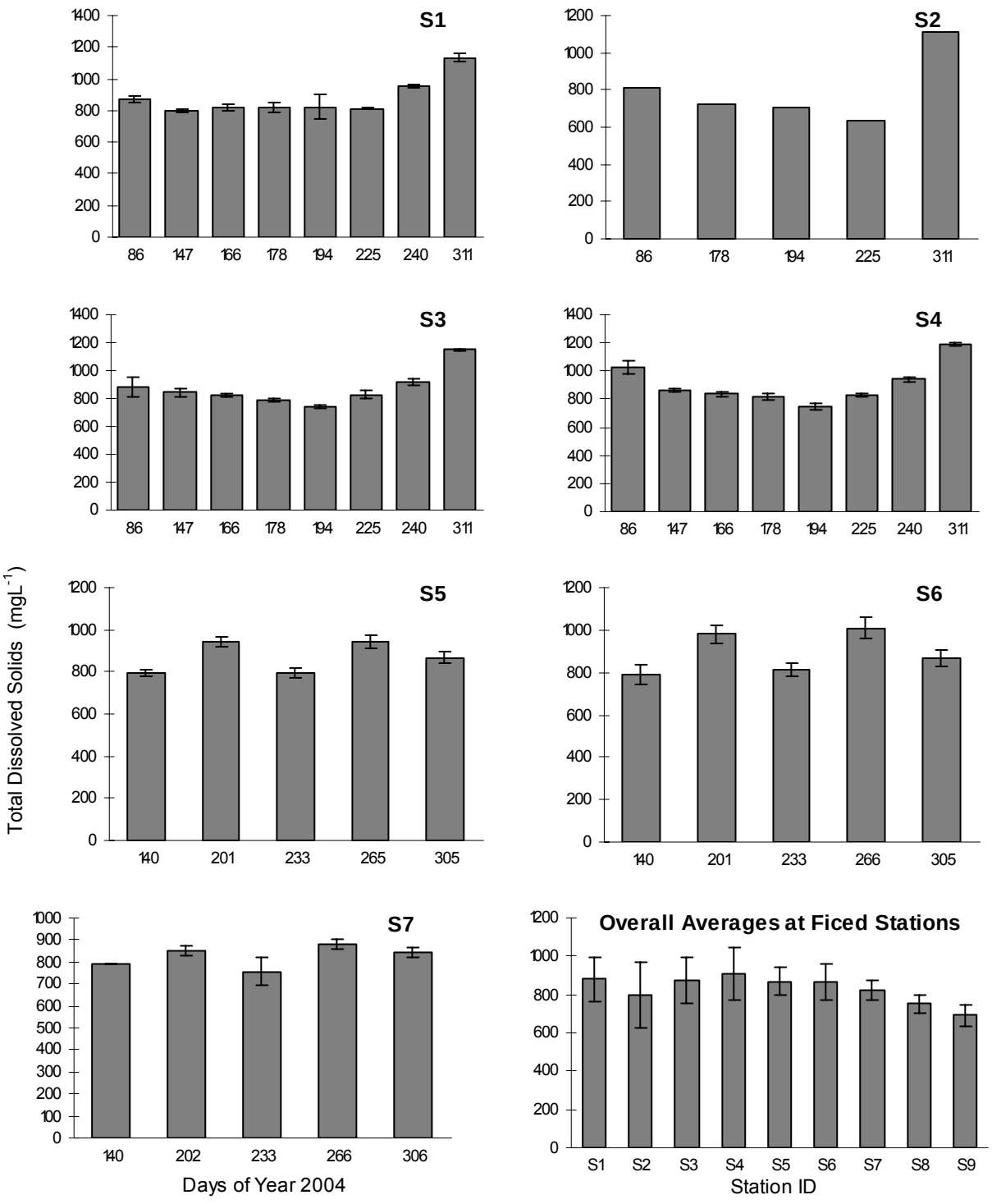

Figure C5. *Average total dissolved solids (mg.L^{-1}) concentration at fixed monitoring stations. Error bars indicate ±1 SD of depth profile measurements.*

Complete List of Volumes

Vol. 1

LARS 2007 Proceedings

Vol. 2

Alumni Summer School - Well Drilling and Rural Water Supply

Vol. 3

Summary of Master Theses from Arba Minch University

Vol. 4

Results from Expert Seminar - Topics of Integrated Water Ressources Management

Vol. 5

Adane Abebe - Hydrological Drought Analysis - Occurence, Severity, Risks: The Case of Wabi Shebele River Basin, Ethiopia

Vol. 6

Bogale Gebremariam - Basin Scale Sedimentary and Water Quality Responses to External Forcing in Lake Abaya, Southern Ethiopian Rift Valley

Vol. 7

Stefan Thiemann et al. Integrated Watershed Management - Financial Aspects of Watershed Management